THE INFLUENCE OF HEATING CONDITIONS ON SEMI-SOLID FORMING OF ALUMINUM ALLOYS

by

Mehmet Önsel

B.S. in M.E., Istanbul Technical University, 2003

Submitted to the Institute of Graduate Studies in
Science and Engineering in partial fullfillment of
the requirements for the degree of
Master Science

Graduate Program in Mechanical Engineering

Boğaziçi Univeristy

2005

ACKNOWLEDGEMENTS

First and foremost, I would like to express my gratitude to my thesis advisor, Prof. Sabri Altıntaş, for his immense support throughout this project, both scientifically and personally. I was able to cope with the research only with his unlimited aids and motivation me.

I would like to gratefully acknowledge Yücel Birol (TÜBİTAK-MAM) for his guidance and insight throughout the study. I would like to express appreciation to Osman Çakır (TÜBİTAK-MAM) for his technical support and to Fahri Alageyik and Ceylan Kubilay (TÜBİTAK-MAM) for their aids in metallographic studies.

I am indebted to Kurt Neulinger (Salzburger Aluminium AG) for supplying thixotropic A356 aluminum alloys for the experimental study.

I would like to thank to Mehmat Aktürk (REPAMET) for supplying induction heating unit. Also, I would like to mention Özcan Özer (REPAMET) for his invaluable assistance and guidance about induction heating machine.

I am grateful to Vedat Akgün (FORD OTOSAN) for his guidance and encouragement at initial stages of my thesis. I also would like to gratefully acknowledge to İbrahim Mutlu for the preparation of the tensile test specimens.

I would like to thank my friend, Uğur Bozkurt, for his encouragement, feedback and numerous suggestions.

Finally, I am forever indebted to my parents for their understanding, endless patience and encouragement when it was most required.

ABSTRACT

THE INFLUENCE OF HEATING CONDITIONS ON SEMI-SOLID FORMING OF ALUMINUM ALLOYS

The use of aluminum alloys for complex parts is receiving a great deal of attention recently in the automotive sector worldwide. Semi-solid forming appears to be a very attractive method for producing complex parts as it offers fewer production steps and allows using lower forming loads. In present study, the effect of heating conditions on thixoforming of A356 and AA6082 aluminum alloys was investigated. The production of a fine, equiaxed, globular microstructure is a must for the success of the thixoforming process. The present study showed that thixotropic structure can be successfully obtained using magnetohydrodynamic (MHD) casting route for A356 alloy and strain induced melt activated (SIMA) route for AA6082 aluminum alloy. Holding temperature, holding time and the number of reheating steps were considered as parameters in reheating experiments of MHD cast A356 alloy. The impact of the extent of deformation and reheating treatment parameters on the globularization of the grains in SIMA process was investigated for AA6082 alloy. Finally, A356 and AA6082 aluminum alloys were thixoformed considering heating conditions that give most successful thixotropic structures. The microstructures and mechanical properties of the produced parts were investigated to get information about the obtained quality of the parts.

ÖZET

ISITMA KOŞULLARININ ALÜMİNYUM ALAŞIMLARININ YARI-KATI HALDE ŞEKİLLENDİRİLMESİ ÜZERİNDEKİ ETKİLERİ

Otomotiv sektöründe, karmaşık geometrideki parçalar için alüminyum alaşımlarının kullanılmasının önemi giderek artmaktadır. Yarı-katı şekillendirme yöntemi de, karmaşık şekilli parçaların daha az sayıda işlem adımı ile ve düşük kuvvetler altında üretildiği en uygun yöntemdir. Bu çalışmada, ısıtma koşullarının A356 ve AA6082 alüminyum alaşımlarının yarı-katı halde şekillendirilmesi üzerindeki etkileri incelenmiştir. Yarı-katı halde şekillendirme yönteminin uygulanabilmesi için, alaşımın ince taneli, eş eksenli ve küresel bir mikroyapıya sahip olması gerekmektedir. Bu çalışma, A356 alaşımı için manyetik karıştırma (MHD) yöntemi ve AA6082 alaşımı için deformasyon verme ve yeniden ısıtma (SIMA) yöntemi uygulanarak söz konusu yapının başarılı bir şekilde elde edilebileceğini göstermiştir. MHD yöntemi ile dökülen A356 alaşımının ısıtılması deneylerinde; bekleme zamanı, ısıtma sıcaklığı ve ısıtma adımlarının sayısı parametrelerinin tane küreleşmesi üzerindeki etkileri incelenmiştir. AA6082 alaşımı için uygulanan SIMA işleminde ise, deformasyon miktarı ve ısıtma parametrelerinin mikroyapı oluşumuna etkileri incelenmiştir. Son olarak, en başarılı mikroyapıları veren ısıtma koşulları göz önüne alınarak bu koşullarda çeşitli ürünler basılmıştır. Üretilen parçaların kalitesi hakkında bilgi edinmek üzere, bu parçalar çeşitli mekanik testlere tabii tutulmuş ve mikroyapıları incelenmiştir.

TABLE OF CONTENTS

LIST OF FIGURES

LIST OF TABLES

LIST OF SYMBOLS/ABBREVIATIONS

E_c	Coil electromagnetic force
f	Frequency
f_s	Solid fraction
f_L	Liquid fraction
I	Current
I_c	Coil current
I_w	Current in workpiece
N	Number of turns
R	Resistance
T_{h1}, T_{h2}, T_{h3}	Holding temperature
t_{h1}, t_{h2}, t_{h3}	Holding time
T_L	Liquidus temperature
T_{Ryc}	Recrystallization temperature
T_S	Solidus temperature
ΔT	Superheat
Φ	Flux
δ	Skin depth
μ	Absolute permeability
σ	Conductivity

AC	Alternating current
CRP	Continuous Rheoconversion Process
DSC	Differential Scanning Calorimetry
FLS	Liquid incorporating solid particles
LF	Liquid flow
MHD	Magnetohydrodynamic
PDS	Plastic deformation of solid particles
RAP	Recrystallization and partial remelting
SIMA	Strain induced melt activated

SS	Solid particles
SSM	Semi-solid metal

1. INTRODUCTION

Until a few years ago the only way to manufacture light, safe and structural parts was forging: transformation in the solid state from the raw material to the final component, with an elevated energy consumption, no near-net-shape geometries, with expensive machining operations, low total production rate. These items lead to a high final cost and shape limitation of possible parts. In order to solve these problems, in recent times a number of innovative technologies were studied and developed: squeeze casting, vacuum pressure die casting, semi-solid metal processing [1]. Today, semi-solid metal processing has established itself as a scientifically sound and commercially viable technology for production of metallic components with high integrity, improved mechanical properties, complex shape, and tight dimensional control [2].

The discovery of shear thinning and thixotropic behaviour of partially solidified alloys under vigorous agitation by Spencer et al. in 1971 was the starting point for semi-solid metal processing. In the same year, the two basic routes of semi-solid metal processing -termed "Rheocasting" and "Thixocasting"- proved their feasibility in industrial trials. The rheo-route involves the preparation of a semi-solid metal slurry from liquid alloys and transferring the prepared slurry directly to a die or mould for component shaping. The thixo-route is basically a two step process, involving the preparation of a feedstock material with thixotropic characteristics, reheating the solid feedstock material to semi-solid temperature and shaping the semi-solid slurry to components [2].

Thixoforming of metals always means that during the forming operation the slug consists of a solid and a liquid phase. Thixoforming, i.e. shaping alloys in their semi-solid state, combines the benefits of conventional primary and secondary forming methods, thereby potentially making it technically and commercially feasible to produce complex parts in a single-stage process. In the temperature interval between solid and liquid state metals show thixotropic behaviour. The phenomenological basis of this behaviour is due to the fact that with increasing shear forces, the solid-phase skeleton of the metallic structure can be completely dismantled. This is the most important precondition to achieve low-

viscous flow, which finally allows the production of complex shaped parts requiring only small forces for forming [3].

There are three key technologies in the thixoforming, which is manufacturing of billets with non-dendrite microstructure, reheating the billets to semi-solid state and forming the semi-solid billets to parts [4]. If the component shaping is performed in a closed die, it is referred to as thixocasting, while if the shaping is achieved in an open die, it is called thixoforging. A schematic of the thixoforming process is shown in Figure 1.1.

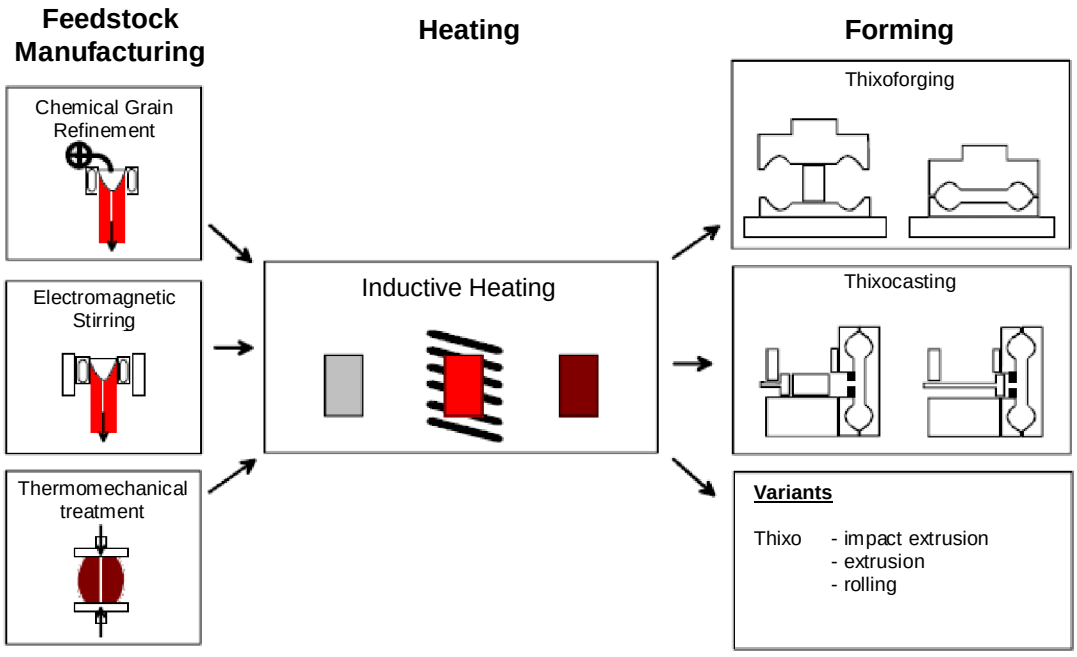

Figure 1.1. Schematic of the semi-solid forming process termed thixoforming [5]

The objective of feedstock production is to provide a material with a characteristic thixotropic microstructure where a non-dendritic (or globular) primary phase with a fine grain size is uniformly distributed in a matrix of lower melting point. Although thixotropic feedstock materials in their semi-solid state may be directly used for component shaping, they are often used as a raw material in the solid state for subsequent reheating into the semi-solid state and component shaping through thixoforming.

The heating process greatly affects the quality of the components. Therefore it is very important to accurately monitor and control the temperature of the semi-solid billet in

order to achieve the desired solid/liquid fraction and microstructure before forming [6]. The actual forming is carried out with modern forging or high-pressure casting machines. Thus, one can distinguish between thixoforging and thixocasting.

Thixoforming technology is relatively new and is currently receiving increased interest by manufacturers. Over the last decade and more the primary driving force for development of semi-solid forming has been the energy efficient automobile. Aluminum usage in the automobile, primarily in cast form, has increased dramatically and with that increase has come the need for parts of higher strength and greater reliability. Thixoforming is one of the important processes filling that niche [7]. One of the main advantages of thixoforming is the production of complex-geometry components within a single production step. Because of the small volume shrinkage during solidification, parts can be produced in near-net-shape quality without additional cutting and shaping, thus saving time and energy. Furthermore, in thixoforging, the driving forces are small compared to conventional forging, leading to smaller plant dimensions and an increase in the forging tool durability. Thixocasting guarantees, in comparison to its conventional counterpart, a laminar filling of complex geometries. Remarkable characteristics of thixoformed products are excellent mechanical properties as well as the possibility of thermal treatment [8].

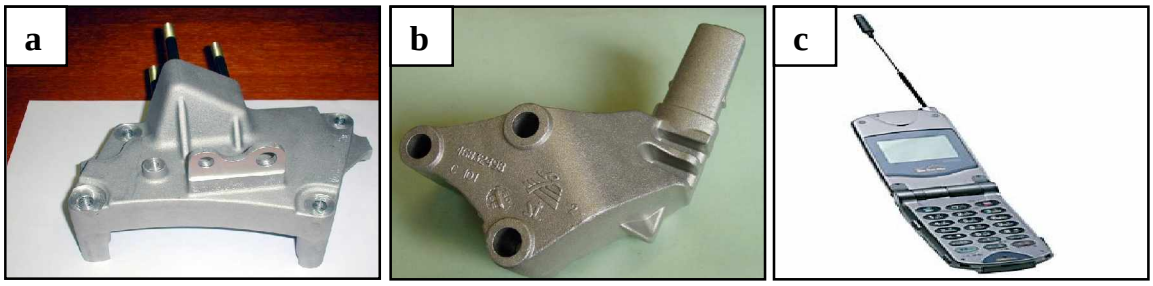

Figure 1.2. Suspension part (a), engine bracket (b) and cell phone frame (c) produced by thixoforming technology [9]

Semi-solid metal processing is rivalling other manufacturing routes for military, aerospace and most notably automotive components. In Europe, suspension parts, engine brackets and fuel rails for automotives are being produced. In the USA, examples include mechanical parts for mountain bikes and snowmobiles, while in Asia there is concentration

on the production of electronic components such as computer notebook cases and electrical housing components [10]. Figure 1.2 provides a few examples of parts produced by thixoforming technology.

2. THIXOTROPIC FEEDSTOCK PRODUCTION

Semi-solid metal processing takes advantage of the unique thixotropic behavior found in the semi-solid state. In this state, the alloy generally exhibits decreasing viscosity with increasing shear [11]. The viscosity of semi-solid material in the liquid phase is as low as 0.001 Pa s, and the behavior is that of a Newtonian fluid that is independent of time and shear-rate. However, the viscosity in the useful forming in the semi-solid state (f_s=0.3-0.7) is changed drastically from 0.1 to 1×10^{-6} Pa s as the function of the temperature and shear force. The material when static can be treated as solid owing to the high viscosity, and in forming it can be looked upon as a visco-fluid causing the good filling [12]. This unique thixotropic nature of semi-solid slurry is exhibited in Figure 2.1 where a semi-solid slug was cut like butter with a knife.

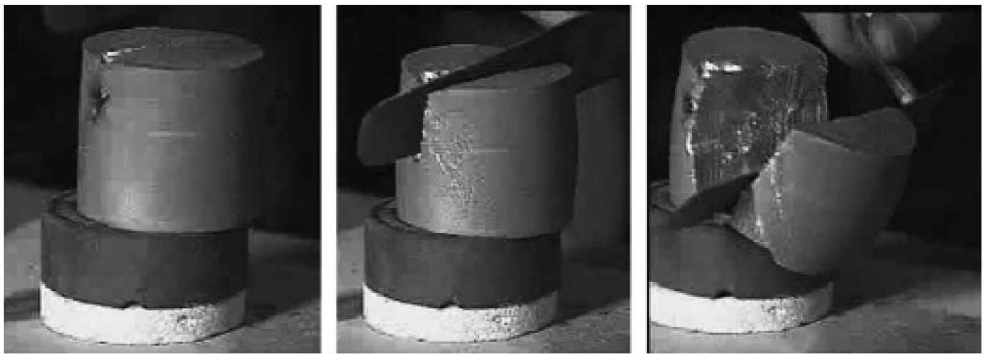

Figure 2.1. A photographic sequence illustrating the thixotropic behaviour of semi-solid alloy slugs [9]

The main requirement for processability in the semi-solid range is that alloys should exhibit a fine equiaxed microstructure devoid of dendrites so that they can be formed to net shape in the semi-solid state by semi-solid metal processing [13]. The ideal microstructure for semi-solid slurry before the component shaping process is an accurately specified volume fraction of fine and spherical solid particles uniformly dispersed in a liquid matrix [14].

The pre-conditions to realize the semi-solid metal processing are a suitable alloy and an appropriate structural state of the feedstock.

2.1. Suitability of Alloys for Thixoforming

The feasibility of semi solid metal processing of various alloys has been investigated in the past 30 years. Initially, the primary focus was on high temperature alloys, notably steels, and practically no attention was given to aluminum and magnesium alloys. This was mainly due to the drive for perfection of steel die casting technology for military applications. Semi-solid processing was considered to be an effective means to reduce the casting temperature. However, because of the oil crises in the 1970s, and increasing environmental concerns since the 1980s, automobile market forces have been pressing hard for weight reduction using high performance light metal parts. As a consequence, since the 1990s, semi solid metal processing has predominantly concentrated on aluminum alloys.

Millions of aluminum alloy components are produced using this process every year in Europe, Japan and the USA, but they are almost all made from conventional casting alloys such as A356 and A357, which provide excellent thixoformability and workability [15]. However, such A356 and A357 cannot match the mechanical properties of wrought aluminum alloys. In the viewpoint of such limitation, it is evident that the application scope of thixoforming technology is considerably narrowed. In order to overcome this limitation, a lot of researches have been done to develop thixoforming process for various wrought aluminum alloys. First, unlike cast Al–Si aluminum alloys, feedstocks for thixoforming of wrought aluminum alloys are not existed in commercial market. Second, because liquid fraction of wrought aluminum alloys is very rapidly changed with temperature change, the careful attention, when a slug is reheated, must be given to obtain the reasonable liquid fraction ensuring good thixoformability. A small decrease in temperature can lead to a considerable increase in solid fraction resulting in a microstructure absolutely not favorable to semi-solid forming. Third, at semi-solid state, wrought aluminum alloys have higher viscosity and hot cracking tendency than cast grade aluminum alloys [16]. However, increasing attention is being given to thixoforming of normally wrought alloys and their mechanical properties and there is significant progress towards reaching the goal of thixoforming alloys with performance approaching that of the

conventionally wrought alloys.

New alloys suitable for thixoforming are desired rather than existing alloys originally designed for casting or forging. In this respect, some alloy modifications can be made. Shape retention is improved by decreasing silicon concentrations with some loss in fluidity and strength. Magnesium additions (0.2 - 1.0 per cent) can be used to provide product strength through heat treatment. Eutectic modifications where necessary are accomplished with small additions of strontium (~0.02 per cent) [17].

Thixoformability is the term usually used to indicate the suitability of alloys for thixoforming. Thixoformability depends on parameters such as the amount and spatial distribution of the fraction liquid (f_L), fraction liquid sensitivity, solidification range, morphology of solid grains [18].

Many criteria are considered for alloy composition selection for thixoforming.

2.1.1. Solidification Range

The solidification range is usually defined as the temperature range between the solidus and liquidus. It is mainly determined by alloy composition and affected by processing conditions, such as cooling rate. Solidification range is an important factor and needs to be optimized during alloy development for semi-solid metal processing. Solidification range should not be too wide (less than 130 K), because this could lead to poor resistance to hot tearing and poor fluidity of the liquid alloy. On the other hand, a too narrow solidification range makes difficult the temperature control of semi-solid billets.

2.1.2. Temperature Sensitivity of Liquid Fraction

For a given alloy composition, liquid volume fraction of a semi solid metal slurry is usually determined by the semi-solid metal processing temperature. The temperature sensitivity can be defined by the slope of the liquid fraction-temperature curve. Alloys designed for semi solid metal processing should have a small temperature sensitivity of liquid fraction.

A typical fraction liquid versus temperature curve is shown in Figure 2.2. The highest 'knee' on the fraction liquid versus temperature curve should occur between 30 and 50 per cent liquid (see schematic in Figure 2.2); this is the temperature at which α - solid solution starts melting. If this occurs between 30 and 50 per cent liquid, liquid formation tends to be controllable because the rate of liquid formation above the knee tends to be slower.

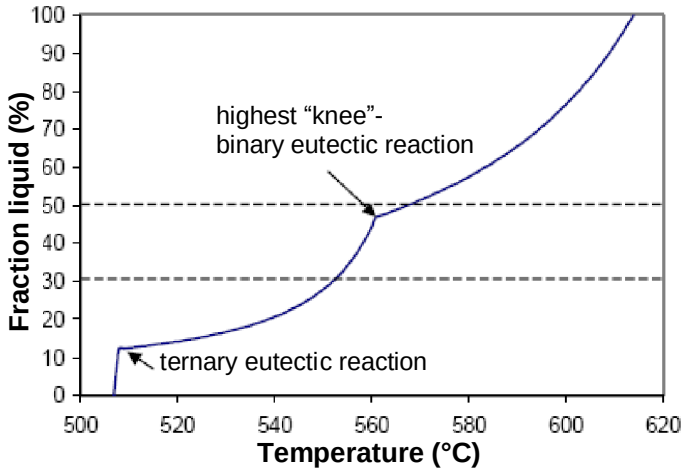

Figure 2.2. Schematic of a typical fraction liquid versus temperature curve [18]

Fraction liquid sensitivity should be as small as possible. Large values will result in substantial variation of the fraction liquid with a small change in temperature. This will lead to unpredictable changes in the rheological behavior of the material and, invariably, to defects and inferior properties in the final product. In most alloys as the temperature approaches the liquidus, the absolute value of the rate of change of the volume fraction of solid with respect to temperature increases. Control and reliability of the process requires a small value of fraction liquid sensitivity. While sophisticated heating systems can control the temperature with a tolerance of ± 0.5 per cent of the working temperature, most industrial heating systems give an accuracy of about ± 1-3 per cent. These variations in temperature can lead to significant variations in solid fraction, which in turn negates the reproducibility of the process. Small temperature gradients may cause significant variations of properties in the billet and are detrimental to the reliability of the process [13].

2.1.3. Morphology of Solid Phase

The rheological properties of semi-solid alloys are basically influenced by the morphology of the solid phase. An ideal slurry for semi-solid metal processing has a controlled volume fraction of fine and spherical solid particles distributed uniformly in a liquid matrix with good fluidity. Such semi-solid metal slurry can ensure smooth mould filling and fine and uniform microstructure after solidification. However, the ease with which the fine and spherical particles can form during semi solid metal processing depends on the actual composition. Accordingly, composition selection during alloy design should facilitate the creation of such an ideal semi solid metal slurry.

2.1.4. Rheological Properties in the Semi Solid State

It is the characteristic rheological properties of semi solid slurries that make semi-solid metal processing unique and advantageous compared with other conventional casting techniques. The processing condition, and the morphology, size, and distribution of the solid phase in the liquid matrix, all have great influence on the viscosity of slurries. The variation in viscosity, on the other hand, will influence the castability. In addition, particle agglomeration strongly affects the rheology of slurries. A reduced tendency for particle agglomeration will facilitate semi-solid metal processing and can be achieved through addition of alloying elements.

Entrapped liquid is stated to be unfavorable as it does not contribute to the ability of the material to flow. In existence of entrapped liquid, semi-solid metal processing has therefore to be done at increased temperature to compensate entrapped liquid.

2.2. Methods for Preparation of Thixotropic Slurries

It has been demonstrated that the initial near equiaxed microstructure of alloys suitable for subsequent semi-solid processing depends on the method used to produce them. Therefore, it is important to study how this initial difference affects the evolution of microstructure in the semi-solid state, i.e. the structure of the solid skeleton, grain growth, and the degree of spheroidization, since microstructure significantly affects the rheological

behavior of alloys during semi-solid forming [19].

A primary goal of slurry preparation is to create such a structure to ensure the favorable rheological characteristics to facilitate the subsequent component shaping process. Technically, this structure can be achieved by a number of different techniques [2]. A first group in which the liquid alloy is stirred by mechanical or magnetic action and a second consisting of plastic deformation followed by a static recrystallization heat treatment. Other methods are being developed and among them the low temperature pouring technique appears to be particularly promising [20].

There are a number of thixotropic feedstock production techniques, which are at different stages of research and development. Among all methods, only electromagnetic stirring has become a widely accepted method for the production of non-dendritic feedstock materials on a commercial scale, although small scale productions via intensive plastic deformation are being used for some components today. In this section, the basic features of those techniques available for feedstock production are given in detail.

2.2.1. Stirring

In the early 1970's, when Spencer and co-workers were conducting hot-tearing tests on a lead-tin alloy through the solidification range, they discovered that under continuous shearing the semi-solid material offered much less resistance than expected. More importantly, the microstructure of the solidified material was radically different than the normal dendritic microstructure. In conventional casting processes one obtains a highly oriented needle-like dendritic structure, whereas solidification in the presence of shearing produced more uniform primary α-globules surrounded by lower melting eutectic phase. The globular microstructure, when partially re-melted, offers much less resistance to flow even at high solid fractions. This property represented a great potential for pressure die forming, and eventually spurred growth of other semi-solid processing techniques [21].

During the initial years of semi-solid metal process development, mechanical stirring was used in various ways to break up dendrites and produce thixotropic metal structures. The combination of rapid heat extraction and vigorous melt agitation was effected by using

different sizes, shapes, and velocities of stirring rods. Various researchers addressed the evolution of the "stircast" structure during this time. A schematic of stir casting device is shown in Figure 2.3. The semi-solid alloy is sheared in a heated tubular zone between a grooved rotor and a crucible. Although these methods worked well in that they effectively produced the desired metal structures, erosion of the stirrer became the "weak link" of the process. Focus was placed on the development of "passive" agitation techniques to mitigate stirrer erosion and ensure impurity-free castings [22].

The first highly effective passive method for producing feedstock material for thixocasting applications was the Magnetohydrodynamic (MHD) casting process developed by Dantzig and co-workers [23]. In this approach, the solidifying melt is not agitated by a mechanical stirrer, but by alternating electromagnetic fields. Although there are other means to produce nondendritic alloys, this process and its variants are of the most commercial importance.

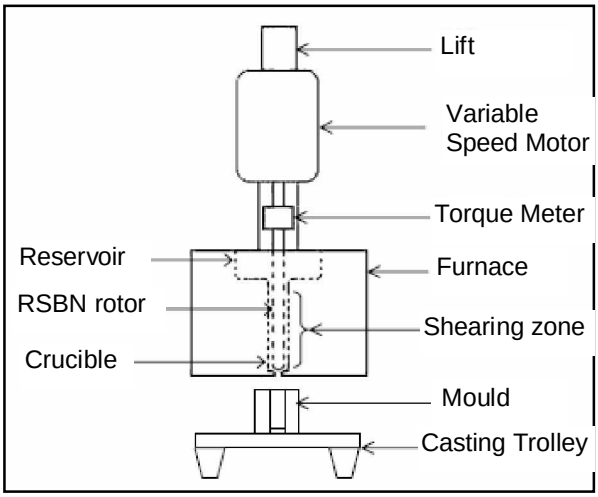

Figure 2.3. Schematic of stir casting device [24]

From a practical standpoint, introducing convection by mechanical or electromagnetic means during the early stages of solidification favors formation of fine, equiaxed grains. There are many references in the older cast metals literature as to effect of such convection on grain structure. Mold oscillation, for example, was sometimes employed to achieve fine grains in sand castings, and stirring with a cold rod was used to refine the structure of ingots. Today, electromagnetic stirring is widely practiced in

continuous casting to achieve fine grain size [11].

MHD casting process can be integrated in the known continuous casting technology, but requires additional investments for appropriate equipment of existing plants. Figure 2.4 is the schematic representation of a lab-scale setup which combines directional solidification with stirring induced by a rotating magnetic field. Induction coils are placed around a crucible to induce these forces. The crucible is equipped with a cooling system to initiate freezing in the alloy while the melt is exposed to the electromagnetic forces. Upon cooling down to ambient temperature, the alloy has an equiaxed, non-dendritic microstructure [21]. The MHD stirring process works remarkably well and is widely used commercially today.

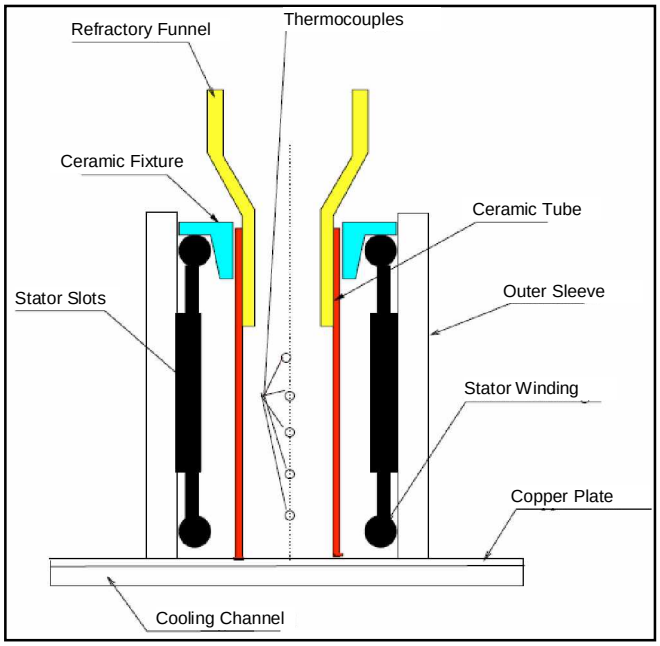

Figure 2.4. Experimental set up to produce magnetic stirring during solidification [21]

Figure 2.5 presents a semi-solid microstructure typically obtained with the MHD process. The resulting microstructure of MHD casting consists of ripened equiaxed dendrites called 'rosettes'. This microstructure is the result of dendrite degeneration. As liquid metal flows through the caster, it is subjected to both stirring by the electromagnetic field and cooling by the cooling system of the caster. When the molten metal enters the cooling zone, the temperature drops below the liquidus temperature and solid starts to nu-

cleate against the mold walls forming dendrites. These dendrites are detached from the mold, flow into the liquid metal and undergo growth and spheroidization transforming into rosettes. At the same time, they may collide with other free-flowing rosettes and coalesce, if their misorientation is favorable, forming agglomerates [25].

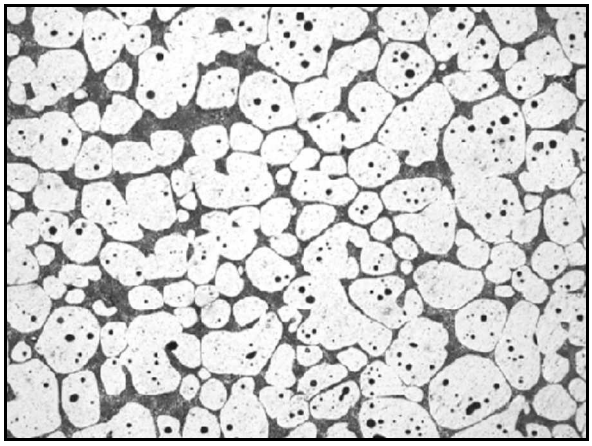

Figure 2.5. Typical semi-solid microstructure obtained using MHD process [26]

The major hurdles to the wide acceptance of this technology for thixotropic feedstock production include high production costs (accounting for up to 50 per cent of the component cost), microstructural non-uniformity in the cross-section of the cast billet, and non-spherical (although non-dendritic) particle morphology. A significant cost factor in the MHD billet process is the casting of the MHD log, sectioning into billets, and reheating the billets to form the semi-solid feedstock for the semi-solid metal forming process [17]. Microstructural deficiency will cause prolonged reheating time and difficulties during subsequent thixoforming, consequently resulting in a further increase of the production costs [2].

2.2.2. Strain Induced Melt Activated (SIMA) Process

Currently, electromagnetic stirring (magnetohydrodynamic, MHD) accounts for most commercial production for thixoforming. However, MHD billets tend to exhibit composition heterogeneity leading to an unequal distribution of liquid, and hence to flow heterogeneity. Additionally, their microstructure favours the occurrence of liquid trapped within the particles, thereby reducing the effective liquid fraction and further impairing

flow behaviour. An alternative method of microstructural conditioning may be strain induced melt activated (SIMA) process, which consists of plastic deformation before heating to semi solid temperature field. During subsequent heating recrystallization takes place, and when liquid starts to form, grain boundaries are wetted and penetrated by it, leading to the formation of equiaxed particles. Melts conditioned by SIMA show a reduced amount of trapped liquid and more spherical particles, compared with MHD billets, thus achieving better thixoformability [27]. In addition, as semi-solid billets with SIMA processing need not be mechanically stirred to break up dendritic structures, equipments used and processes are simple [28].

SIMA process consists of four discrete stages. First, the alloy is cast in convenient sizes to obtain a typical dendritic microstructure. Subsequently, it is hot worked so a directional microstructure is introduced and the thickness of the casting is decreased. The third stage involves the introduction of a critical level of stored energy in the alloy by cold working. Finally, the deformed alloy is semi-solid partially remelted, and held isothermally [29]. The transformation of the deformed dendritic microstructure into equiaxed could be explained by the grain deformation-recrystallization model: when the alloy is deformed during the third stage of the process, its dislocation density increases. During the final stage, as the temperature increases and while the deformed alloy is still in the solid state, it is subjected to recovery and recrystallization. New, strain-free grains nucleate and grow at the expense of strained grains. These new grains are characterized by high-angle grain boundaries. Upon heating above the solidus temperature, the high-energy grain boundaries are penetrated by liquid, causing the fragmentation of the original grains. The presence of liquid phase enhances grain growth and spheroidization of the newly formed grains. The soaking time and temperature in the semi-solid state are expected to control the extent of grain growth and the degree of spheroidization [26].

The preferred starting-material in SIMA process is a fully solidified alloy which may or may not have initially a dendritic microstructure. The starting material may be deformed by some suitable means such as by extrusion, rolling, tensile extension or compression. The deformation may be performed at low temperatures but to such an extent that, on raising the temperature, recrystallization of the structure occurs. The subsequent step of raising the temperature allows partial melting of the alloy. This melting will start normally

in the lowest melting point regions which were the last to solidify in the original casting and comprise regions at the grain boundaries and between dendrite arms where microsegregation has occurred. In most cases high angle grain boundaries introduced by the recrystallization process will also melt causing each grain to separate as a discrete solid particle within the matrix liquid. Even where the boundaries are not completely wetted by the liquid phase (i.e. melted), a groove will be established down the grain boundary at the liquid/solid interface such that the surface tension forces are locally balanced. With fine enough microstructures these grooves may be deep enough to cause fragmentation of the solid into small discrete particles surrounded by matrix liquid. The recrystallization and melting steps can occur successively in the same heating operation or may be separate stages of production. In either case the discrete particles produced on partial melting will rapidly spheroidize under surface tension forces to produce a dispersion of near round solid particles within the melt. Such a semi-solid/semi-liquid slurry behaves as a thixotropic material and may be formed, cast or forged to any required shape. If desired the material may be cooled and then reheated to a temperature between its solidus and liquidus temperatures to regain its thixotropic properties. An advantage of a material which exhibits thixotropic properties between its solidus and liquidus temperatures is that it can be formed, for example cast or forged, under reduced loads [30].

Up to date, most of the studies on the thixoforming of wrought aluminum alloys have been done by SIMA process. This process is based on the scientific understanding that high angle grain boundaries induced by plastic deformation and recrystallization will be wetted by liquid metal at the semi-solid temperature, resulting in a fine and globular structure. A modification of the SIMA process was made by Kirkwood and co-workers by changing the cold working to warm working at a temperature below the recrystallization temperature to ensure the maximum strain hardening. The process sequence is shown in the schematic diagram in Figure 2.6. Further research work on the SIMA process for other alloys has allowed increased understanding of the effects of processing parameters (such as amount of plastic deformation, reheating temperature, and time duration) on the resulting microstructure in the semi-solid state. With appropriate choice of processing conditions, the resulting solid phase particles are usually fine in size, globular in morphology, and uniform in distribution.

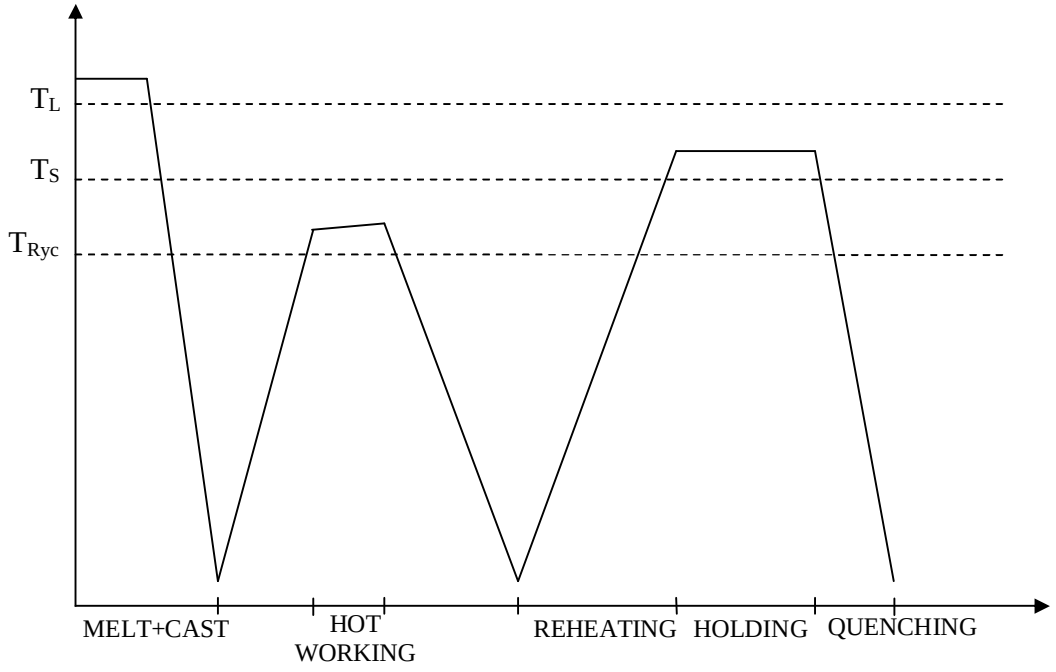

Figure 2.6. Schematic process sequence for the modified SIMA method

Partial melting can produce thixotropic structure simply by heating dendritic structures to $T > T_{solidus}$; however, holding at high temperatures can promote undesirable grain/globules growth. As far as rheocast slurries are concerned, spherical solid particles with small size are required for appropriate rheological properties, and so the stimulation of nucleation associated with restriction of growth could lead to the desirable structure [31]. While spheroidization has a positive effect on flow behaviour, further particle growth and coalescence may impair it by building up a three dimensional skeleton [27].

2.2.3. Cooling Slope Casting

A major factor contributing to the higher costs of the thixoforming process is the high premium associated with the costs of producing the specialized ingots required for thixoforming, i.e. ones that possess spheroidal microstructures. Typically ingots for thixoforming are continuously cast using some form of electric stirring (magnetohydrodynamic (MHD) stirring route), and then they are cut to a suitable size and reheated to the semisolid state for thixoforming. If one could eliminate the casting and cutting process steps, one would remove a major element of the costs in the thixoformed

products. The equipment and running costs associated with the cooling slope are very low [32].

The essence of the cooling slope is a very simple water-cooled plate as shown in Figure 2.7. In this process, molten metal with a suitable superheat is cast into the mould after flowing along the slope plate made from mild steel. The surface of the cooling slope is frequently coated with boron nitride, in order to prevent sticking of solidified metal. Solid nuclei are formed because of contacting between the melt and slope plate which causes rapid heat transferring. These nuclei are detached from the surface as a result of applying shear stress and melt flow. Finally they are distributed into the melt [33].

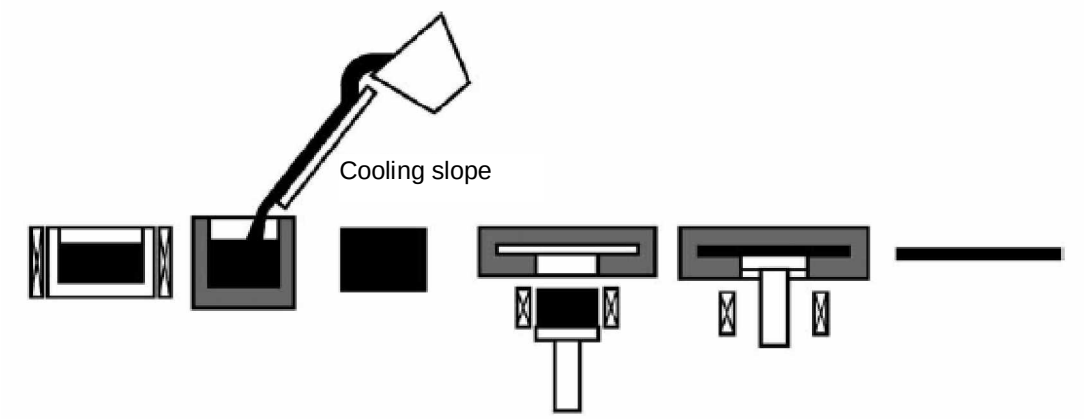

Figure 2.7. Schematic illustration of the thixoforming process using a cooling slope [32]

Cooling slope provides globular or spheroidal microstructure when cast alloy is heated to the semi-solid temperature. The first main influence on the evolution of a globular microstructure is the forced nucleation, by pouring the melt over the cooling channel. The temperature of the melt has to fall quickly into the semi-solid area. The second main influence is the decelerated cooling of the semi-solid billet to the processing temperature [34]. In cooling slope casting method different parameters such as superheat, length of slope plate, mould material, slope and inclined plate's material can affect the final microstructure.

A drawback of this process may be the formation of casting defects, such as pores and oxide. This would cause the mechanical properties of thixoformed cooling slope

products to be lower, e.g. than those of thixoformed SIMA products [35].

2.2.4. Liquidus Casting

Foundry men and ingot casters have long understood that equiaxed grains are favored over columnar grains by low pouring temperature (low “superheat”). As pouring temperature is lowered further, the equiaxed grains become finer [11]. Liquidus casting, also known as low superheat casting, has been developed recently as an alternative technique for production of thixotropic feedstock. In liquidus casting, melt with a uniform temperature just above its liquidus is poured into a mould for solidification. The resulting microstructures are usually fine and non-dendritic. Upon reheating, the liquidus cast microstructure spheroidizes rapidly to produce microstructural features suitable for thixoforming operations. So far, this technique has been tested on both cast and wrought aluminum alloys [2]. Figure 2.8 shows the process using the low superheat casting. Low superheat casting is simpler than the cooling slope casting process.

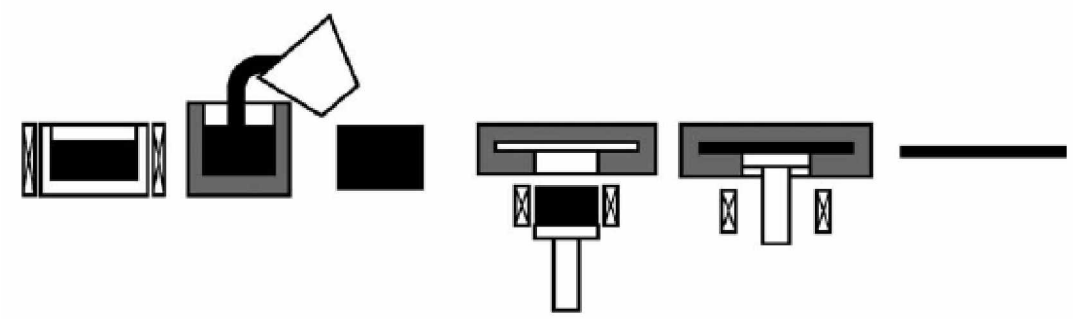

Figure 2.8. Schematic illustration of the thixoforming process using low superheat casting [32]

Liquidus casting, with liquidus rheocasting in particular, is gaining more attention as a simple and cost effective technique for feedstock production and seems to have a promising future. In this ingot production process, the only 'special equipment' needed is the die, resulting in very low equipment and running costs [32]. However, the major obstacles for industrial application may arise from difficulties related to accuracy and uniformity of temperature control, and consistency and uniformity of resulting microstructure in large scale production. It seems much effort is still required to establish

the exact mechanism for the formation of the fine and non-dendritic structure during liquidus casting [2].

In recent years, a novel semi-solid process has been developed. The process is termed the Continuous Rheoconversion Process (CRP), and is a passive liquid mixing technique that utilizes the principle of liquidus casting. The CRP is a simple process in which two melts (either of the same alloy or two different alloys), held at a particular level of superheat, are passively mixed within a reactor. The reactor provides heat extraction and forced convection during the initial stage of solidification, leading to the formation of thixotropic structures. Figure 2.9 illustrates the concept of the CRP process. The advantages of the CRP include process simplicity, flexibility, tight control over thixotropic structure evolution, fast adjustment of solid fraction, and incorporation of scrap metal for recycling. The term "flexibility" refers to the ability of the process to be viable for both thixocasting and rheocasting applications. Important parameters include the superheat and chemical composition of the melts, the heat extracting rate of the reactor, and the temperature of the receiving reservoir [36].

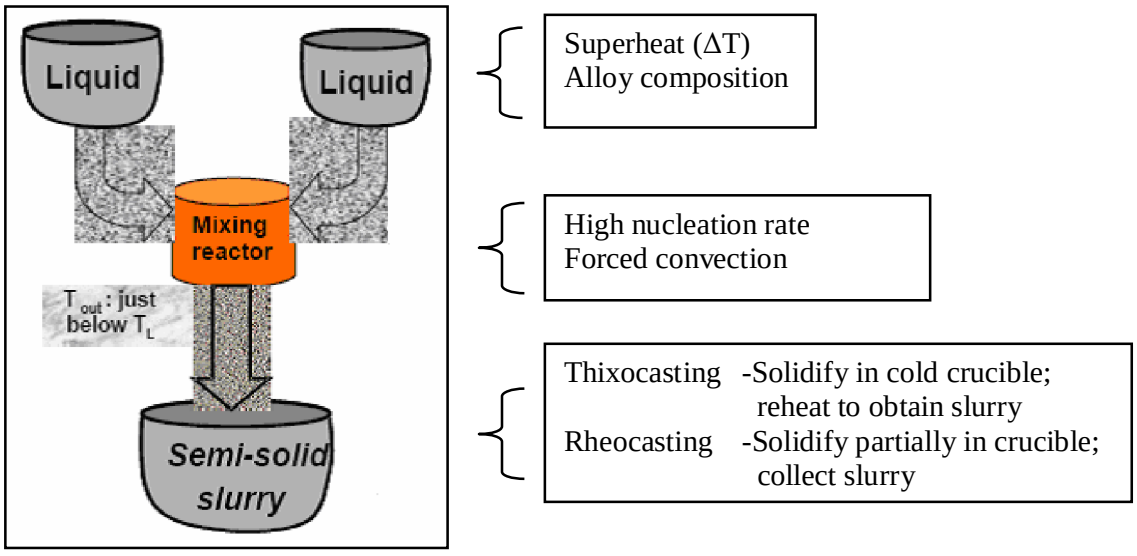

Figure 2.9. Conceptual schematic of the new Continuous Rheoconversion Process [36]

2.2.5. Spray Casting

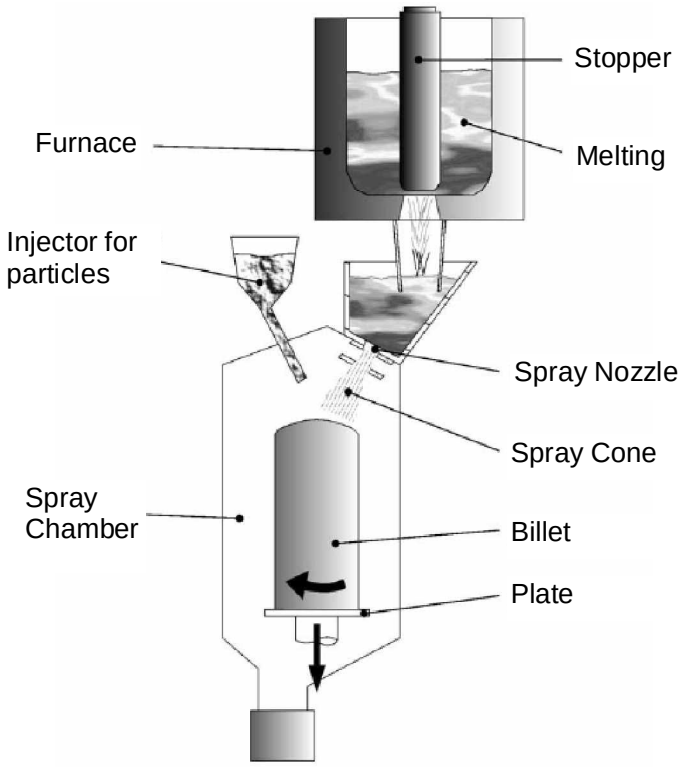

Figure 2.10. Spray forming process [37]

Spray casting (Osprey process) is another non-agitation process for feedstock production. Figure 2.10 describes a usual spray forming lay-out and process. In this process, molten metal is directed through a nozzle to meet the high pressure inert gas (nitrogen or argon). The liquid metal stream is atomized by the high pressure gas into micrometre sized droplets that experience high cooling rate during their flight, the cooling rate being in the order of $10^3 Ks^{-1}$. While the large droplets remain fully liquid and the small droplets solidify during atomization, those of intermediate sizes become semi-solid. The droplets are collected on a moving substrate and consolidated to form a coherent preform. A second stage of solidification takes place on the substrate at the beginning of the deposition, and subsequently on the upper surface of the preform. Liquid and semi-solid droplets with high liquid fraction splat upon impact, while solid and semi-solid droplets with high solid fraction fragment. A portion of the solid grains undergoes remelting and resolidifies slowly. Typical local solidification time on the preform surface is of the order of 100 s indicating that more than 90 per cent of the solidification time of a

spray cast preform occurs in the deposit at high solid fraction. The resulting microstructure comprises very fine equiaxed grains. The spray casting process has been investigated extensively over the past two decades and several models have been proposed to describe the process in detail [2].

Various alloys produced by spray casting have been evaluated experimentally as feedstock materials for semi-solid processing. It is generally believed that spray cast materials are suitable as feedstock for thixoforming, especially for high temperature alloys, such as steels and superalloys [2]. Spray casting is a relatively expensive route but one which can be used to produce alloys, which cannot be produced in any other way, such as aluminum-silicon alloys with greater than 20 per cent silicon e.g. [9].

2.2.6. Grain Refinement

Equiaxed grains typically also range in size from less than 0.1 mm to over 1 cm. Effective grain refiners (heterogeneous nucleating agents) are available for most nonferrous alloys. Through use of these, it is possible, in practice (especially with aluminum and magnesium alloys), to obtain grain sizes consistently under about 0.1 mm [11].

Chemical grain refinement is nowadays a common practice in continuous casting of aluminum alloys. This technique has also been considered for feedstock production. In most cases, a pre-alloyed wire is proportioned into the hot metal flow into the launder where it releases heterogeneous nucleation agents, usually titanium and boron based. Owing to the enhanced heterogeneous nucleation rate and suppression of dendritic growth, a fine and equiaxed structure can be achieved. With an appropriate grain refining procedure, such a structure can also be suitable for subsequent reheating and thixoforming. However, chemical grain refining is not used alone, but used in conjunction with other feedstock production methods, such as MHD stirring and liquidus casting. One disadvantage of the chemical grain refinement method is that nucleation agents are only effective to specific alloy systems; another is that in some cases these additives will remain present in the product as non-metallic inclusions, which may impair both the

proccessibility of the semifinished stock and the mechanical properties of the final product [2].

Compared to MHD techniques, the grain refinement approach is more flexible and is relatively cost-effective. Therefore, grain refined aluminum alloys are being employed for semi-solid processing by many die casters. However, there are some drawbacks inherent to the current Al- Ti/Al-Ti-B grain refined materials such as lack of grain size uniformity, the fading of nucleating agents, and the agglomeration and settling of insoluble nucleating particles in the melt. These can negatively affect the quality and productivity of the thixoforming process. In the recent past, a permanent grain refining technology has emerged. This new technology is termed SiBloy®. Unlike traditional grain refining techniques, the grain refining effect of SiBloy® is achieved by adding Si-B master alloy into the melt. During cooling, fresh AlB_2 particles (instead of insoluble TiB_2, $TiAl_3$ etc.) precipitate out from the melt just above the liquidus temperature, which, in turn, serve as potent nucleating agents, and thus grain refining the melt. In this technique, the grain refining effect was found to be: 1) independent of holding time (no fading); 2) unaffected by remelting treatments (permanent effect), 3) almost independent of cooling rate in the range between 0.5 and 15°C/s, and 4) effective for Al-Si alloys with Si content between 5 and 11 per cent [38].

Grain refined alloys can give equiaxed microstructures but it is difficult to ensure the grain structure is uniformly spheroidal and fine and the volume of liquid entrapped in spheroids tends to be relatively high [9].

3. REHEATING PROCESS FOR THIXOFORMING

Reheating to the semi-solid state is a particularly important phase in the thixoforming process. It aims to provide semi-solid slug with an accurately controlled solid fraction of fine and spherical particles uniformly dispersed in a liquid matrix of low melting point. To achieve this semi-solid microstructure, the important processing parameters during the reheating process include accuracy and uniformity of heating temperature and heating duration. It is the heating temperature that determines the solid fraction in the slug. Too high a heating temperature causes instability of the slug resulting in difficulties for slug handling, while too low a heating temperature leads to unmelted, coalesced, polyhedral silicon phase in the slug in the case of hypoeutectic cast aluminum alloys having a detrimental effect on the rheological properties during die filling and on the ductility of the finished parts. In addition, as discussed previously, the composition of the alloys currently used are not optimised for semi-solid metal processing, a small variation in temperature can cause a large difference in solid fraction. Therefore, temperature accuracy affects the stability of the forming process and the consistency of the product quality. Furthermore, a uniform temperature distribution throughout the slug is important, because a non-uniform distribution of temperature may lead to fluctuation in solid fraction and rheological characteristics, which in turn may cause solid/liquid separation during mould filling. Generally speaking, the maximum temperature difference in the billet should be less than 6 °C. Finally, the heating duration has to be optimized; too long a heating time will cause structural coarsening, while too short a heating time will lead to incomplete spheroidization of the solid particles compromising the rheological properties and leading to difficulties during mould filling [2].

Billet heating by direct resistance heating is not feasible, as the part of the material under and beyond the electrodes is not heated, and would be scrapped in a forging application. A further limitation on the application of direct resistance heating is the contact pressure required between the electrode and the work piece. This can be considerable, and can damage some more fragile materials.

Currently, reheating is achieved mainly by induction heating, although a convection furnace is also used in some cases. Because conventional electric furnace heating involves too long a heating time, and cannot be controlled to obtain a uniform temperature distribution, the induction heating method is usually used in the reheating process [39].

Induction heating has the advantage of precise and fast heating, which is necessary for semi-solid metal processing. During induction heating, the relationship between time and temperature must be controlled exactly to obtain a uniform temperature distribution over the entire cross sectional area [40]. Another feature of induction heating is its repeatability. For a given material, the power input repeats accurately over the heating cycle. This allows time to be used as the measure of temperature, since the material, heated for a measured time, can be assumed to be at the given temperature with high accuracy. This is useful where there is a constant production rate, using automatic feeding and ejection. Because the initial billet temperature of the forming process is the key parameter to filling results in the semi-solid forming process, an accurately controllable induction heating method must be selected for the reheating process. In the case of the reheating of aluminum alloys in the thixoforming process, multi-heating steps and woven glass-coated coils with various numbers of turns are usually used for the through-heating of the billet [12].

It is clear from the above discussion that reheating is a complex process. Heating up the metal slug to the semi-solid temperature range is a crucial part of the process. The slug has to be uniformly heated to the required working temperature as quickly as possible [3]. In order to provide a successful design for modern induction heating systems, it is necessary to have a full understanding of the features of the process. Optimization of the processing parameters is a critical step to ensure a high quality of formed parts.

3.1. Basics of Induction Heating

Induction heating (Figure 3.1) is a non-contact heating method; one in which an electrically conductive material (typically a metal) is heated by an alternating magnetic field. Invisible lines of force are created by a work coil when a current flows through it, the result of which is an induced current in the conductive workpiece. Heating results due to

the Joule effect and, to a lesser degree, magnetic hysteresis (i.e., power loss other than by eddy currents in a magnetic material caused by reversals of the magnetic field). Joule's Law states that the rate at which heat energy is produced in any part of an electric circuit is measured by the product of the square of the current (I) times the resistance (R) of that part of the circuit.

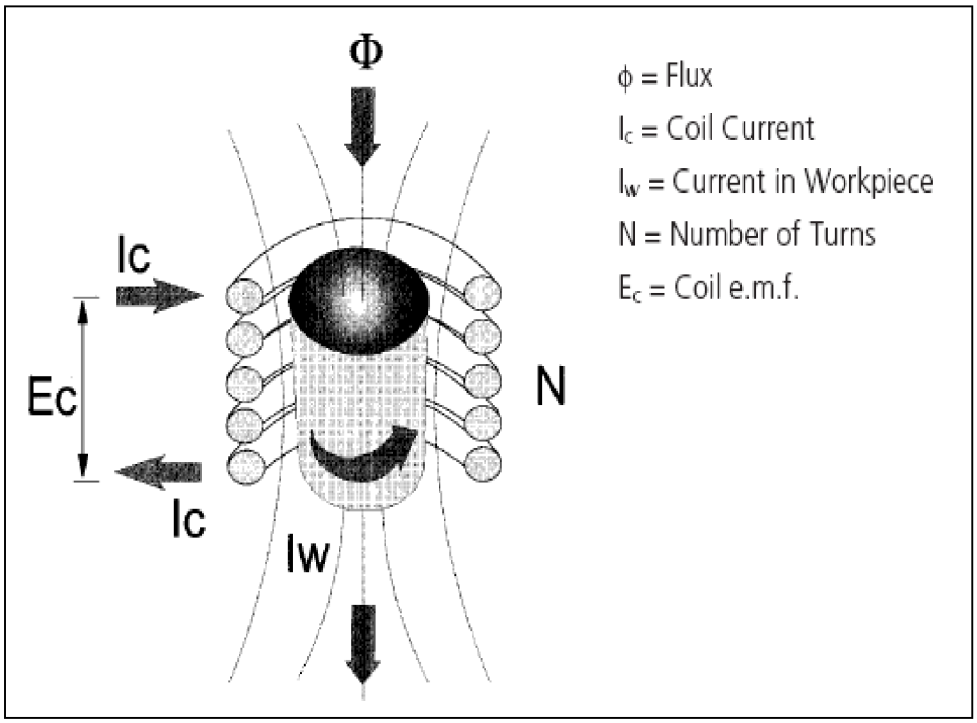

Figure 3.1. Induction heating of a cylindrical workpiece [41]

The principle of induction heating is a consequence of the Faraday Effect, named for the physicist Michael Faraday who was the first to produce an electric current from a moving magnetic field. The basic principle of induction heating, which is an applied form of Faraday's discovery, is the fact that AC current flowing through a circuit affects the magnetic movement of a secondary circuit located near it [42]. The alternating magnetic field induces a current flow in the conductive workpiece. The arrangement of the work coil and the workpiece can be thought of as an electrical transformer. The work coil is like the primary where electrical energy is fed in, and the workpiece is like a single turn secondary that is short-circuited. This causes tremendous currents to flow through the workpiece [43]. Induction heating is based on the principle of resistance to these induced currents. These

currents, called eddy currents, are similar in magnitude and opposite in direction to the current produced by the induction coil (also known as the inductor).

A number of other independent variables, including the workpiece's magnetic permeability (a measure of how magnetic the material is), the air gap (coupling distance between the inductor coil and workpiece) and the frequency influence the induction process and its efficiency.

Depending on application and workpiece geometry, the shape of an induction coil can be noticeably different. In some cases, induction coils are simple single-turn or multi-turn geometries, where the workpiece is placed inside of the coil. In other cases, induction coil geometries are more complex, such as butterfly-shape, split-return, pancake, etc. Although any current carrying conductor can serve as an induction coil, coils usually are made of copper, which has good electrical conductivity, economy and availability.

In induction heating, heat is generated within the work itself; it does not rely on transmission heat energy by radiation or convective as in a furnace or oven. Therefore, hardening to a specified depth below the surface is possible without excessively long process times or excessively high surface temperatures. In addition, the heating can be applied to a specified area. Induction processes are accurate, consistent and repeatable. Because heating occurs in the part itself, induction heating is considered a very high (energy) efficiency process (and more efficient than the majority of alternative methods).

An induction heating system comprises a basic induction power source, which provides the required power output at the required power frequency, complete with matching components, an induction coil assembly, a method of material handling and some method of water cooling and quenching. Most induction heating systems are water cooled with the exception of small, low-power units. The methods of material handling and the induction coil arrangement depend entirely on the application. The choice of induction power source is related to the application requirements and to production rate [44].

3.2. Key Factors to Consider for Induction Heating

3.2.1. Operating Frequency

There is a relationship between the frequency of the alternating current and the depth to which it penetrates in the workpiece; low frequencies of 5 to 30 kHz are effective for thicker materials requiring deep heat penetration, while higher frequencies of 100 to 400 kHz are effective for smaller parts or shallow penetration as shown in Figure 3.2 [45].

The choice of frequency is defined not only by the required temperature profile in the slug, but also by the requirement for providing high electrical efficiency in the induction system and minimum electromagnetic forces. During induction heating, aluminum slugs experience electromagnetic forces which are directed out of the coil. Under normal process conditions, slugs consist of a significant amount of liquid fraction. Essential electro magnetic forces may result in uncontrollable removal of liquid metal from inductor. Therefore, special attention should be paid to their minimization [46].

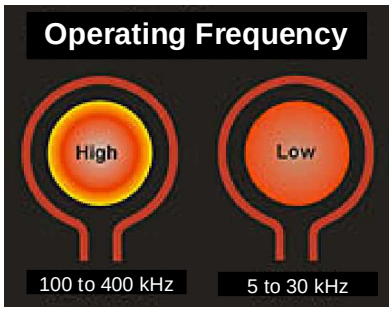

Figure 3.2. Relationship between operating frequency and penetration depth in induction heating [45]

3.2.2. Material Characteristics

The material being heated by induction furnace need not to be a magnetic material to heat efficiently. All that is required is that it has reasonably good electrical conductivity. Most ferrous and non-ferrous metals can be heated inductively. The eddy currents induced in the workpiece or charge are primarily responsible for the heating.

For ferrous metals like iron and some types of steel, there is an additional heating mechanism that takes place at the same time as the eddy currents. The intense alternating magnetic field inside the work coil repeatedly magnetizes and de-magnetizes the iron crystals. This rapid flipping of the magnetic domains causes considerable friction and heating inside the material. Heating due to this mechanism is known as Hysteresis loss, and is greatest for materials that have a large area inside their B-H curve. This can be a large contributing factor to the heat generated during induction heating, but only takes place inside ferrous materials. For this reason ferrous materials lend themselves more easily to heating by induction than non-ferrous materials.

It is interesting to note that steel looses its magnetic character when heated above approximately 700°C. This temperature is known as the Curie temperature. This means that above 700°C there can be no heating of the material due to hysteresis losses. Any further heating of the material must be due to induced eddy currents alone. This makes heating steel above 700°C more of a challenge for the induction heating systems. The fact that copper and aluminum are both non-magnetic and very good electrical conductors can also make these materials a challenge to heat efficiently [43].

3.2.3. Depth of Penetration

During the heating stage of thixoforming process, the whole part has to be heated homogeneously up to the temperature needed for the process. Induced eddy currents are not uniformly distributed within the slug. The maximum value of the current density is located on the surface. Current density then decreases from the surface of the slug towards its center. This phenomenon of non-uniform current distribution within the slug cross-section is called the skin effect. Because of the skin effect, most of the power will be concentrated in a slug surface layer. This layer is called the skin (or current penetration) depth and is a function of frequency and electrical resistivity. During the heating cycle of an aluminum slug, the resistivity of the aluminum will increase more than three times. This results in growth of the penetration depth during the heating cycle [46]. The skin depth decreases when resistivity decreases, permeability increases or frequency increases. Skin depth can be calculated by the equation below:

$$\delta = \frac{1}{\sqrt{\pi \mu f \sigma}} \tag{3.1}$$

where δ is the skin depth, f is the frequency, μ is the absolute permeability, and σ is conductivity.

Non-uniformity of the heating profile at the coil and slug ends is related to the distortion of the electromagnetic field in those areas. This distortion is called the electromagnetic end effect. Generally speaking, end effect is considered one of the most complicated problems in induction heating. This effect can result in either overheating or underheating of the slug ends. The required temperature distribution along the end of the slug depends on the frequency, the coil and slug geometry (including the slug-to-coil air gap and coil overhang), the material properties of the slug, the refractory, power density and cycle time [46].

3.2.4. Coupling Distance

Coupling refers to the proportional relationship between the amount of current flow in the workpiece and the distance between the workpiece and the coil. Close coupling generally increases the flow of current and therefore increases the amount of heat produced in the workpiece [45].

Preferred coupling distance depends on the type of heating and the type of material (ferrous or nonferrous). In static surface heating, in which the part can be rotated but is not moved through the coil, a coupling distance of 1.5 mm from part to coil is recommended. For progressive heating or scanning, a coupling distance of 1.9 mm is usually necessary to allow for variations in workpiece straightness. For through heating of magnetic materials, multi-turn inductors and slow power transfer are utilized. Coupling distances can be looser in these cases - on the order of 6.4 to 9.5 mm. It is important to remember, however, that process conditions and handling dictate coupling. If parts are not straight, coupling must decrease. At high frequencies, coil currents are lower and coupling must be increased. With low and medium frequencies, coil currents are considerably higher and decreased

coupling can provide mechanical handling advantages [47].

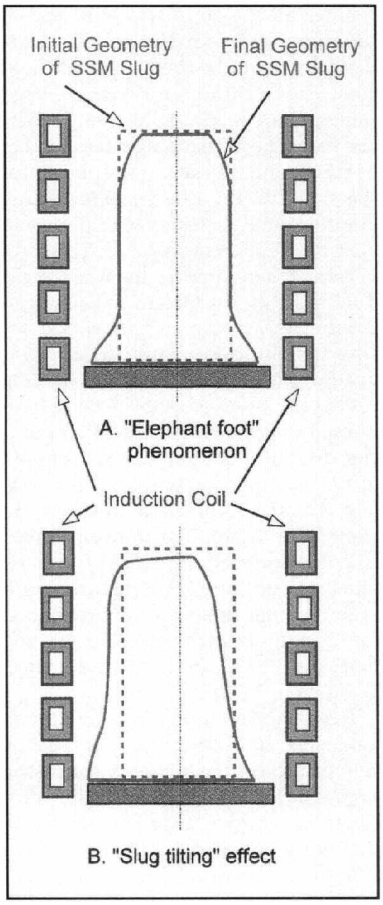

Figure 3.3. “Elephant foot” phenomenon (a) and “slug tilting” (b) effect [46]

There are two phenomena affecting the coupling distance in reheating process for thixoforming. In a vertical type coil arrangement, the existence of the "elephant foot" phenomenon is an indication that the slug has obtained a semi-solid condition. As a result of that phenomenon, the coil-to-slug air gap will not be the same along the coil height (Figure 3.3 (a)). The variation of the air gap changes the electromagnetic coupling between the coil and different areas of the slug. Thus, the power density distribution along the slug height will vary as compared to a perfect cylindrical body. In addition to the "elephant foot" phenomenon, a "slug tilting" effect and "surface erosion" at the top of a slug makes the situation even more complex (Figure 3.3 (b)). Due to tilting, certain areas of the slug will have better coupling with the inductor than areas located on the opposite side of the slug. The areas with better coupling will receive more intensive heating which will result in

more intense tilting. Due to "surface erosion" at the top of a slug and the "elephant foot" phenomenon at the bottom, the length of the eddy current paths at slug's top, bottom and central areas will be different. This will result in distinct resistances to eddy current flow in different surface areas of the slug and, therefore, in different Joule losses. In other words, from electromagnetic point of view, slug will be seen by the magnetic field as a number of disks made from metals with different electrical conductivity [46].

3.2.5. Coil Design

The inductor, or heating coil, is similar to a transformer primary, and the workpiece is equivalent to the transformer secondary. Therefore, several of the characteristics of transformers are useful in the development of guidelines for coil design.

One of the most important features of transformers is the fact that the efficiency of coupling between the windings is inversely proportional to the square of the distance between them. In addition, the current in the primary of the transformer, multiplied by the number of primary turns, is equal to the current in the secondary, multiplied by the number of secondary turns. Because of these relationships, there are several conditions that should be kept in mind when designing any coil for induction heating:

1) The coil should be coupled to the part as closely as feasible for maximum energy transfer. It is desirable that the largest possible number of magnetic flux lines intersect the workpiece at the area to be heated. The denser the flux at this point, the higher will be the current generated in the part.

2) The greatest number of flux lines in a solenoid coil is toward the center of the coil. The flux lines are concentrated inside the coil, providing the maximum heating rate there.

3) Because the flux is most concentrated close to the coil turns themselves and decreases farther from them, the geometric center of the coil is a weak flux path. Thus, if a part were to be placed off center in a coil, the area closer to the coil turns would intersect a greater number of flux lines and would therefore be heated at a higher rate, whereas the area of the part with less coupling would be heated at a lower rate; the resulting pattern is

shown schematically in Figure 3.4. This effect is more pronounced in high-frequency induction heating.

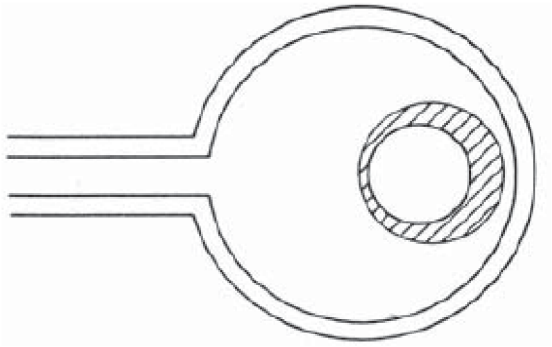

Figure 3.4. Induction heating pattern produced in a round bar placed off center in a round induction coil [47]

4) At the point where the leads and coil join, the magnetic field is weaker; therefore, the magnetic center of the inductor is not necessarily the geometric center. This effect is most apparent in single-turn coils. As the number of coil turns increases and the flux from each turn is added to that from the previous turns, this condition becomes less important. Due to the impracticability of always centering the part in the work coil, the part should be offset slightly toward this area. In addition, the part should be rotated, if practical, to provide uniform exposure.

Because of the above principles, some coils can transfer power more readily to a load because of their ability to concentrate magnetic flux in the area to be heated. In general, helical coils used to heat round workpieces have the highest values of coil efficiency. Coil efficiency is that part of the energy delivered to the coil that is transferred to the workpiece. This should not be confused with overall system efficiency. Besides coil efficiency, heating pattern, part motion relative to the coil, and production rate are also important. Because the heating pattern reflects the coil geometry, inductor shape is probably the most important of these factors [47].

With good coil design, the proper heat pattern is achieved and the efficiency of the induction heating power supply is maximized without making it difficult to insert and retrieve the workpiece [45].

3.2.6. Power Supply

The power supply produces a magnetic field around the workpiece by sending an alternating current through the induction coil. The power supply's output determines the relative speed at which the workpiece can be heated. For example, a typical heating process accomplished with a 3 kW power supply could be completed more quickly with a 5 kW power supply. However, additional power capability may increase the power supply's, size and weight and utility requirements; larger power supplies typically require 3-phase electrical connections and facilities for water cooling [45].

During heating of billets, a uniform power distribution along the end of the slug will not necessarily correspond to uniform temperature profile. This is due to additional heat losses (radiation and convection losses) at the slug end area compared to its central part. By properly choosing the design parameters, it is possible to obtain a situation where the additional heat losses at the left end of the slug are compensated for by the additional power (power surplus) due to the electromagnetic end effect. This allows one to obtain a reasonably uniform temperature distribution along the length or height of the slug.

3.3. Evolution Mechanisms during Reheating Step in Thixoforming Process

Slug reheating is a critical stage in the thixoforming process. Its purpose is not only to obtain the desirable nominal liquid fraction, but also to ensure transformation of the solid phase to a spheroidal morphology with fine particle size. The driving force for such morphological evolution in the semi-solid state is the reduction of the interfacial energy between the solid and liquid phases. Microstructural evolution during reheating is therefore a diffusion controlled process. On the one hand, the holding time should be long enough to complete the morphological transition from dendritic (or rosette) to spherical, but, on the other hand, the holding time should be short enough to prevent excessive grain growth, which is detrimental to the mechanical properties of thixoformed parts. Consequently, the reheating process needs to be optimized to achieve the most desirable slurry characteristics for thixoforming. Understanding the structural evolution mechanisms would be a critical step towards such optimization [2].

Several mechanisms are discussed during reheating step before semi-solid forming. One is melting mechanism: melting of the arm at its root as a result of normal ripening. The melted arm is considered whose curvature radius of root is slightly smaller than that of remainder, so the arm tends to melt from the necked region firstly. Particularly in SIMA process, the melting at the root is accelerated by the strain induced at the dendrite root as a result of the predeformation. During the heat treatment at semi-solid temperature, the melted fragmentation of arm evolves into spheroidal (or in some case, ellipsoidal) grain, usually having no entrapped liquid. The size of the individual grain after evolution depends on that of the initial arm fragmentation.

The second is a combining mechanism: if the spacing of two dendrite arms is short, the two arms will touch each other and combine into a large structure with some liquid phase entrapped in it during the following heat treatment. With heating continuously to semi-solid temperature and holding predetermined time, it also evolves toward spheroidal morphology, but is very large and has some liquid islands in it.

The third is recrystallization mechanism which is a specific of SIMA process: recrystallization is produced as a result of the strain induced by the predeformation. During holding above eutectic temperature, the liquid penetrates along the new recrystallization grain boundaries. As the temperature is further increased, the recrystallization grain boundaries remelt, which results in the separation of recrystallization and then the recrystallization structure removes from the primary dendrite. After semi-solid heat treatment, recrystallization evolves into the spheroidal and small particles. There is no liquid island in the spheroidal structure after evolution, since the liquid phase entrapping does not occur during this process.

The former two mechanisms are present in both non-deformed and deformed alloy. While the recrystallization mechanism is only present in predeformed alloy, it will be predominant gradually with the increasing of the compression ratio for more recrystallization occurs in more heavily deformed alloys. So more grains are obtained based on this evolution mechanism during semi-solid heat treatment, which can explain why the smaller, more globular grains are attained in more heavily deformed alloys. In order to make these three mechanisms clear, the whole microstructural evolution of the

alloys during heat treatment after deformation is characterized in Figure 3.5. After deformation, the initial dendritic fragment is produced first (Figure 3.5 (a)) and then recrystallization is attained during the following heat treatment within the recrystallization temperature range (Figure 3.5 (b)). Subsequently, the dendritic fragment begins to melt, touch, and the liquid phase penetrates along the recrystallization grain boundaries above eutectic temperature (Figure 3.5 (c)). After heating continuously, the recrystallized and the melted fragments are removed from the primary dendrite, and the combined dendrites evolve into a microstructure and entrap some liquid phase in it. After isothermal heat treatment at semi-solid temperature, the spheroidal microstructure is attained (Figure 3.5 (e)) [29].

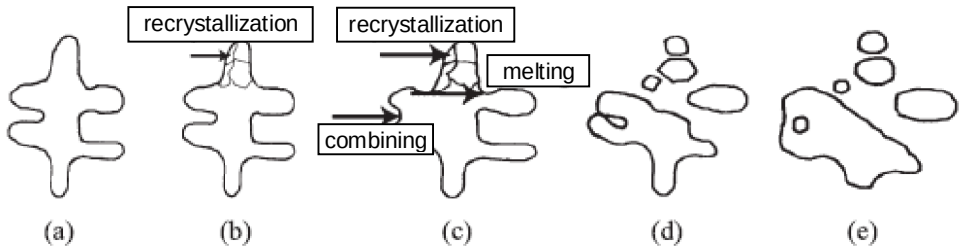

Figure 3.5. Schematic illustration of evolution of structure during heat treatment after deformation: (a) initial dendritic, (b) recrystallization, (c) melting, touching and liquid penetration, (d) combining and removing, and (e) spheroid [29]

4. FORMING OPERATION

Thixoforming is a forming technology, where a semi-solid slug is formed to a near-net-shape part. Depending on whether forming takes place in a die casting machine or a forging press, one talks of thixocasting or thixoforging. These methods are shown schematically in Figure 4.1.

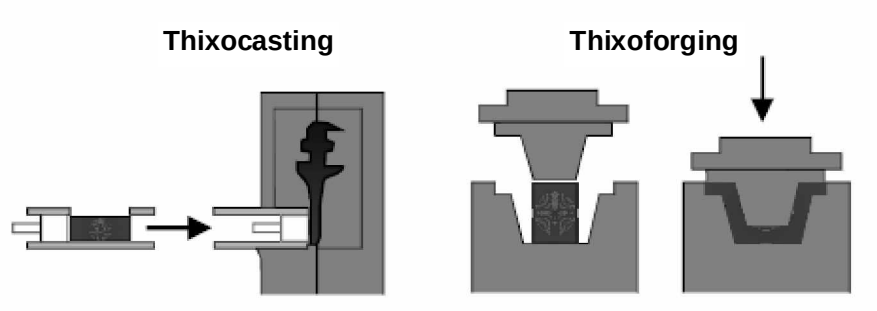

Figure 4.1. Thixoforming variants [8]

Thixocasting usually means that the alloy is solid initially and has been treated in such a way that when it is heated into the semi-solid state it will have a non-dendritic microstructure. It is reheated into the semi-solid state and 'casting' is implying that the liquid content prior to forming is relatively high i.e. above about 50 per cent [9].

Thixoforging describes the process where suitable material is heated into the semi-solid state and placed between dies halves. The parts of the die are then brought together by a ram. The direct insertion of the slurry into the die reduces material use because of the lack of runners, gate and press discard [9]. All initial material is formed to the finished part and so, due to drip of losses, the height of the component is varying. After form filling the forming pressure operates on the whole component. Until this day several parts have been produced with cast and wrought aluminum alloys. The forming experiments show that parts using aluminum cast and wrought alloys can be formed in just one step. Figure 4.2 shows the parts of which nearly 100% of the initial material can be obtained. The figure demonstrates the variety of thixoforged parts. It is possible to produce different parts with variable wall thickness, sharp edged thickness changes, sharp radii and undercuts [48].

Figure 4.2. Thixoforged parts of aluminum alloys [48]

One of the unique metallurgical features of the semi-solid metal processing is the microstructure developed within the formed part. As an example, Figure 4.3 illustrates the structures of a cast MHD billet, a reheated and quenched billet, and a solidified thixoformed part showing the divorced eutectic (the dark regions) structure with rounded primary aluminum particles and rosettes of entrapped eutectic. If laminar flow conditions are maintained during die fill, then the microstructural similarity evident in Figures 4.3 (b) and (c) occurs throughout the part. This unique forming property is due to the rheological behavior of the semi-solid formed from the reheated MHD billet [17].

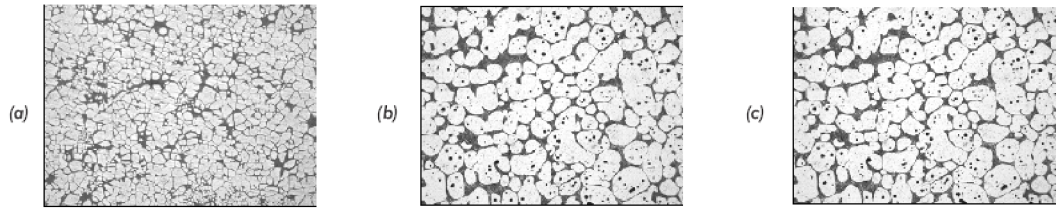

Figure 4.3. (a) As cast MHD billet structure; (b) reheated MHD billet structure; (c) thixoformed part structure [17]

4.1. Press Requirements for Thixoforging Process

The forming of metals in semi-solid state places great demands on the forming unit. Because of the shear-rate dependent viscosity of the metal, the thixoforging technique requires extremely low punch forces at the beginning of the forging process. Only towards the end of the process is a higher punch force needed, because the material cools down to

temperatures which are closer to the solidus temperature and also because the surface of the workpiece gets larger. The punch force of the traditional forging process, however, increases during the whole punch stroke. After the cavity has been filled, the press works with a constant force over a certain period of time during which the workpiece has to solidify completely. The given punch force has to produce pressure within the workpiece in order to avoid inner porosities in the workpiece. These porosities could be caused by the shrinkage of the material while it changes from the semi-solid to the solid state and also while it cools down to room temperature.

Immediately upon inserting the heated raw part into the die, the punch stroke starts. The punch velocity should be as high as possible in order to close the dies as fast as possible. This is necessary because the differences in temperature of the material and the die cause a quick cooling of the workpiece. The stroke of the punch should be as short as possible because the cycle time should also be kept short. The minimum length of the stroke is conditioned by the fact that an insertion of the part and a removal of the workpiece after the stroke has ended have to be ensured.

The impact velocity of the upper die when it meets the heated part should be reduced significantly to avoid a bursting of the semi-liquid material. During the following forging process the chosen punch velocity depends on the alloy and on the geometry of the workpiece.

Attention has to be given to the fact that the workpieces cool down very quickly - depending on the relation between the part's surface and its volume. To avoid "freezing" of the material during the forging process, the punch velocity has to be optimized in such a way that the forging process is finished before the material solidifies. By increasing the temperature of the die, an extension of the time during which thixoforging is possible could be easily achieved, yet this would extend the cycle time because the forged part should solidify as quickly as possible within a very short period of time. In order to meet this demand, the temperatures of the material and the dies should differ greatly. Another reason for using relatively low temperatures is the thermal load to which the lubricants are subject.

Still another reason for thixoforging with optimized punch velocities is to fill the cavity with a laminar flow of the semi-solid material. If there are large variations in the cross sections of a workpiece the punch velocity will have to be adjusted during the filling process. When the material is solid, the workpiece has to be cooled down to a temperature level at which the workpiece can be removed from the die without any plastic deformation [49].

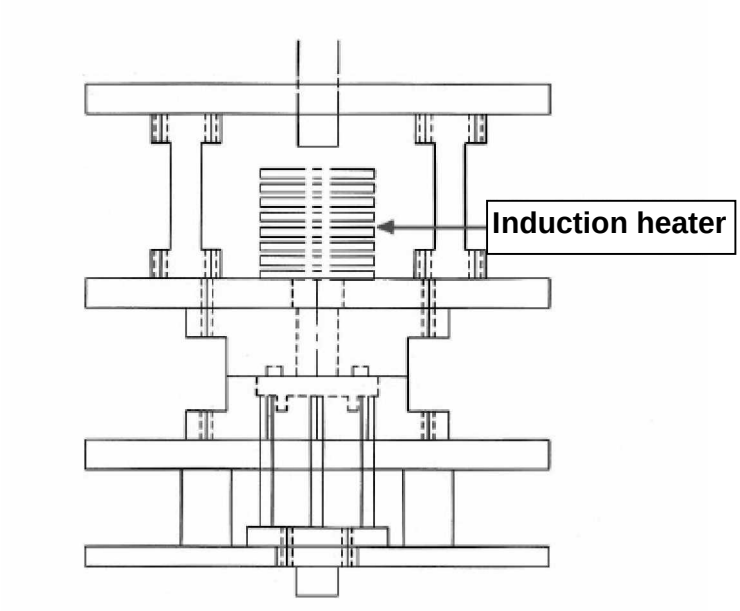

Figure 4.4. The couple induction heating die sets [12]

In order to retain the billet shape and to prevent heat loss, it is an important part of the forming process to transfer the reheated material to the die cavity. When the reheating system is apart from the die set, it is difficult to design the device controlling the heat loss due to the temperature loss during transferring the billet, and the heat loss causes bad filling results. To solve the filling limitation due to the heat loss and difficulties to billet handling, Kang et. al. [50] proposed a reheating system coupled with the die set, which has the induction coil located just above the die gate, as shown in Figure 4.4. This system reduces the over-heating of the billet considering heat-transfer and provides the necessary time for the soaking process. The most invaluable of this system is that it can enlarge the solidification range in the thixoforming process, because this system has no problems of billet heating. In this type of system, a uniformly shaped billet is needed in order for it to

be able to be inserted easily into the die cavity by the pressure of the punch [12].

4.2. Deformation Behaviour of Semi-Solid Metals

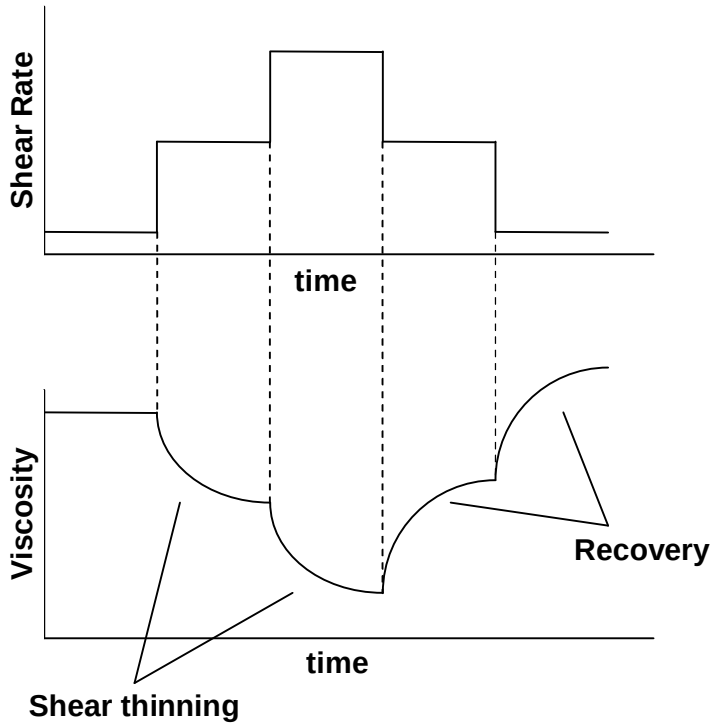

Figure 4.5. Schematic diagram to illustrate the thixotropic behaviour of semi-solid slurries [51]

The rheology of semi-solid metal slurries is attracting increasing attention from research scientists owing to the complexity of the flow response, and from production engineers since it must be controlled carefully for successful forming operations [2]. Semi-solid slurries exhibit time dependent, non-Newtonian, flow known as thixotropy, which is manifested by a fall in viscosity with time at constant shear rate after a step increase in shear rate, and, conversely, viscosity increasing with time following a step decrease in shear rate (Figure 4.5). A finite time is therefore required to establish a new steady-state viscosity following a change in shear rate. The flow behaviour of the slurry is also sensitively dependent on the fraction solid present, and therefore on the temperature. Semi-solid metal forming (or thixoforming) exploits this thixotropic behaviour since an undeformed partially melted slug may be stiff and handleable, whereupon after shearing on

entering the die its viscosity dramatically decreases allowing it to flow easily and to fill the die. A knowledge of the rheology of alloy slurries must therefore contribute to quantitative understanding of the thixoforming process [51].

Advantages of thixoforming process are due to the mechanism of deformation, which is different than in the conventional metal forming. Due to a localization of the liquid phase at grain boundaries, the plastic deformation involves sliding along the boundaries and rotations of grains. The contribution given by the grain deformation of grains to the overall deformation is negligible. This mechanism of deformation involves low yield stress while the workability of the alloy increases significantly [52]. Deformation mechanisms of thixotropic materials are given in more detail below.

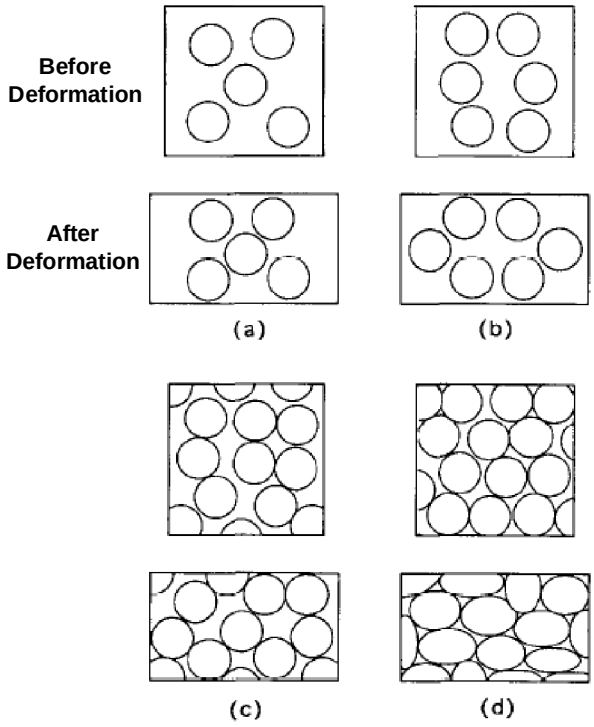

Figure 4.6. Four main deformation mechanisms controlling deformation of alloys in the semi-solid state: (a) liquid flow; (b) flow of liquid incorporating solid particles; (c) sliding between solid particles; and (d) plastic deformation of solid particles [53]

Four deformation mechanisms are proposed to be the main mechanisms controlling deformation of alloys in the semi-solid state, as shown in Figure 4.6. Two mechanisms are dominant when the solid particles are surrounded by the liquid phase, which are the liquid flow (LF) mechanism and the flow of liquid incorporating solid particles (FLS) mechanism. The other two mechanisms are dominant when the solid particles have contacted with each other, which are the sliding between solid particles (SS) mechanism, and the plastic deformation of solid particles (PDS) mechanism.

Figure 4.6 (a) shows schematically the LF deformation mechanism. The material shown by the shaded area is deformed from the top square shape into the bottom rectangular shape. The solid particles are surrounded by the liquid phase and the deformation is achieved mainly by liquid flow. During the deformation, the liquid flows laterally to accomplish the deformation of the material, while the solid particles move towards each other in the vertical direction solely to serve the purpose of accommodating the shape contraction in the vertical direction. However, the solid particles do not have lateral movement relative to each other at all, since the shape expansion in the lateral direction is achievable by solely the liquid flow. As a result, a solid/liquid segregation is produced by the LF mechanism, in which the solid particles segregate in the center portion, while the liquid segregates around the edge. The deformation force required by the LF mechanism is thus very small. Figure 4.6 (b) shows schematically the FLS deformation mechanism. The deformation is achieved by a cooperative movement of the solid particles and liquid phase. The solid particles move along with the liquid flow during the deformation not only in the vertical direction as in the LF mechanism, but in the lateral direction also. As a result, the deformation force required by the FLS mechanism is larger than that required by the LF mechanism, since the solid particles are involved in the lateral movement as well.

Figure 4.6 (c) shows schematically the SS deformation mechanism. The deformation is achieved by sliding among solid particles. The deformation force required is to overcome the friction generated from the sliding between solid particles, and also to overcome the restriction of the solid particle movement due to the spatial constraint imposed by the surrounding particles. Consequently, the deformation force required by the SS mechanism is larger than that required by the FLS mechanism. Figure 4.6 (d) shows

schematically the PDS deformation mechanism. The deformation is accomplished by plastic deformation of the solid particles. The deformation force is mainly to overcome the yield strength and subsequently, if any, strain hardening of the solid particles, which thus is the largest deformation force required among all the mechanisms. Admittedly, sliding between the solid particles is still required to accommodate the PDS mechanism; however, the sliding is not significant in the PDS mechanism, and is relatively small compared with that in the SS mechanism.

During semi-solid deformation, a large amount of segregation of the solid particles and liquid phase is observed, and the extent of the segregation is a function of time, which means that the variations of the macrostructures during the deformation are a function of time as well as position. To explain these phenomena in terms of the four deformation mechanisms proposed above, the effects of the deformation parameters, i.e. solid fraction and deformation rate (strain rate), on the dominance and shift of the deformation mechanisms are discussed below.

The effects of the solid fraction are equivalent to the deformation temperature effects, since the solid fraction is a function of the deformation temperature. As the solid fraction decreases, or the deformation temperature increases, the LF and FLS mechanisms are dominant since the deformation forces required by them are less than those required by the other two mechanisms. However, when the solid fraction increases, or the deformation temperature decreases, the SS and PDS mechanisms become dominant for the deformation to proceed. In the extreme, where nearly no liquid phase is present and there is no room for the solid particles to slide by each other, all the deformation can be accomplished by the PDS mechanism, and the deformation force required is the largest.

For the LF mechanism to be active, the liquid requires time to flow laterally outwards to accomplish the deformation. Consequently, the LF mechanism can only be activated at lower deformation rate. The amount of response time required by the other three mechanisms to be activated is the largest for the FLS mechanism, in which liquid flow is also involved, and is the smallest for the PDS mechanism, in which no significant movement of either solid particles or liquid phase is required. By considering the response time and the force required by the four mechanisms together, the LF mechanism is

dominant at the lowest deformation rate, since it is an active mechanism and requires the least deformation force. On the other hand, the PDS mechanism is dominant at the highest deformation rate, since it is the only active mechanism due to no response time allowed.

Figure 4.7 shows schematically a summary of the effects of the deformation rate and the solid fraction, or deformation temperature, on the four deformation mechanisms. As the solid fraction and the deformation rate increase, the SS and PDS mechanisms become more dominant.

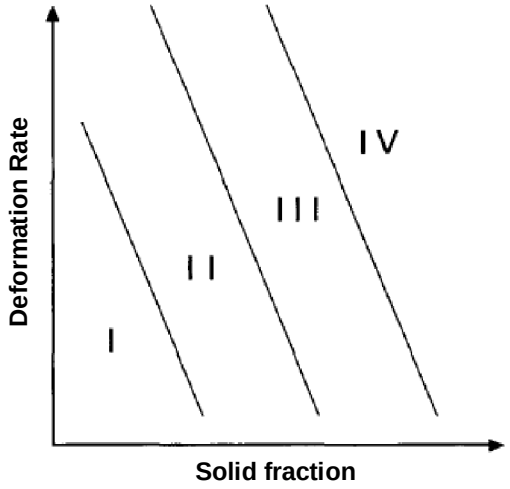

Figure 4.7. The effects of the deformation rate and the solid fraction on the dominance of the four deformation mechanisms [53]

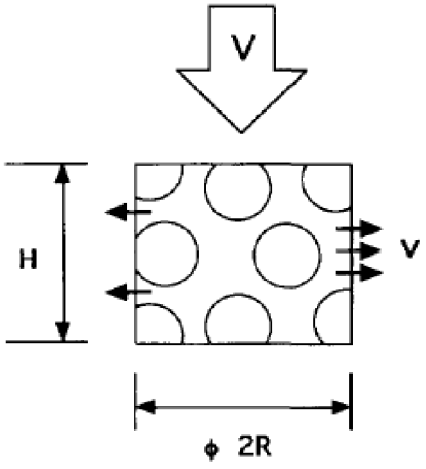

Figure 4.8. The LF deformation mechanism – *V*=deformation rate; *v*=liquid flow rate [53]

The effects of the deformation rate on the LF deformation mechanism in the center portion can be demonstrated as shown in Figure 4.8. As the cylindrical material shown by the shaded area is deformed in the direction indicated by the arrow sign, the liquid starts to flow between the solid particles to accomplish the deformation. During deformation by the LF mechanism, the deformation is accomplished only by lateral flow of the liquid phase, as indicated previously. Consequently, in accordance with the rule of constant volume, the lateral flow rate (v) of the liquid phase can be expressed as a function of the compressive or deformation rate (V) and solid fraction (f_s) as follows:

$$v = \frac{\left(\frac{R}{2H}\right)}{(1-f_s)}V \tag{4.1}$$

where R = radius of the cylindrical material; H = height of the cylindrical material. Figure 4.9 shows the plot of the liquid flow rate vs. the solid fraction at various deformation rates for a given *R/H*. As the deformation rate increases, the required liquid flow rate to achieve the deformation increases, which, in turn, creates a larger back pressure to resist further deformation. As a result, for the LF mechanism, a larger deformation force is required for a higher deformation rate. It is also shown that as the solid fraction increases, the required liquid flow rate increases, which, in turn, requires a larger deformation force as discussed above.

However, the fact that the deformation rate affects the segregation of the solid and liquid phases must be taken into consideration during deformation, and the total effects are called the composite deformation rate effects. During segregation, the solid fraction in the center portion increases as the deformation strain increases, which means $df_s / d\varepsilon > 0$, while the solid fraction around the edge decreases as the deformation strain increases, which means $df_s / d\varepsilon < 0$, as shown in Figure 4.10. Since the LF mechanism, which is the mechanism creating the segregation, dominates in the beginning for the lower deformation rate, the segregation phenomenon is more significant for the lower deformation rate than for higher deformation rate, as shown in Figure 4.10.

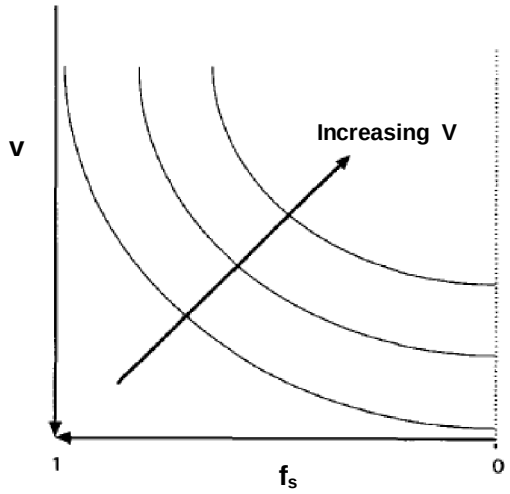

Figure 4.9. The liquid flow rate vs. the solid fraction at various deformation rates for a given R/H for the LF mechanism [53]

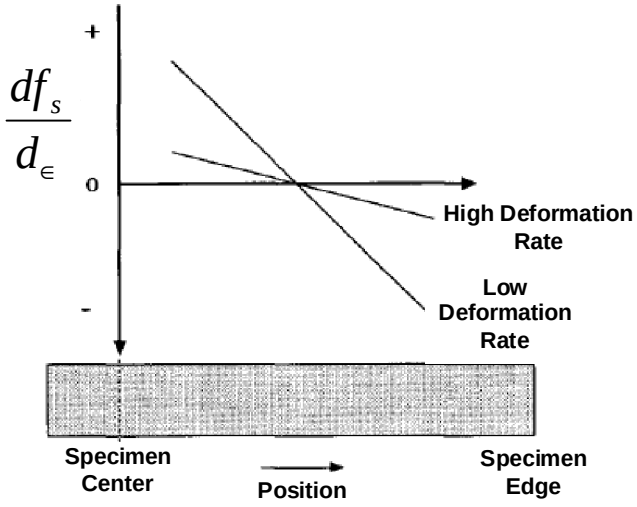

Figure 4.10. The variations of the solid fraction variation rate with the position in the specimen for different deformation rate [53]

Figure 4.11 shows schematically typical phenomenological semi-solid deformation behavior of a cylindrical material, in which all four deformation mechanisms are in operation at the very beginning. As the deformation proceeds, the distributions of the solid and liquid phases are varied as shown in Figure 4.11 from the top to the bottom figures. In the beginning of the deformation, no segregation of solid and liquid phases is present. The dominant deformation mechanism is the LF mechanism since the deformation force

required by it is the least, and the liquid between the solid particles flows laterally to achieve the deformation. Consequently, the center of the cylinder becomes depletive of liquid, and segregation of the solid and liquid phases becomes evident. As the solid fraction increases in the center portion, the other mechanisms start to set in, as discussed in the previous section. The first mechanism is the FLS mechanism, since the deformation force required by it is the second least. As the solid particles start to have contact with each other, the SS and PDS mechanisms become dominant. Eventually, the only deformation mechanism available in the center portion is the PDS mechanism, since only the solid phase exists in the center. Similar phenomena take place in the other portion of the cylindrical material as shown in Figure 4.11. Towards the end of the deformation, the whole cylindrical material can typically be separated into four different layers in terms of the dominant deformation mechanisms from the center to the edge, which in sequence are the layers dominant by (1) the PDS mechanism; (2) the SS mechanism; (3) the FLS mechanism; and (4) the LF mechanism [53].

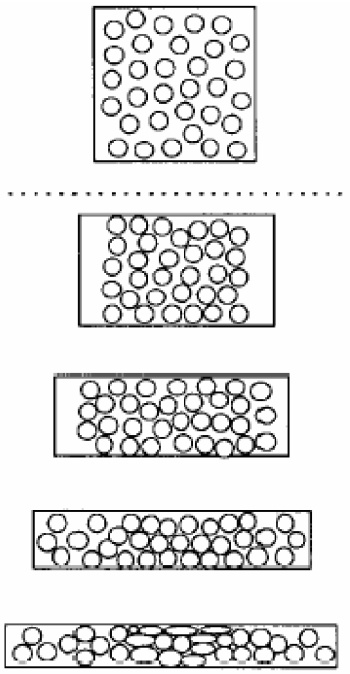

Figure 4.11. Typical phenomenological semi-solid deformation behaviors with increasing deformation strains from top to bottom [53]

4.3. Formability in the Semi-solid Range

Formability in the semi-solid range depends on the following parameters:

Volume fraction of solid: The behavior of a semi-solid material is very sensitive to the volume fraction of solid. A large volume fraction of solid results in increased apparent viscosity and significant internal damage during deformation, as a result of strain localization, which in turn causes difficulties in die filling and defects in the final product. Although no specific limits have been explicitly suggested in the literature, it is generally accepted that the volume fraction of solid during processing should be about 0.6.

Morphology of solid grains: The MHD material contains near equiaxed rosette-like solid grains in the semi-solid state. In this case, the resistance to shear is high, and isothermal holding for spheroidization is required to reduce the apparent viscosity of the material.

Spatial distribution of the liquid phase: Occasionally part of the liquid resides inside the solid grains, a result of the grain growth process. This type of liquid adversely affects the ability of the material to deform, since it decreases the amount of interconnected effective liquid available for deformation and results in increased temperature requirements for semi-solid metal processing.

Viscosity of liquid phase and connectivity of solid phase: These parameters are expected to play an important role in semi-solid processing; their effects have not been adequately quantified yet. In addition, the resistance of the solid phase to deformation depends on grain boundary cohesion that is reduced when microsegregated species are present along the grain boundaries, compared to fully homogenized alloys [13].

In terms of formability, thixoforming has an advantage over solid state forming. The desired microstructure for semi-solid forming is one free of dendrites, with the solid present in as spherical a form as possible and with minimum entrapped liquid. The resulting semi-solid mixture then flows homogeneously, Figure 4.12, behaving as a thixotropic fluid with viscosity depending on fraction solid, morphology, shear rate and

time. To achieve the desired formability, all semi-solid processes employed commercially today seek to achieve formation of as large a number as possible of grain “nuclei” [54].

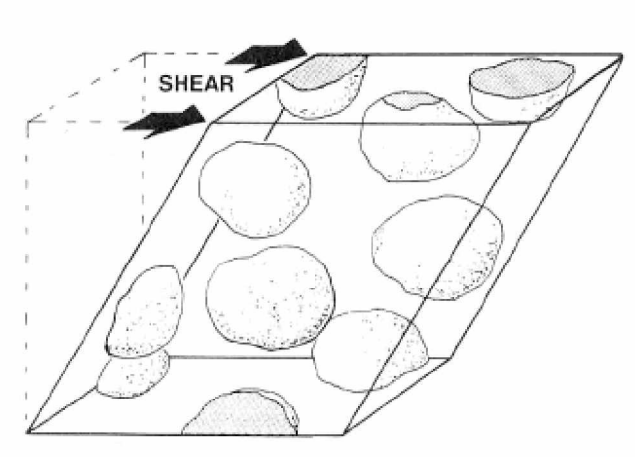

Figure 4.12. Schematic diagram of homogenous flow of semi-solid alloys [54]

5. EXPERIMENTAL STUDY

5.1. Materials Used in the Experiments

Semi-solid metal processing is believed as a promising near-net shape forming technology for its unique features compared with conventional metal forming methods. It has been more than thirty years since it was pioneered by Flemings *et al.* and more than ten years since it was put into commercial application. However, up to now, components produced by semi-solid forming are generally made from conventional Al-Si casting alloys such as A356 or A357. Although the properties of the components are superior to casting ones, the advantages of semi-solid metal processing have not been fully realized. Therefore, it is necessary to expand some new alloys in order to satisfy the development of semi-solid metal processing [55].

Table 5.1. Chemical composition of A356 aluminum alloy used in the study (as per cent)

Si	Fe	Cu	Mn	Mg	Zn	Ti	Sr	Al
6,99	0,107	0,0056	0,0071	0,3118	0,0078	0,0982	0,0298	92,413

Table 5.2. Chemical composition of AA6082 aluminum alloy used in the study (as per cent)

Si	Fe	Cu	Mn	Mg	Cr	Zn	Ti	Al
1,194	0,189	0,004	0,625	0,677	0,002	0,004	0,014	97,25

In present study, thixoforming characteristics of both cast and wrought aluminum alloys were investigated. In these experiments, the applied cast aluminum alloy used is A356, which was fabricated by electromagnetic stirring process in the SAG Company, Austria. The diameter of received billets was 76 mm and the length was 90 mm. Billets were cut into cylindrical specimens of 30 mm in diameter and 35 mm in height by machining. As wrought aluminum alloy, AA6082 was used and thixotropic structure was obtained via SIMA process in the laboratory. The diameter of the received billets was 208 mm and they had been produced by vertical casting system in ASAŞ Aluminum Company. They were extruded to 27 mm and 44 mm diameters in SIMA process and then cut to 35

mm length. The chemical composition of the alloys used in the present study is shown in Table 5.1 and Table 5.2. Note that A356 alloy is strontium modified and this affects the formation of the eutectic silicon. The formation changes from a lamellar to a modified structure.

A356 alloy is the most popular Al alloy for semi-solid automotive components because of its wide solidification interval, its well castability and its good mechanical properties. AA6082 aluminum alloy is heat treatable, high strength wrought alloy and it is used in Europe as structural profiles in automotive parts. However, its susceptibility to hot cracking and poor fusion of confluent melt fronts greatly restrict the application range [56].

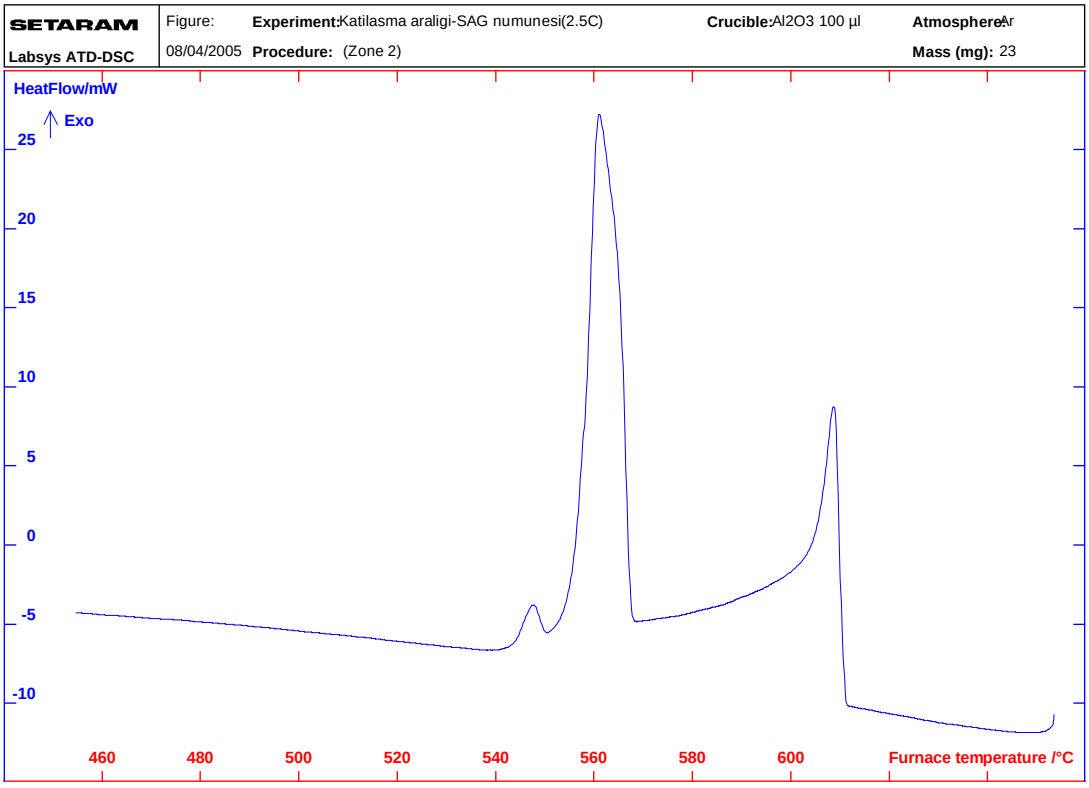

Figure 5.1. DSC curve of A356 alloy during solidification

It is well known that the liquid/solid fraction is calculated using Scheil's equation customarily. However, it is very difficult to determine the distribution coefficient for complex alloys, such as AA6082 alloy [57]. The melting range and solid fraction against temperature of A356 and AA6082 aluminum alloys were determined by Differential

Scanning Calorimetry (DSC) technique. The DSC tests were also used to determine the amplitude of phase transformations during heating. A356 and AA6082 aluminum alloys were cut into small pieces for DSC tests. DSC tests were performed using carbon pans and lids in an argon atmosphere to prevent oxidation. All DSC studies were executed in Setaram DTA-DSC device in TÜBİTAK-MAM.

For A356 alloy; the DSC runs increased from room temperature to 650 °C at a heating rate of 20 °C/min, then the sample was held at 650 °C for 10 minutes and finally cooled from 650 °C to 450 °C at 2.5 °C/min. The temperature and heat flow were plotted during solidification (exothermic effect) and is shown in Figure 5.1.

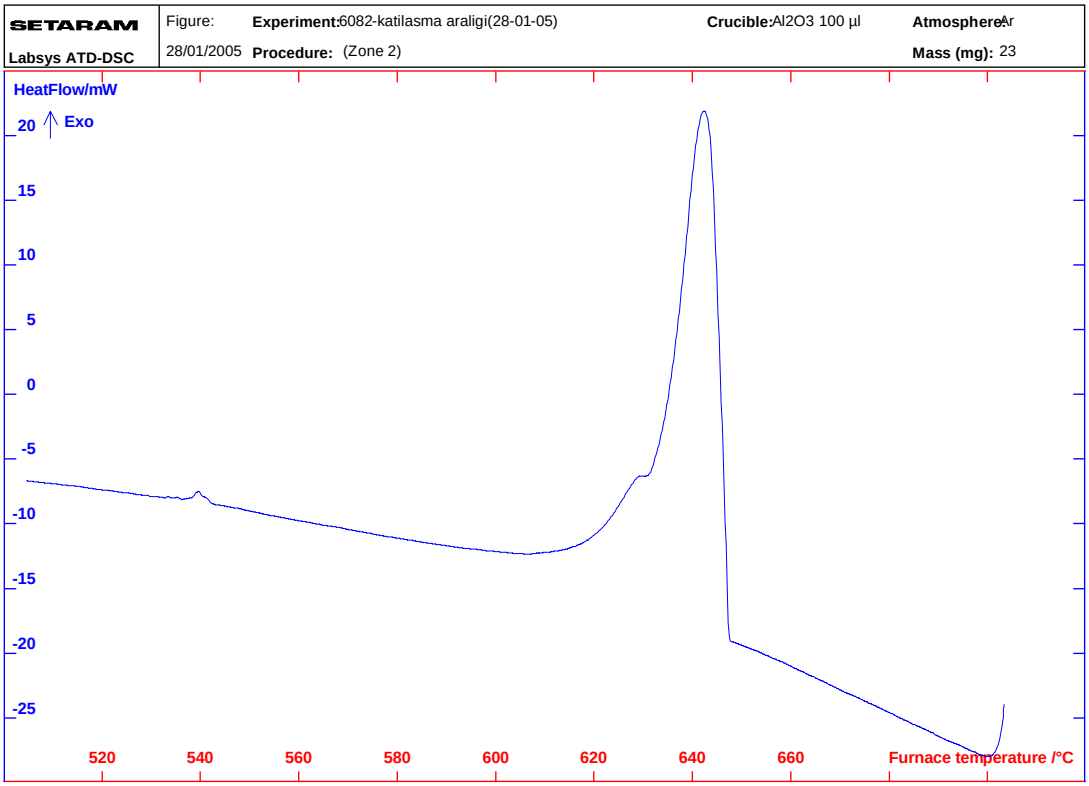

Figure 5.2. DSC curve of AA6082 alloy during solidification

For AA6082 alloy; the DSC runs increased from room temperature to 700 °C at a heating rate of 20 °C/min, then the sample was held at 650 °C for 10 minutes and finally cooled from 700 °C to 500 °C at 2.5 °C/min. The temperature and heat flow were plotted during solidification (exothermic effect) and is shown in Figure 5.2.

Table 5.3. Thermal properties of A356 and AA6082 aluminum alloys

Material	Solidus Temperature (°C)	Liquidus Temperature (°C)	Solid-liquid interval (°C)
A356	553	615	62
AA6082	603	649	46

Solidus temperature, liquidus temperature and solidification range of A356 and AA6082 aluminum alloys are given in Table 5.3 in accordance with DSC curves. Working temperatures are lower in A356 alloy. Also, A356 alloy has a wider solidification range than AA6082 alloy.

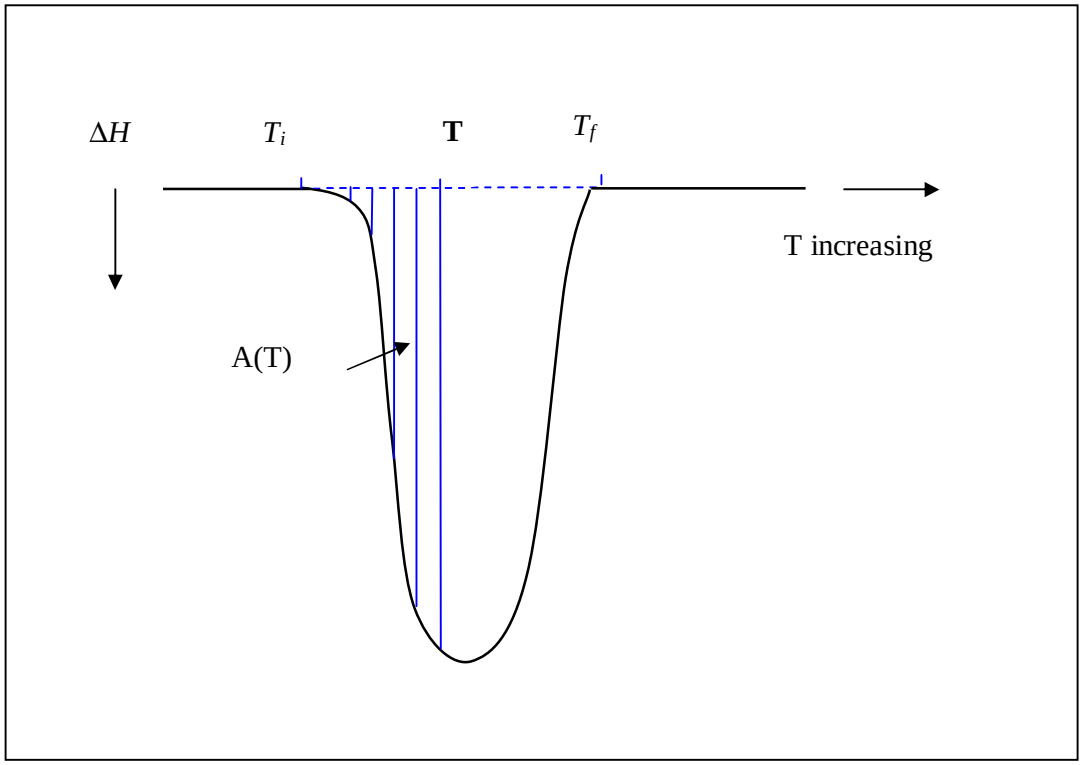

Figure 5.3. Schematic illustrating the estimation of fraction liquid from the heat flow plot from DSC

Solid fraction-temperature relationship for each alloy was calculated from the method of partial areas using DSC curves. The assumption was that the weight fraction of liquid was proportional to the evolution of heat during melting i.e. the fraction of

transformation was the proportion of the area under the DSC curve. Therefore liquid fractions of each material against temperature were evaluated from the peak area, A(T), between solidus temperature (T_i) and instantaneous temperature (T) and divided by the total area under the peak, $A(T_f)$, of heat flow against temperature. The baseline defining the peak area was a linear baseline (Figure 5.3). Therefore, the fraction of transformation i.e. fraction liquid, $f_L(T)$, could be expressed as

$$f_L(T) = \frac{A(T)}{A(T_f)} \tag{5.1}$$

Solid fraction-temperature curves of A356 and AA6082 aluminum alloys were estimated from the DSC plots and are shown in Figure 5.4 and Figure 5.5. For AA6082 alloy, liquid content increases rapidly at temperatures above 630 °C. Therefore, temperature control is more critical for AA6082 alloy.

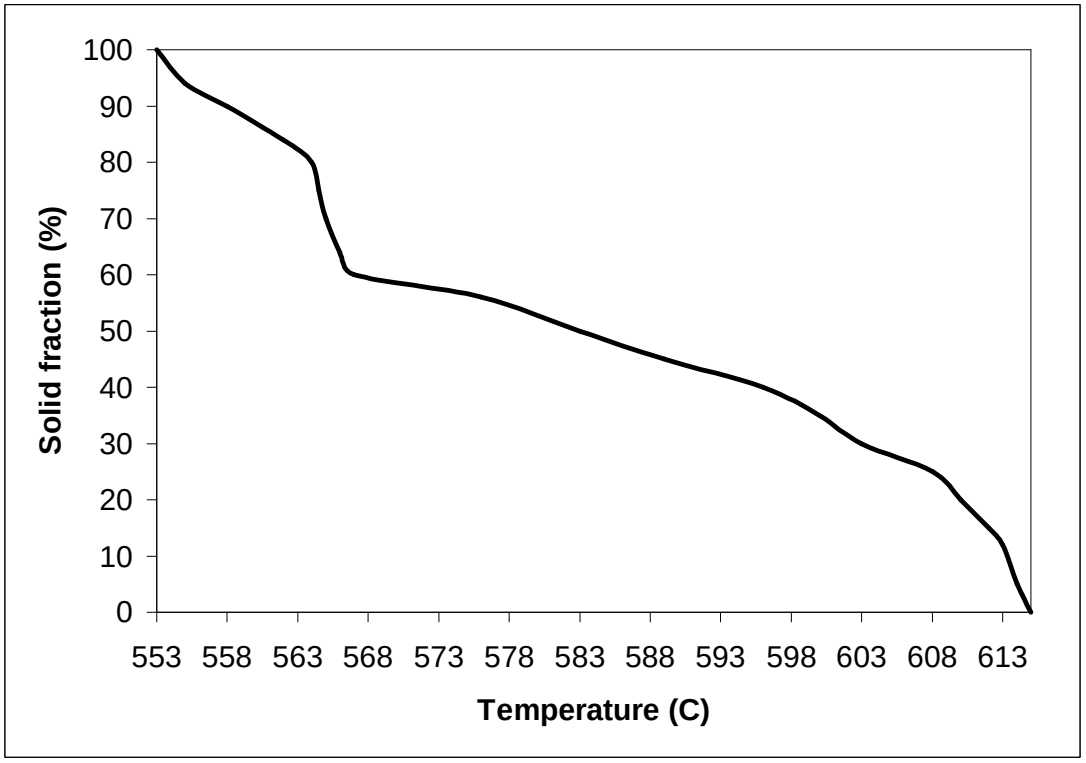

Figure 5.4. Solid fraction vs. temperature curve of A356 aluminum alloy

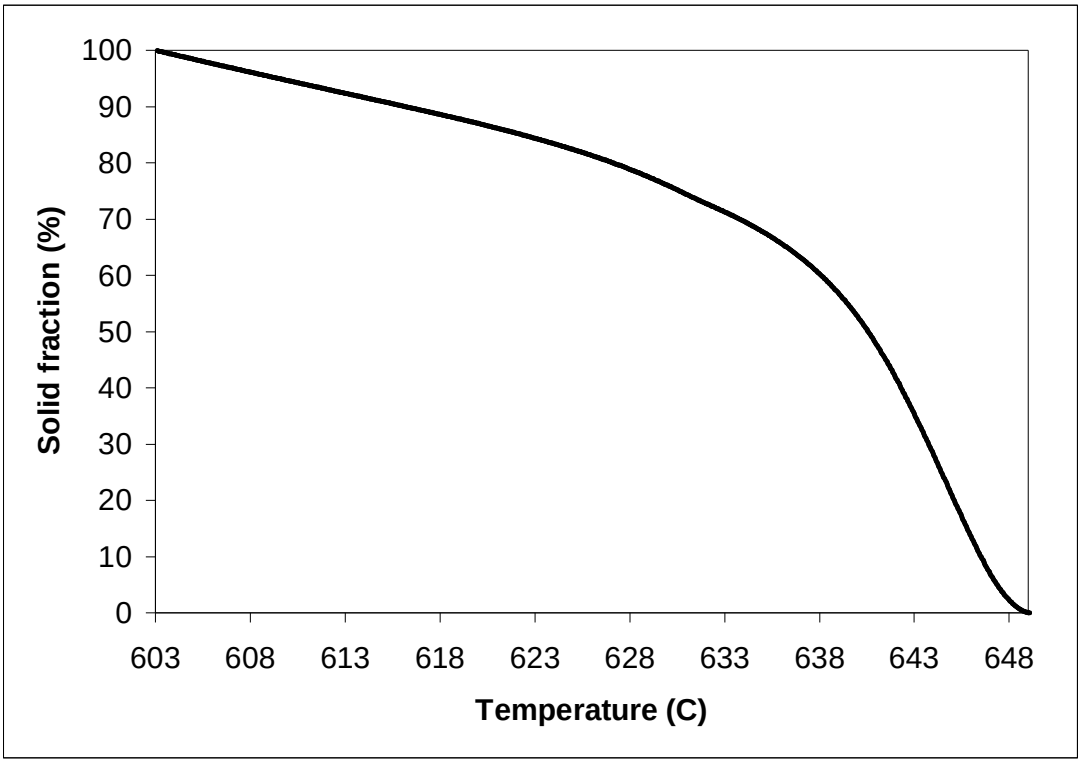

Figure 5.5. Solid fraction vs. temperature curve of AA6082 aluminum alloy

5.2. Experimental Setup

5.2.1. Induction Heating Unit

A high frequency induction heating unit was used in all experiments for heating of aluminum billets. Induction heating unit is shown in Figure 5.6. The dimensions of the induction heating unit are 50 cm × 50 cm × 30 cm and the weight is about 20 kg. This device uses an electrical source to drive alternating current (AC) through a coil to heat metal objects. The passage of current through the electrically conductive coil generates an intense and rapidly changing magnetic field that causes eddy currents to flow through the workpiece.

There are three indicator screens on the front side of induction furnace indicating voltage, current and frequency values. The frequency of the induction heating furnace differs from 90 kHz to 140 kHz with respect to material remains fixed during heating

period. Power value is calculated by multiplying measured voltage and current values displayed on the panel of the induction heating furnace. Power adjustment from zero (%0) to the highest power level (%100) is realized with a power controller. Current and voltage values displayed on the screen vary according to position of power controller. Maximum attainable power is about 3 kW with this machine. The heating power has to be controlled precisely and timely according to the billet state in order to obtain efficiently the desired and uniform liquid/solid fraction in the billet without changing the microstructure. Moreover, two warning lamps are included on the panel of the heater, one for excess current and the other for excess heat. This system can be used for both heating and melting purposes by changing the work coil and moving up or down the switch placed at the lower part of the panel.

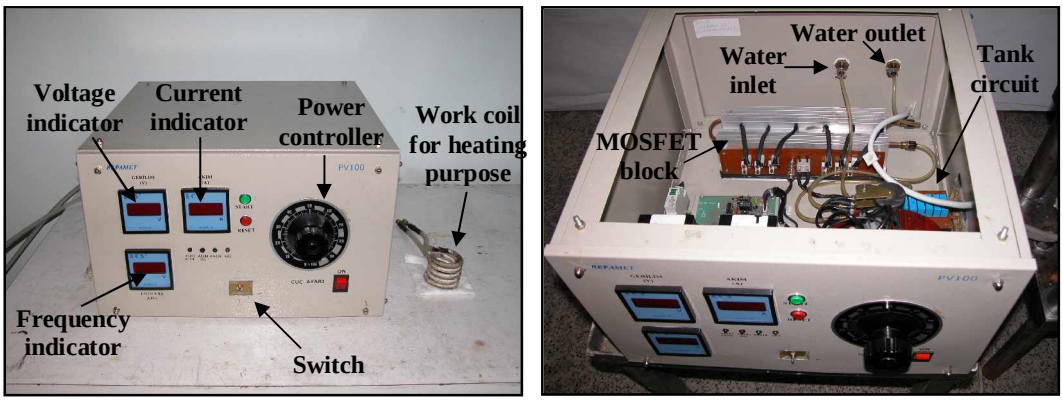

Figure 5.6. Induction heating unit

The work coil is incorporated into a resonant tank circuit. The work coil is made to resonate at the intended operating frequency by means of a capacitor placed in parallel with it. This causes the current through the work coil to be sinusoidal. Work coil consists of few turns of a thick copper conductor but with large currents of many tens or hundreds of amps flowing. Water cooling is used to remove excess heat generated by the passage of the large high frequency current through the work coil and its associated tank capacitor. In this respect, there are water inlet and outlet locations on the back side of the induction heating unit and water is circulated through hosepipes. Flow requirement of the cooling water is about 2-3 lt/min.

Induction heating unit can be used for both heating and melting purposes by changing the working coil. Thus, there are two working coils for this machine, one for heating purpose and the other is for melting purpose. In the scope of thesis, all experiments were related to the heating, so only heating coil was used in the experiments.

Figure 5.7 shows the photo and specifications of the heating coil. The diameter of A356 billets used in the experiments was 30 mm and that of AA6082 billets was 27 mm. The inner diameter of the coil is 50 mm. In this respect, the coupling distance is 10 mm for A356 billets and 11.5 mm for AA6082 billets. These values of coupling distance are appropriate according to the values given in Section 3.2.4.

Heating coil specifications	
Outer diameter	65 mm
Inner diameter	50 mm
Wire diameter	7.5 mm
Height	50 mm
Number of turns	5

Figure 5.7. The photo and specifications of the heating coil

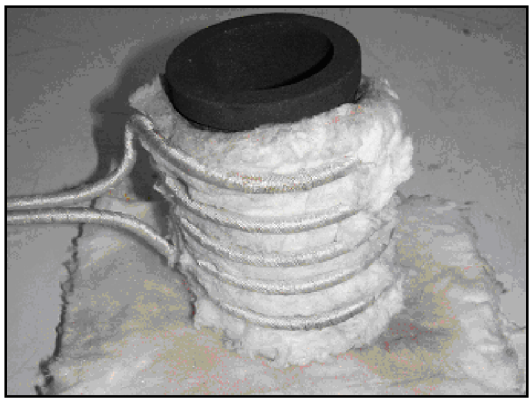

Melting coil specifications	
Outer diameter	103 mm
Inner diameter	89 mm
Wire diameter	7 mm
Height	100 mm
Number of turns	5

Figure 5.8. The photo and specifications of the melting coil

Figure 5.8 gives the photo and specifications of the melting coil. Melting coil is used together with a graphite crucible. Material to be melted is put in this crucible. Melting coil heats the crucible inductively, and the material melts conductively by contacting hot crucible. The response of graphite to inductive heating is very strong.

5.2.2. Die

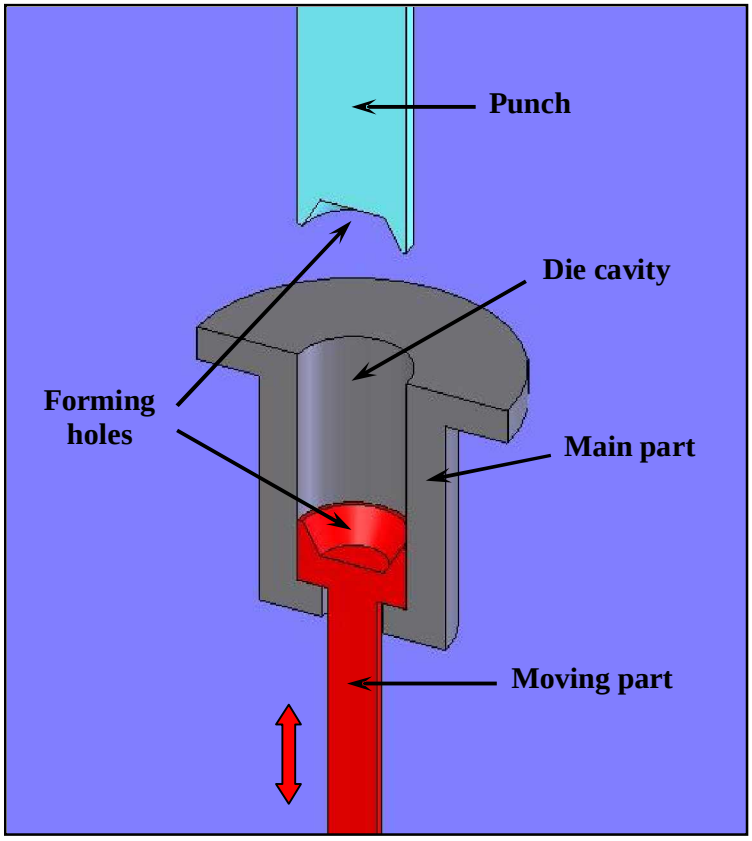

Figure 5.9. Schematic view of die prepared using Solid Works 2005

Two different dies were designed in the thixoforming process for different purposes. Their design criteria are alike but the dimensions are different. One is shorter in length and used for microstructural evaluation and hardness tests while the other is longer and designed to match ASTM tensile test specimen standards. Solid Works 2005 software program was utilized while designing the dies. The die is composed of three parts namely punch, main part and moving part. Both punch and moving part include forming holes. Figure 5.9 shows the schematic diagram of the die prepared in Solid Works 2005. Between

two die designs, only difference is in dimensions of conical depths of forming holes.

According to this die design, reheated slug is directly entered into die cavity having the product shape. Two advantages, in the commercial view point, can be taken from this new tool design concept: (1) without a separate gate and runner structure, the size of the tool could be considerably reduced; (2) the additional hydraulic ejecting system was not needed because part ejection can be done using the moving part as an ejector. Additionally, since the die filling distance and time could be effectively reduced by use of this tool design, the slow injection ensuring non-turbulent laminar flow may be easily realized without the problems related to incomplete filling. This point has more important meaning when wrought aluminum alloys are used for thixoforming. Wrought aluminum alloys have relatively narrow solidification range; accordingly, the cooling of wrought aluminum alloys occurs far more rapidly during die filling process than that of cast grade aluminum alloys. Therefore, in the case of wrought aluminum alloys, this new tool design concept can make thixoforming of large and complex shapes much easier.

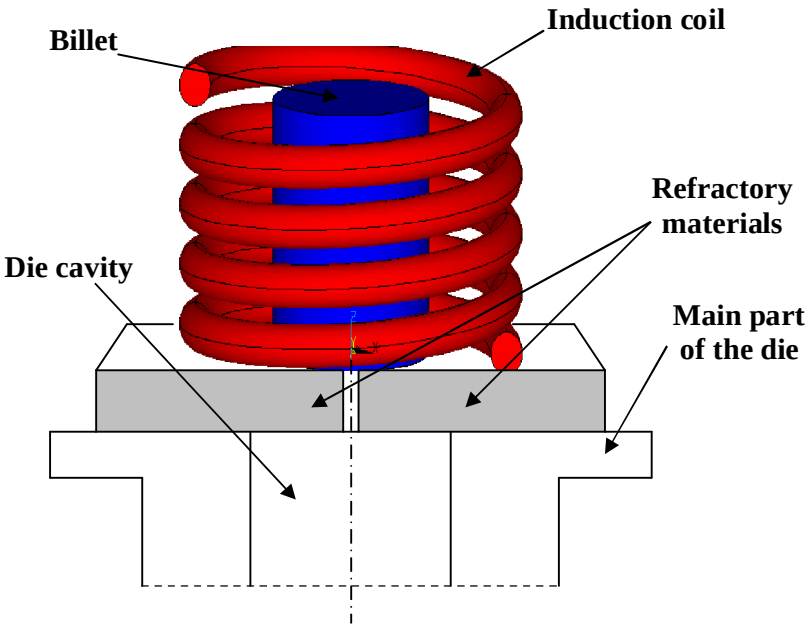

Figure 5.10. The position of the billet and refractory materials during heating

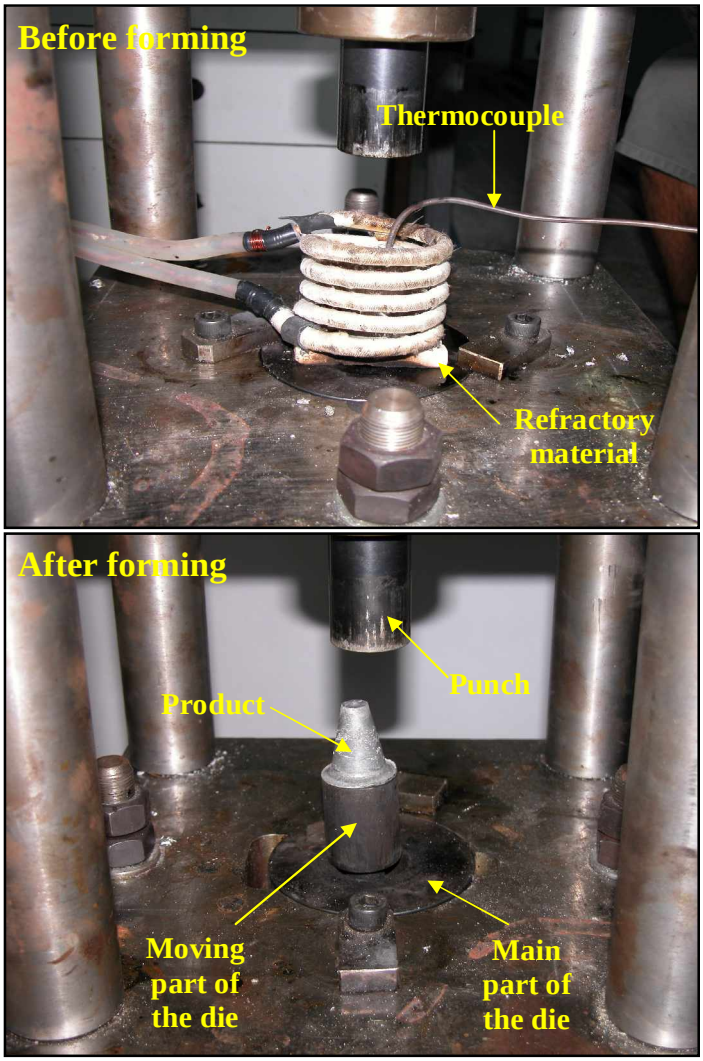

Figure 5.11. The photos of the system just before and after forming

The billet is heated just above the hole of the main part of the die. A refractory material lies between the billet and the die to prevent the drop of the billet into the hole during heating stage. Refractory material is also useful to minimize the possible heat loss of the billet. Refractory material is composed of two parts. The position of the billet and the refractory material during heating is shown schematically in Figure 5.10. During heating, the position of the moving part of the die is as like in Figure 5.9. When the billet comes to the desired temperature in the semi solid range, refractory materials are pulled and the billet drops into the die cavity. Simultaneously, forming operation is performed. In this die concept, moving part acts like an ejector, so it facilitates the extraction of the product after thixoforming operation. After forming, the moving part is moved upwards for

extraction of the product. Figure 5.11 gives the position of the billet and die system both before and after forming operation. After forming operation, the product is removed from the die and then quenched in water.

In thixoforming experiments, die was preheated to 300 °C to reduce the rate of heat transfer from the aluminum billet to the die. In order to maintain a constant die temperature, the die was heated by a 900 W ring resistance. The heater is set to a constant temperature with the use of temperature controller units. The ring heater is shown in Figure 5.12 in combination with the die. The ring heater is attached to the main part of the die. The material of the die is H13. H13 is a very versatile hot work tool steel giving good hot toughness and wear resistance and is suitable for many hot work applications. The die was heat treated HRC 52 before usage.

Figure 5.12. The ring heater in combination with the main part of the die

5.2.3. Forming Unit

Forming unit is composed of a hydraulic cylinder, a main body to hold the punch and die, and a hydraulic power generator to apply necessary load. The photo of the semi-solid forming unit is shown in Figure 5.13. The semi solid forming unit specifications are shown in Table 5.4 [58]. In order to prevent the movement of the die under injection load locking blocks are used. Hydraulic power unit was designed in accordance with specifications

required by the system also to provide high efficiency and a rigid construction. In thixoforming operation, a ram that actuates fast and applies the necessary load is needed. Therefore a 7.5 kW electric motor was used to provide the necessary pump flow and operational pressure. Also the hydraulic pump provides 42 liters/minute for the system, which is necessary for high speed of the ram. Hydraulic power unit specifications are shown in Table 5.5.

Figure 5.13. Semi-solid forming unit

Table 5.4. Semi-solid forming unit specifications [58]

Dimensions of the forming unit	300 x 300 x 765 mm
Maximum load	7.8 ton-f
Maximum speed of the ram	89 mm/s
Ram stroke	120 mm

Table 5.5. Hydraulic power unit specifications [58]

Electric motor……:	Power……..: 7.5 kW
	Voltage……: 380 V
Hydraulic pump……:	Flow Rate ……..: 42 lt/min
	Type……: Gear pump
Directional control valve...:	Nominal flow…..……..: 70 lt/min
	Nominal pressure……..: 215 bar
Throttle valve…..:	Nominal flow rate……...: 75 lt/min
	Nominal pressure……: 315 bar
Tank……....:	Dimensions…..……....: 50x 60 x 80 mm

5.3. Induction Heating Practices for A356 Alloy

For the thixoforming process, the billet must be reheated to the semi-solid state. The reheating process is very important in the forming process of a billet, the process not only being necessary to achieve the required semi solid billet state, but also to control the microstructure of the billet [40]. In this part of the study, the effects of reheating temperature, number of heating steps and holding time on the globularization of microstructure for MHD A356 alloy was investigated.

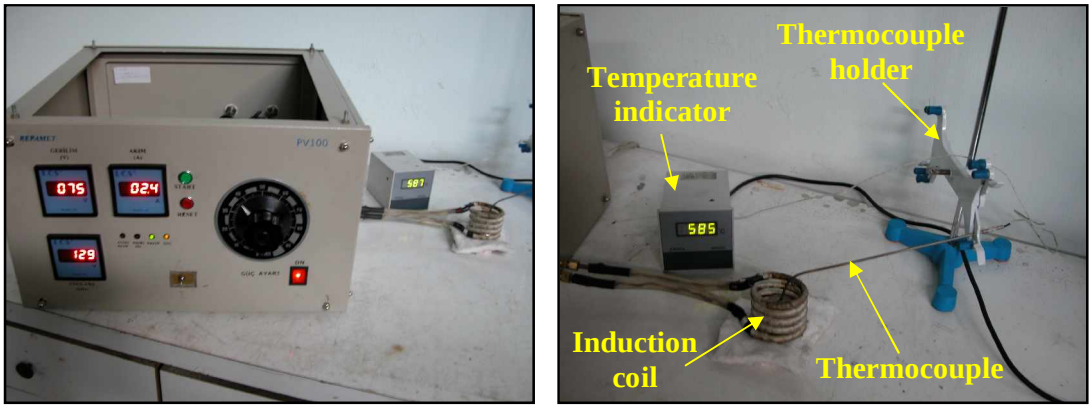

Figure 5.14. Induction heating unit in operation

A356 alloys fabricated by electromagnetic stirring were received from SAG Company, Austria in dimensions of 76 mm diameter and 90 mm length. These billets were then machined to 30 mm diameter and 35 mm height to adapt the billet dimensions to the coil of the induction heating unit. The induction heating experiments was performed using the induction heating furnace set in Boğaziçi University Materials & Manufacturing laboratory. The capacity of the induction heating furnace is 3 kW and the frequency is 90 – 130 kHz differing with respect to material. The heating process is usually monitored and controlled by the billet temperature. To monitor the temperature variation of the billet during reheating process, a hole of 3.5 mm diameter was machined at the center of samples and K-type thermocouple was inserted to the hole to precisely measure and control the temperature of slurry. The thermocouple was attached to a temperature indicator. This indicator displays the instantaneous temperature of the billet. Figure 5.14 represents an induction heating experiment in operation along with measurement technique.

The heating power has to be controlled precisely and timely according to the billet state in order to obtain efficiently the desired and uniform liquid/solid fraction in the billet without changing the microstructure. At the first stage, billets were rapidly heated with high power input (about 1.5 kW) from beginning to the solidus temperature of 553 °C. Once this temperature was reached, the power was reduced and the billet was gradually heated to the semi-solid temperature at the second stage. Because in this range there are two phase transformations in A356: the melting of the ternary Al–Si–Mg at 555 °C and the melting of binary Al–Si eutectic at 575 °C. Those endothermic phase transformations a little bit delay the heating process [59]. It is important to note that rapid temperature rise occurs when the eutectic is melted at 575 °C; the care must be taken to control the temperature at that time. Finally, the temperature is fixed at a semi-solid temperature for a soaking time. In these experiments, constant power for each stage was supplied to the coil by setting current and voltage to a fixed value during heating because of simplicity of the heating power control. In this way, all specimens were heated with same heating rate. Average heating rate was 150 °C/minute.

In order to optimize the reheating step of A356 alloy, several specimens were heated to semi-solid temperatures under different heating conditions. In order to obtain uniform temperature distribution through billets, step heating trials were included in reheating

experiments. The temperatures for holding in the steps were chosen in relation to the reaction temperatures. At the end of the final holding time, the specimens were quenched in water. During the heating period, temperature of billets was noted periodically, and temperature-time curves were plotted for each specimen.

Preparation of metallographic specimen consisted of grinding with SiC paper of different fineness and subsequently polishing with 3 μm diamond paste and colloidal alumina. For microstructural characterization, the samples were chemically etched with 0.5 ml HF in 100 ml water for 20 s. The metallographic observation was carried out by optical microscopy. All microstructural observations were made at mid-radial region (midway between surface and center) of the specimen.

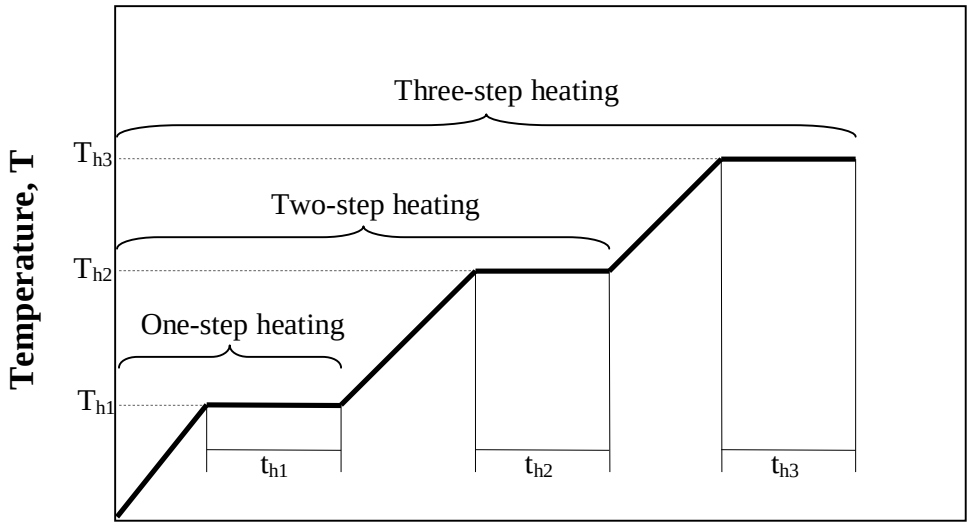

t_{h1}, t_{h2}, t_{h3}	T_{h1}, T_{h2}, T_{h3}
Holding time	Holding temperature

Figure 5.15 Input data diagram of the reheating conditions to obtain a globular microstructure

To determine the optimal reheating conditions for the globularization of the microstructure and a small temperature gradient, the following parameters were considered: the holding temperature (T_h), the holding time (t_h), and the number of

reheating steps. The reheating experiments were performed for the conditions in Table 5.6. The meanings of the symbols used in Table 5.6 are the same as those shown in Figure 5.15. A number was given to each experiment for clear expression.

Table 5.6. Experimental conditions for the reheating of semi-solid aluminum alloy (A356)

Experiment no.	Holding temperature, T_h (°C)			Holding time, t_h (minute)		
	T_{h1}	T_{h2}	T_{h3}	t_{h1}	t_{h2}	t_{h3}
1	584	-	-	2	-	-
2	584	-	-	5	-	-
3	584	-	-	15	-	-
4	575	584	-	3	2	-
5	575	584	-	3	5	-
6	575	584	-	3	10	-
7	350	575	584	1	3	0.5
8	350	575	584	1	3	2
9	350	575	584	1	3	5
10	350	575	584	1	3	10
11	350	575	584	1	1	5
12	578	-	-	5	-	-
13	570	578	-	3	5	-
14	350	570	578	1	3	5

5.4. SIMA Process for AA6082 Alloy

Parameters such as heating time and temperature, and the degree of hot working, are critical factors in controlling the semi-solid microstructures in the SIMA process. Microstructure of an alloy prepared in the semi-solid state depends on its microstructure prior to partial remelting, so it is important to study the initial microstructure and subsequent evolution process during partial melting. In this part of the study, the impact of the extent of deformation and reheating treatment parameters on the globularization of the grains in the AA6082 alloy was investigated.

AA6082 aluminum alloy was used in the SIMA process. The diameter of the received billets was 208 mm and they had been produced by vertical casting system in ASAŞ Aluminum Company. These billets were again melted and casted die cast molds of 100 mm diameter in TÜBİTAK Marmara Research Center. These billets of 100 mm diameter were then heated to 460 °C and were extruded to cylindrical profiles of 27 mm and 44 mm. Extrusion process is shown in Figure 5.16. Unlike conventional SIMA, all billets used for this study were processed by only hot extrusion without any subsequent cold working treatment. 27 mm and 44 mm diameter billets were then cut into pieces of 35 mm length. These rods are generally called a slug in thixoforming technology.

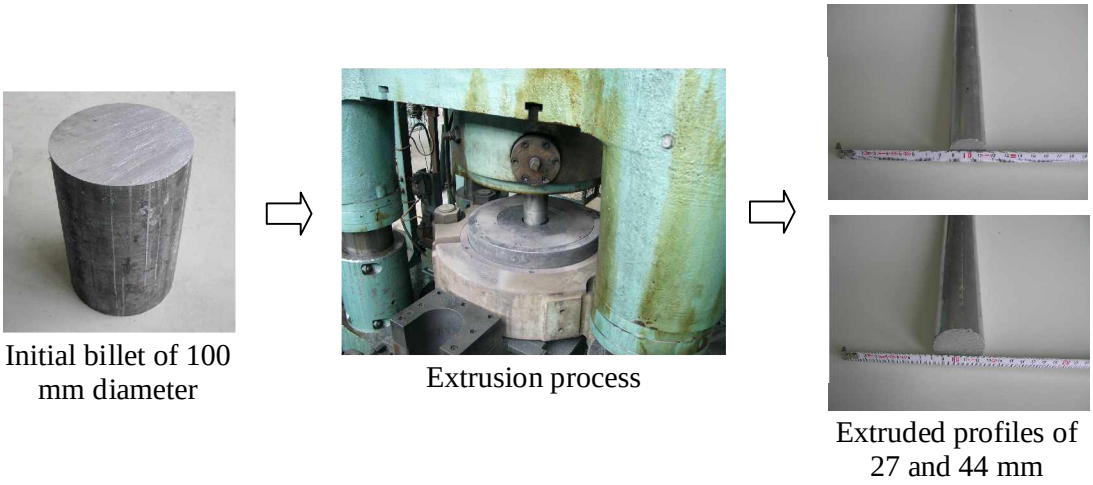

Figure 5.16. Extrusion process of AA6082 from 100 mm diameter to 27 and 44 mm diameters

DSC (Differential Scanning Calorimetry) technique was utilized to define solidus and liquidus temperatures (solidification range) of the alloy. The solidification range of AA6082 alloy was found to be 603-649 ℃ in accordance with Figure 5.5. These specimens were heated to temperatures varying between 630 ℃ and 645 °C in the induction furnace which was installed in Boğaziçi University Materials & Manufacturing Laboratory. Average heating rate was 150 °C/minute. To monitor the temperature variation of the billet during reheating process, a hole of 3.5 mm diameter was machined at the center of samples and K-type thermocouple was inserted to the hole to precisely measure and control the temperature of slurry. Specimens heated to semi-solid temperatures were hold at those temperatures for several holding times. At the end of holding time, the

specimens were quenched in water. The cross sections of the specimens were ground with progressively finer SiC paper, and polished by 3-μm diamond paste and colloidal silica, and finally etched in %0.5 HF solution before microstructural investigation. The metallographic observation was carried out by optical microscopy. All microstructural observations were made at mid-radial region (midway between surface and center) of the specimen.

5.5. Thixoforming of A356 and AA6082 Aluminum Alloys

In this part of the study, A356 and AA6082 aluminum alloys were heated to semi-solid range and thixoformed under pressure. External appearance, microstructure and mechanical properties of thixoformed specimens were investigated after forming.

In thixoforming experiments, many types of equipment were employed in combination and many parameters were controlled successfully. An appearance of the thixoforming system in operation is shown in Figure 5.17. The operation of the system seems complex at first sight. However, there are three different stages in combination in this process: heating of the billets by an induction heating unit, heating of the die by a ring heater, and forming of the billets by a hydraulic press.

The specimens for thixoforming were made by machining to 30 mm diameter and 35 mm length. An induction heating unit (3 kW, 100 kHz) was used to heat the billets. The billets were placed in the induction coil and heated until the required liquid fraction was reached. The billets were heated to semi-solid temperature on a pair of refractory material placed just above the hole of the main part of the die. The position of the billet and the refractory material during heating is shown schematically in Figure 5.10. This design eliminates billet handling after heating process. The instantaneous temperature of the billets was measured by inserting a K-type thermocouple to the center of the billets. When the billets came to the desired temperature in the semi solid range, refractory materials were pulled and the material dropped into the die cavity without handling. Simultaneously, the punch was moved down and squeezed the billet in the die cavity. Thixotropic nature of the material allowed the metal to flow into the cavity at very low pressures. The duration of the forming operation was just a few seconds. Only at the end of

the forming stroke does the pressure increase to the selected level to form the fully dense component. After forming operation was completed, the punch was moved back and the sample was removed from the die by pushing the moving part of the die upwards.

Figure 5.17. An appearance of thixoforming system in operation

A ring heater with a capacity of 900 W was used to heat the die. The temperature of the ring heater was set to a fixed value and controlled by a heat control unit. In order to prevent the sticking of the billet to the die during forming operation graphite oil was smeared to internal surfaces of the die.

In the experiments, 3 ton-f punch load and maximum punch speed (89 mm/s) was provided to minimize the heat loss of the reheated material and to obtain good thixoformability. Die temperature was fixed at 300 °C in forming experiments. The applied pressure was held for 20 seconds after filling.

Thixoforming trials were executed considering most successful heating conditions according to microstructural images found in Section 6.1 and Section 6.2. In this respect, four different heating conditions were applied for A356 and two different heating conditions for AA6082. The experimental conditions of thixoforming trials are given in Table 5.7 as whole.

Table 5.7. Experimental conditions for thixoforming experiments

Product No.	Material	Holding temperature, T_h (°C)			Holding time, t_h (minute)		
		T_{h1}	T_{h2}	T_{h3}	t_{h1}	t_{h2}	t_{h3}
1	A356	584	-	-	5	-	-
2	A356	584	-	-	15	-	-
3	A356	350	575	584	1	1	5
4	A356	350	575	584	1	3	10
5	AA6082	645	-	-	5	-	-
6	AA6082	645	-	-	15	-	-

The microstructures and mechanical properties of the produced parts were investigated to get information about the obtained quality of the parts.

The thixoformed specimens were given a T6 heat treatment in conventional electric furnaces before mechanical testing in accordance with ASTM standards [60]. T6 heat treatment corresponds to the solution treatment and artificial aging. The T6 conditions for each alloy are as follows: (1) A356: solutionizing (10 h at 538 °C) → quenching → aging (6 h at 171 °C); (2) AA6082: solutionizing (1 h at 560 °C) → quenching → aging (6 h at 185 °C).

Hardness tests were carried out from the samples that are shorter in length. Hardness measurements were made before and after T6 heat treatment to evaluate the contribution of T6 treatment. Figure 5.18 shows the positions for hardness tests. Hardness values were taken from both transversal and longitudinal sections, 8 points for each section with 4 mm intervals. Totally 16 points were measured for each specimen for Vickers micro-hardness testing.

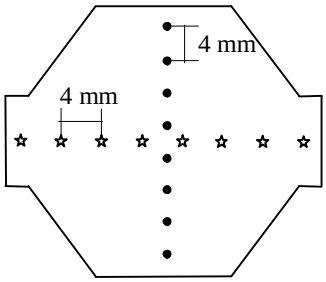

Figure 5.18. Positions for hardness tests

Tensile tests were conducted according to ASTM E-8M [61] for tension testing of cast aluminum alloys. Specimens for tensile testing were machined from thixoformed parts after T6 post-forming heat treatment. Tensile test specimens are small size specimens proportional to standard. Tensile test specimens are shown in Figure 5.19 with dimensions. It should be noted that difficulties exist in the reproducibility of the quality. In this respect, three tensile specimens were prepared for each product to guarantee the reliability of the results. Tensile tests were performed using TESTOMETRIC MICRO-500 apparatus in KOSGEB laboratory.

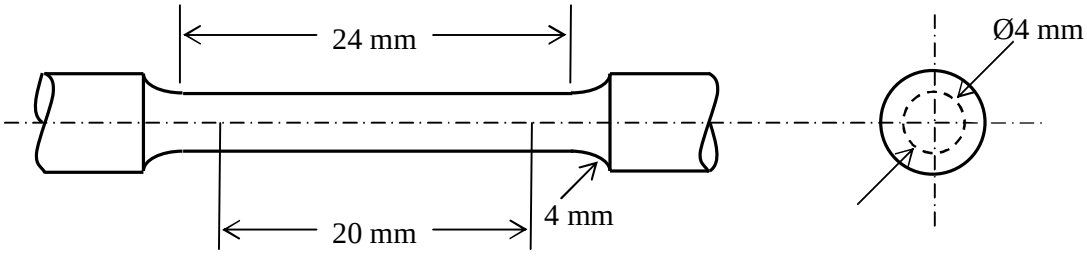

Figure 5.19. Tensile test specimens

6. RESULTS AND DISCUSSION

6.1. Reheating of A356 Alloy Produced by MHD Casting

The microstructure of semi-solid material after reheating must be globular. Moreover, when the semi-solid material is fed from the induction heating system to the die, the shape of the billet must be maintained. Therefore, holding temperature (T_h), holding time (t_h), and the number of reheating steps were considered as parameters of the experiments to observe the globularization of the microstructure.

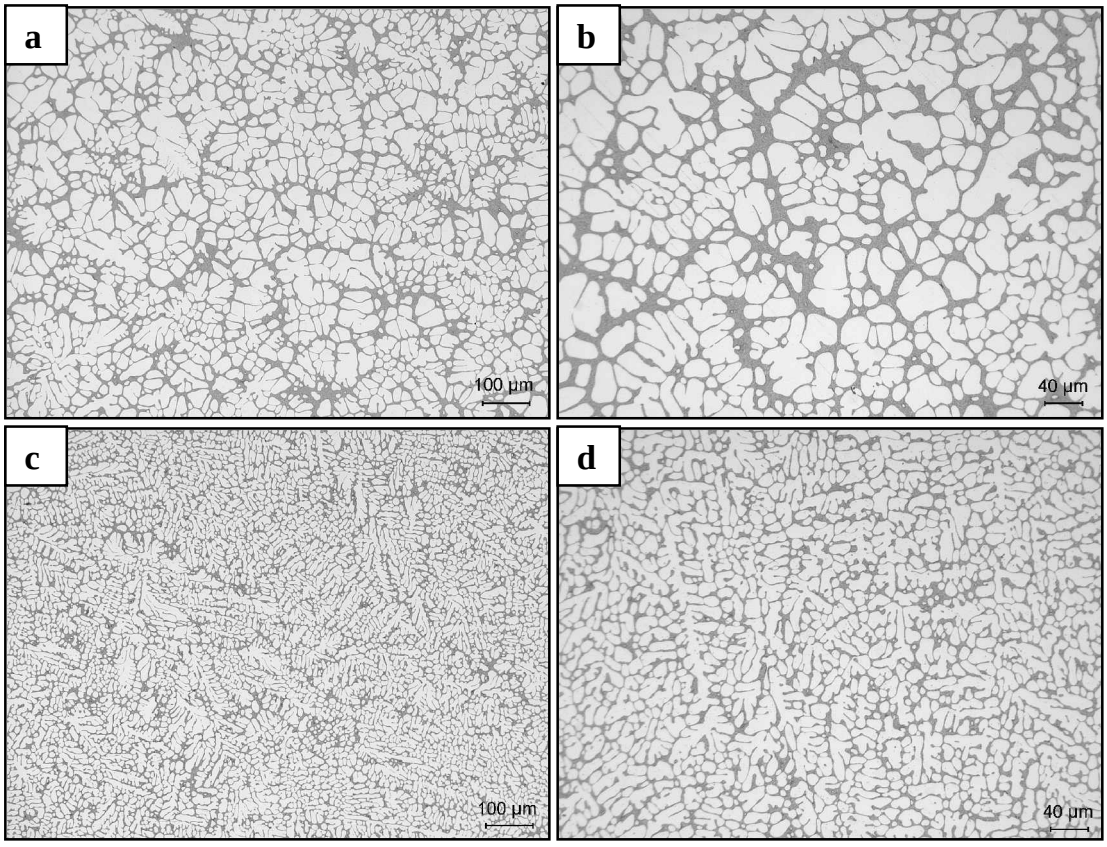

Figure 6.1. Microstructure of A356 alloy in as-received form: (a),(b) center; (c), (d) surface region

The semi-solid material used in this part of the study was A356 alloy fabricated by electro-magnetic stirring, made by SAG Company in Austria. The microstructure of the raw material is shown in Figure 6.1. The microstructure is composed of a eutectic phase and a primary aluminum phase broken up by electromagnetic stirring during solidification. Dendritic structure is fully broken in center region whereas in surface region there exists dendritic arms partially.

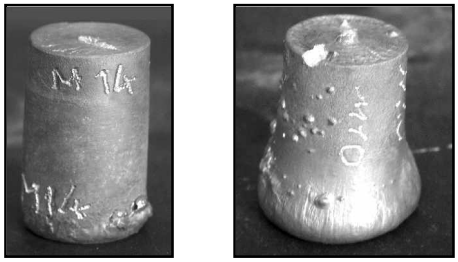

578 °C 584 °C

Figure 6.2. Deformed billet shapes resulting from the induction heating process

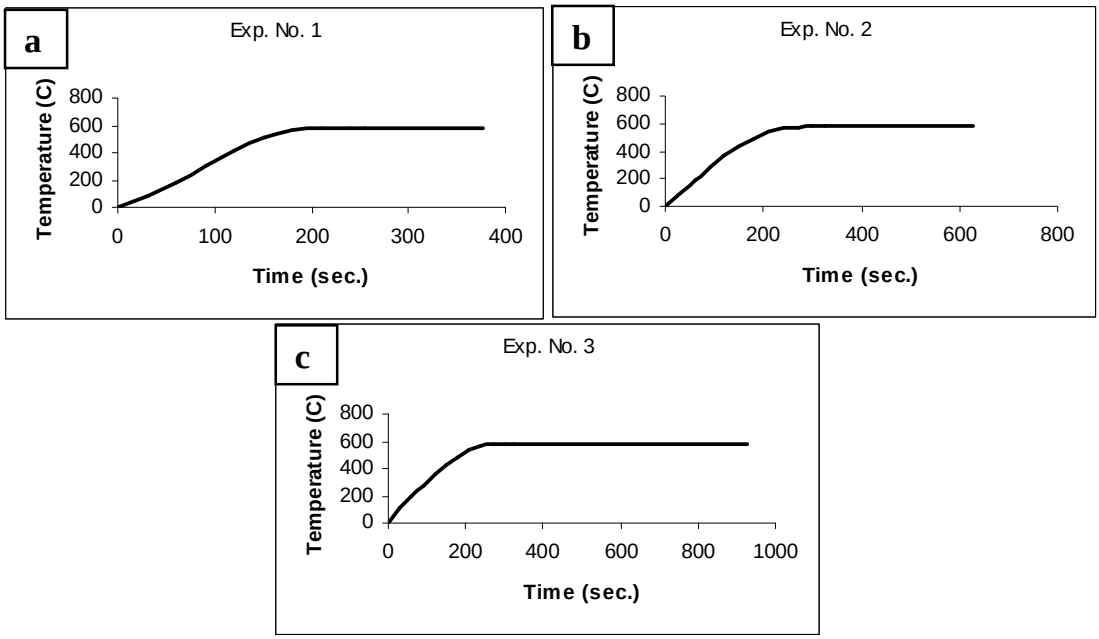

Figure 6.3. Heating curves in the one-step reheating process of A356 alloy (T_{h1} =584 °C): (a) experiment no. 1, t_{h1}=2 min; (b) experiment no. 2, t_{h1}=5 min, (c) experiment no. 3, t_{h1}=15 min

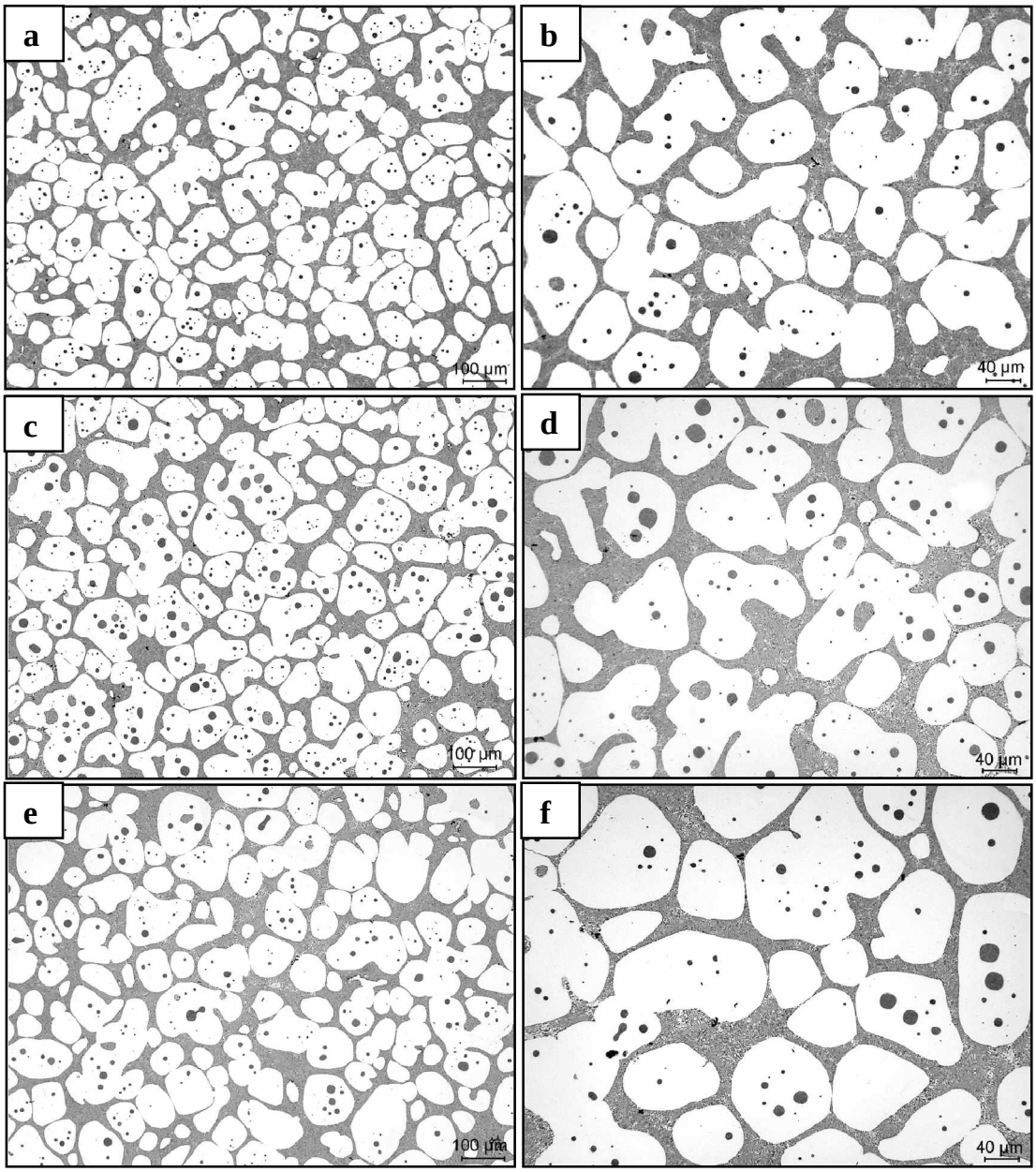

Figure 6.4. Microstructures in the one-step reheating process of A356 alloy (T_{h1} =584 °C): (a), (b) experiment no. 1, t_{h1}=2 min; (c), (d) experiment no. 2, t_{h1}=5 min, (e), (f) experiment no. 3, t_{h1}=15 min

One of the processing requirements with the MHD billet is that the billet must retain its shape during the reheating process. In induction heating experiments, two different semi-solid temperatures were applied: 578 °C and 584 °C. These temperatures correspond to the solid fractions of 55% and 50% in accordance with Figure 5.4. External appearance

of the billets heated to 578 °C and 584 °C and then quenched is shown in Figure 6.2. Deformation of the billet which was heated to 578 °C is small, whereas the billet of 584 °C deforms to elephant foot shape by its own weight.

For experiment nos. 1-11, the reheating experiments were performed for 584 °C which corresponds to solid fraction of 50%. Experiment nos. 1-3 corresponds to one-step heating, experiment nos. 4-6 corresponds to two-step heating and experiment nos. 7-11 corresponds to three-step heating conditions.

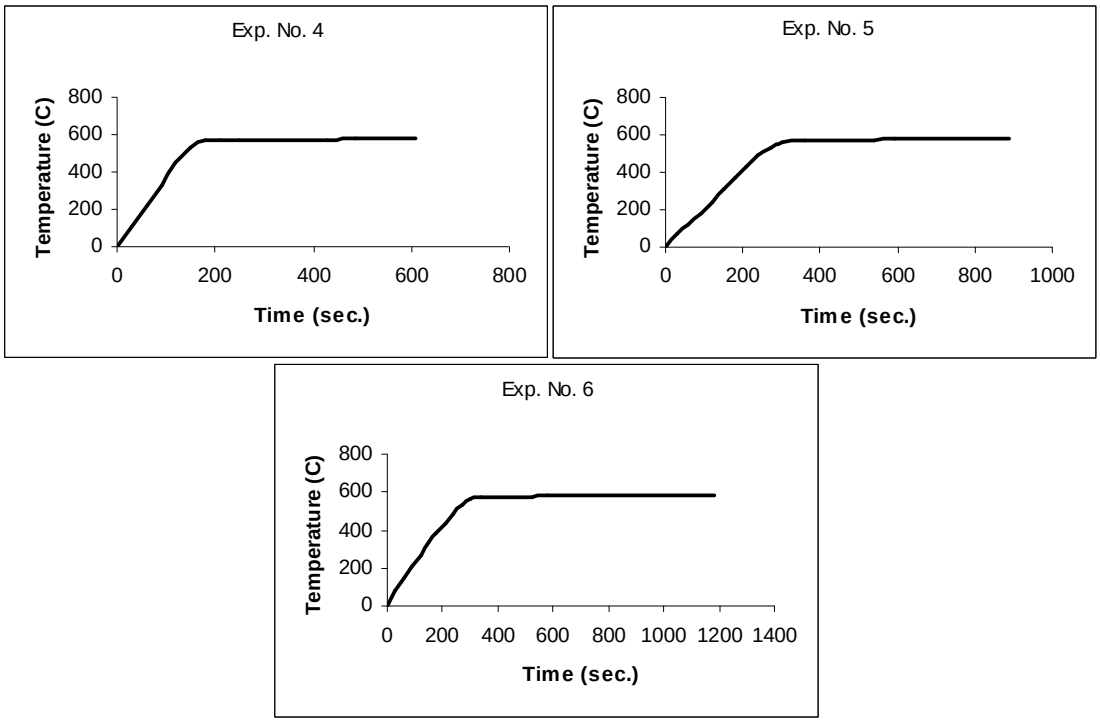

Figure 6.5. Heating curves in the two-step reheating process of A356 alloy (T_{h1} =575 °C, t_{h1} =3 min, T_{h2} =584 °C): (a) experiment no. 4, t_{h2}=2 min; (b) experiment no. 5, t_{h2}=5 min, (c) experiment no. 6, t_{h2}=10 min

Experiment numbers 1, 2 and 3 were performed under conditions of one-step heating with different holding times at 584 °C. Figure 6.3 shows the heating curves of those samples, and Figure 6.4 shows the microstructures of these specimens. As holding time increases, grain size increases and grains become more globular. Experiment number 1 shows a quite inhomogeneous microstructure that is surely not suitable for thixoforming.

Due to the lack of sufficient holding time for globularization of a small Si primary crystal, one-step heating with 2 minutes holding time is unsuitable. As holding time increases, the degree of inhomogeneity gradually decreases. However, it can be said that grain distribution is not homogenous for one-step heating. Microstructures consist of a significant amount of liquid entrapped within the grains.

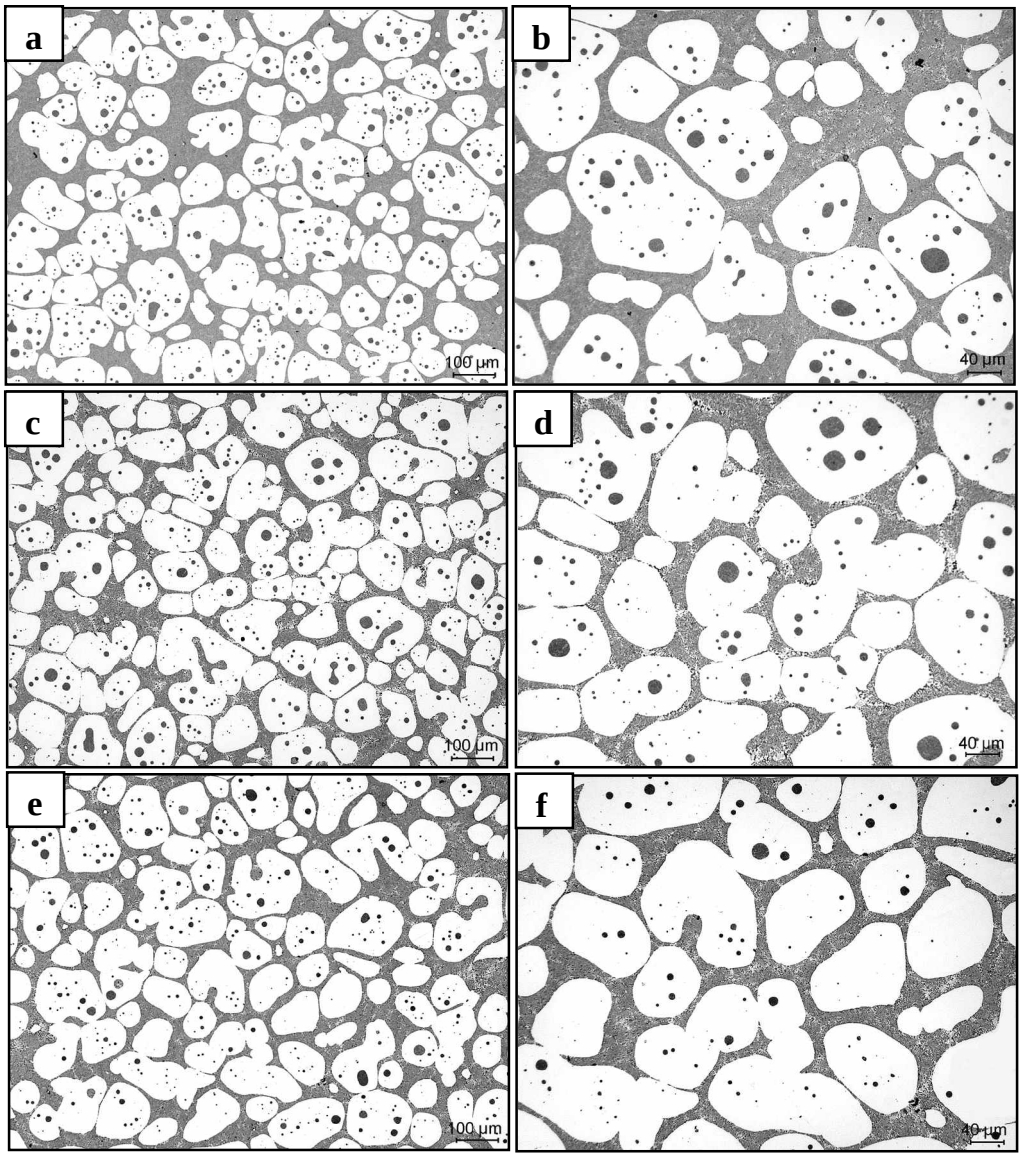

Figure 6.6. Microstructures in the two-step reheating process of A356 alloy (T_{h1} =575 °C, t_{h1} =3 min, T_{h2} =584 °C): (a), (b) experiment no. 4, t_{h2}=2 min; (c), (d) experiment no. 5, t_{h2}=5 min, (e), (f) experiment no. 6, t_{h2}=10 min

Experiment number 4, 5 and 6 were performed under two step heating conditions with different holding times at 584 °C. Figure 6.5 and Figure 6.6 show the heating curves and microstructures of these specimens. Compared to one step heating, grain globularization is better but is not enough. Another feature is that the entrapped liquid decreases with increasing holding time.

Experiment number 7, 8, 9 and 10 were performed under three-step heating conditions with different final holding times. Figure 6.7 and Figure 6.8 show the heating curves and microstructures of these specimens. Comparing Figure 6.8 and Figure 6.6, it can be concluded that microstructure of the specimens with three-step heating is finer and more globular than that of specimens with two step heating.

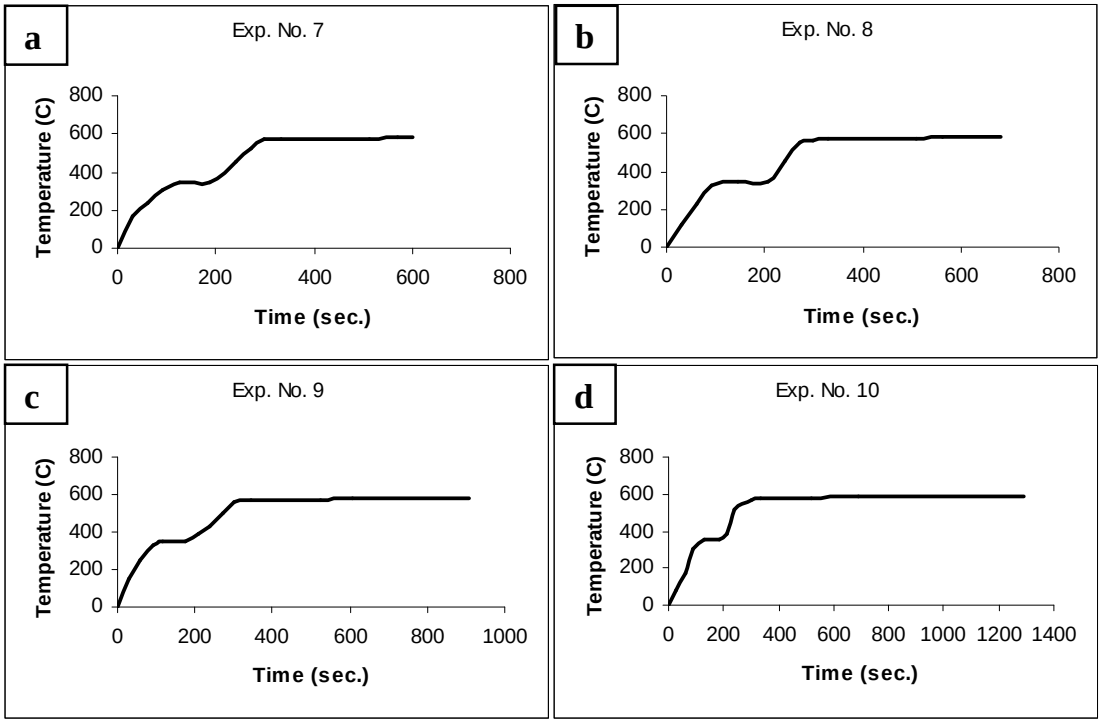

Figure 6.7. Heating curves in the three-step reheating process of A356 alloy (T_{h1} =350 °C, t_{h1} =1 min, T_{h2} =575 °C, t_{h2} =3 min, T_{h3} =584 °C): (a) experiment no.7, t_{h3}=0.5 min; (b) experiment no. 8, t_{h3}=2 min, (c) experiment no. 9, t_{h3}=5 min, (d) experiment no.10, t_{h3}=10 min

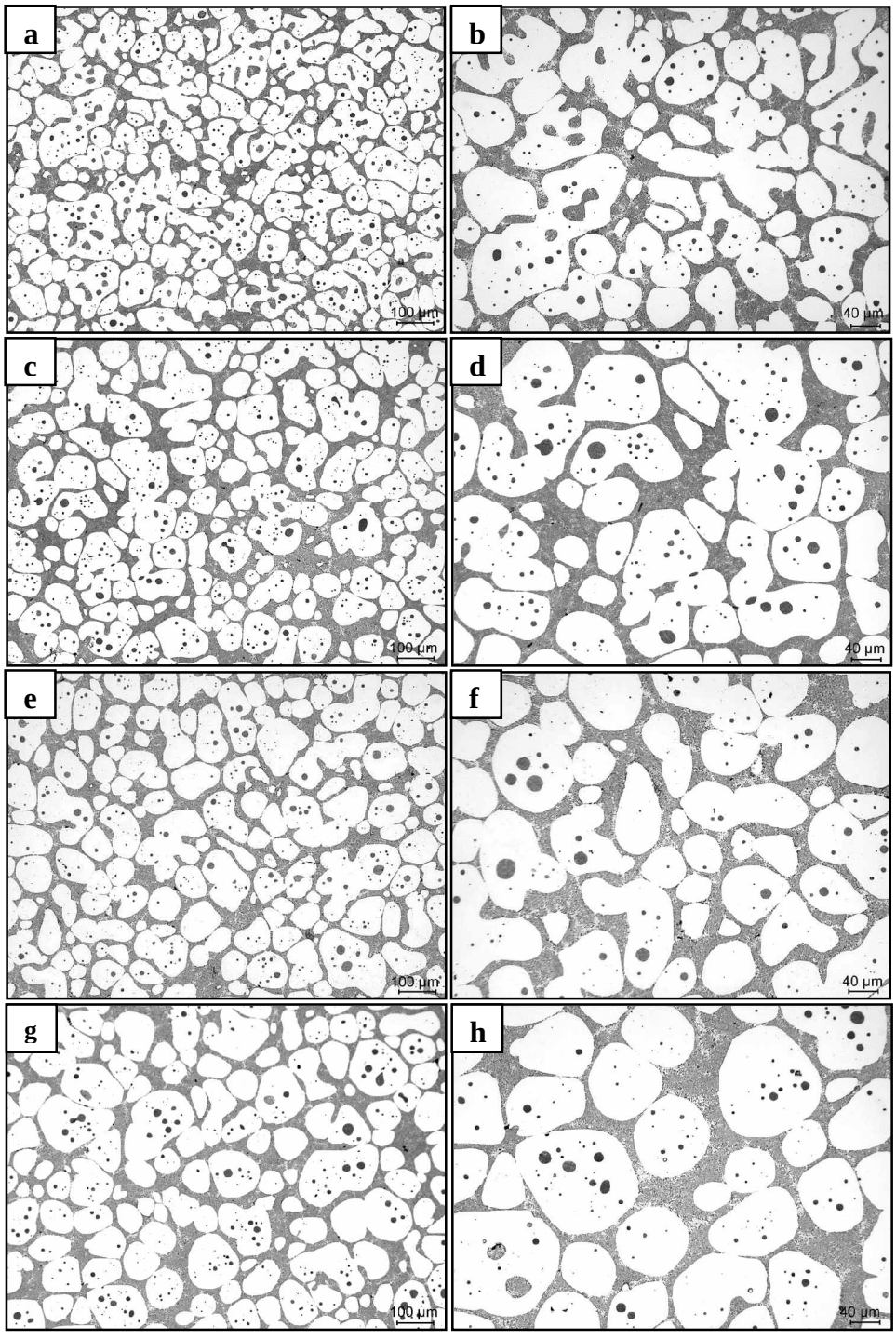

Figure 6.8. Microstructures in the three-step reheating process of A356 alloy (T_{h1} =350 °C, t_{h1} =1 min, T_{h2} =575 °C, t_{h2} =3 min, T_{h3} =584 °C): (a),(b) experiment no. 7, t_{h3}=0.5 min; (c),(d) experiment no. 8, t_{h3}=2 min, (e),(f) experiment no. 9, t_{h3}=5 min, (g),(h) experiment no. 10, t_{h3}=10 min

The holding time of the final step is very important in the three-step reheating process. As shown in Figure 6.8 (a) and (b), if the holding time of the final step is short, the microstructure of globularization is not obtained, due to the lack of sufficient holding time for the separation between solid and a liquid, before and after phase change, and for globularization of the solid particles. On the other hand, if the holding time of the final step is too long, the microstructure becomes coarse, due to the cohesion of the solid regions and the decrease in the liquid regions, as shown in Figure 6.8 (e) and (f). Therefore, the optimal holding time of the final step to obtain a fine globular microstructure without agglomeration seems to be 5 minutes in three-step heating.

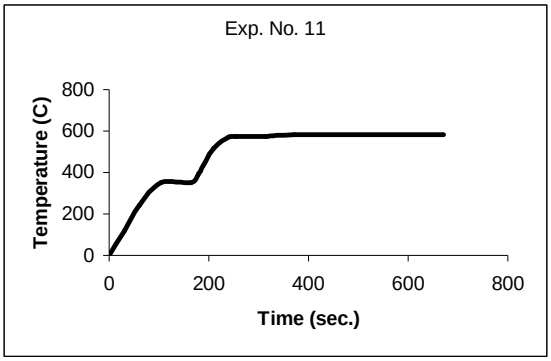

Figure 6.9. Heating curve of the specimen with heating conditions T_{h1} =350 °C, t_{h1} =1 min, T_{h2} =575 °C, t_{h2} =1 min, T_{h3} =584 °C, t_{h3} =5 min (experiment no. 11)

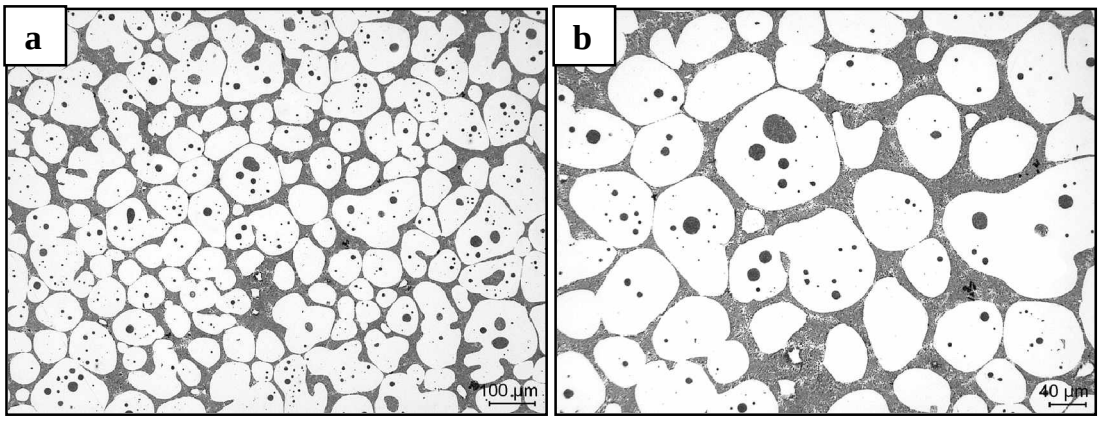

Figure 6.10. Microstructure of the specimen with heating conditions T_{h1} =350 °C, t_{h1} =1 min, T_{h2} =575 °C, t_{h2} =1 min, T_{h3} =584 °C, t_{h3} =5 min

Experiment number 11 was performed under three step heating condition with T_{h1} =350 °C, t_{h1} =1 min, T_{h2} =575 °C, t_{h2} =1 min, T_{h3} =584 °C, t_{h3} =5 min. Only holding time at 575 °C was changed from 3 minutes to 1 minute compared to experiment no. 9. Heating curve is shown in Figure 6.9 and the microstructure is shown in Figure 6.10. Holding for 1 minute at 575 °C gives finer and more globular microstructure compared to 3 minutes.

For experiment nos. 12-14, the reheating experiments were performed for 578 °C or 55% solid fraction. Experiment no. 12 corresponds to one-step heating, experiment no. 13 corresponds to two-step heating and experiment nos. 14 reflects to three-step heating conditions.

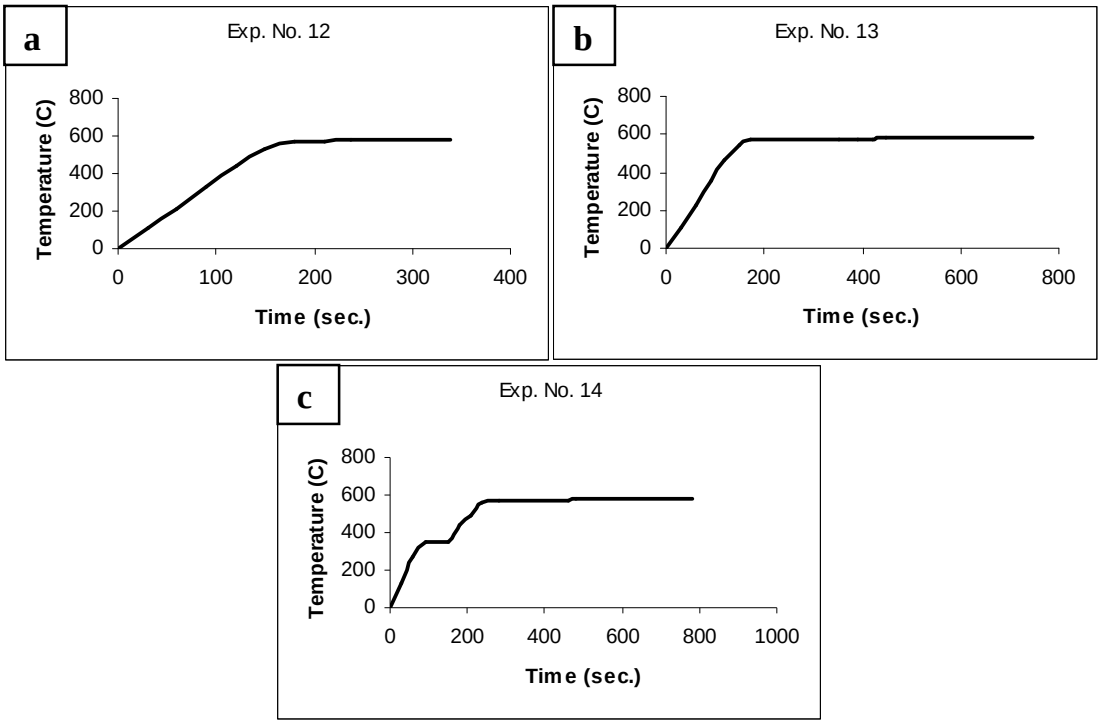

Figure 6.11. Heating curves for final holding temperature of 578 °C: (a) experiment no. 12, T_{h1} =578 °C; (b) experiment no. 13, T_{h1} =570 °C, t_{h1} =3 min, T_{h2} =578 °C, t_{h2} =5 min; (c) experiment no. 14, T_{h1} =350 °C, t_{h1} =1 min, T_{h2} =570 °C, t_{h2} =3 min, T_{h3} =578 °C, t_{h3} =5 min

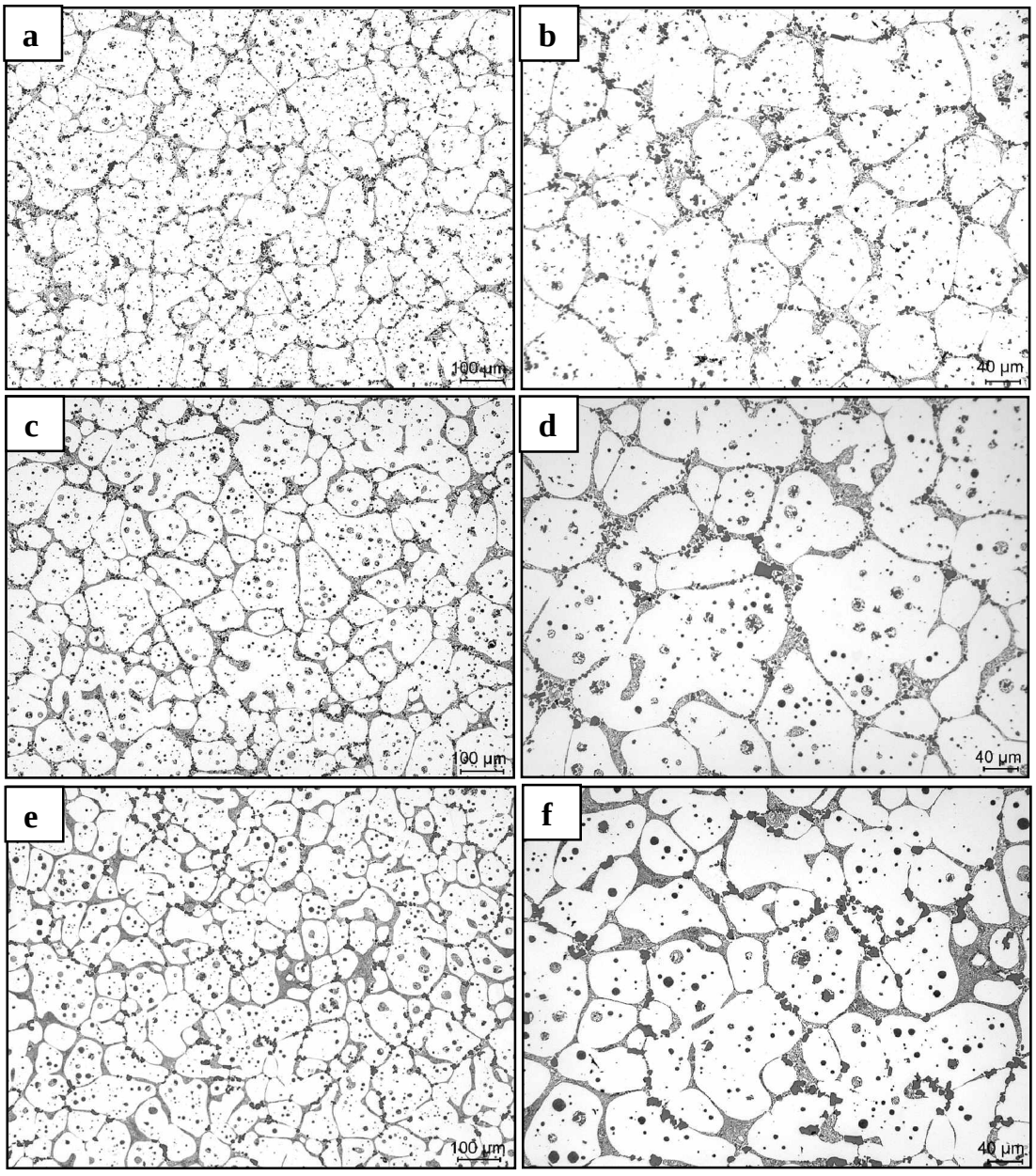

Figure 6.12. Microstructures for final holding temperature of 578 °C: (a), (b) experiment no. 12, Th1 =578 °C, th1 =5 min; (c), (d) experiment no. 13, Th1 =570 °C, th1 =3 min, Th2 =578 °C, th2 =5 min; (e), (f) experiment no. 14, Th1 =350 °C, th1 =1 min, Th2 =570 °C, th2 =3 min, Th3 =578 °C, th3 =5 min

In experiment number 12, the specimen was heated to 578 °C at one step and hold for 5 minutes. Experiment number 13 was performed under two step heating condition with T_{h1} =570 °C, t_{h1} =3 min, T_{h2} =578 °C, t_{h2} =5 min. Experiment number 14 was

performed under three step heating condition with T_{h1} =350 ℃, t_{h1} =1 min, T_{h2} =570 °C, t_{h2} =3 min, T_{h3} =578 °C, t_{h3} =5 min. The heating curves and microstructures of these specimens are shown in Figure 6.11 and Figure 6.12. The advantage of three-step heating seems more clearly for 578 °C. The boundary between solid and liquid regions is clearer in three-step heating. From Figure 6.12 (a) and (b), it can be concluded that one-step reheating is not a good process, because the size of the solid particles is small, and the microstructure of globularization is not obtained. 578 °C corresponds to higher solid fraction than 584 ℃, and it was found that the higher the solid fraction, the worse the accuracy of globularization.

As shown from the above micrographs, three-step reheating is better than two-step reheating with respect to small solid particles and the accuracy of globularization. Finest globular microstructure was achieved in experiment number 11 which was performed under three-step heating conditions with T_{h1} =350 °C, t_{h1} =1 min, T_{h2} =575 °C, t_{h2} =1 min, T_{h3} =584 ℃, t_{h3} =5 min.

It was found that the eutectic is melted completely at over 575°C, complete eutectic melting being necessary to obtain a fine globular microstructure. The temperature rise does not occur until sufficient thermal energy is provided to melt the eutectic, much thermal energy and time being necessary. Before and after the melting of the eutectic, the solid fraction is rapidly changed, and a rapid temperature rise occurs when the eutectic is melted. Due to this temperature rise, the temperature difference becomes large, and controlling the reheating temperature is difficult. Therefore, to homogeneously control the temperature distribution and the solid fraction of the semi-solid material, the billet must be reheated in three steps.

6.2. Thixotropic Feedstock Production for AA6082 via SIMA Process

Figure 6.13 shows as-cast microstructure of AA6082 aluminum alloy. This AlMgSi alloy includes Fe and Mn at relatively high content and is typically composed of AlFe(Mn)Si compound particles arranged in dendrite boundaries.

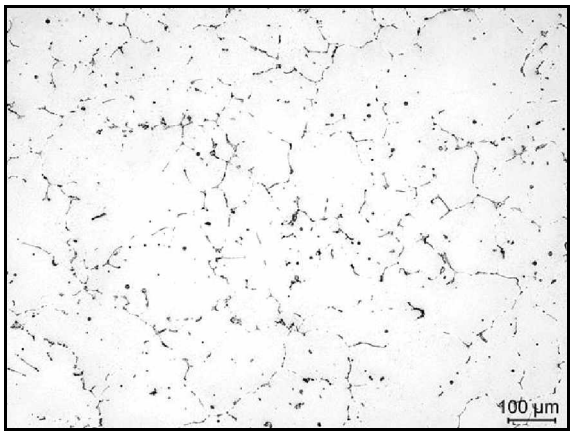

Figure 6.13. As-cast structure of 6082 alloy after casting to 100 mm diameter

6082 aluminum alloy was extruded from 100 mm diameter to 27 mm (extrusion ratio ~13:1) and 44 mm diameter (extrusion ratio ~5:1). Microstructures along longitudinal section of extruded specimens are shown in Figure 6.14. It can be seen that grains are elongated in the extrusion direction and AlFeSi intermetallic compounds are arranged in the extrusion direction.

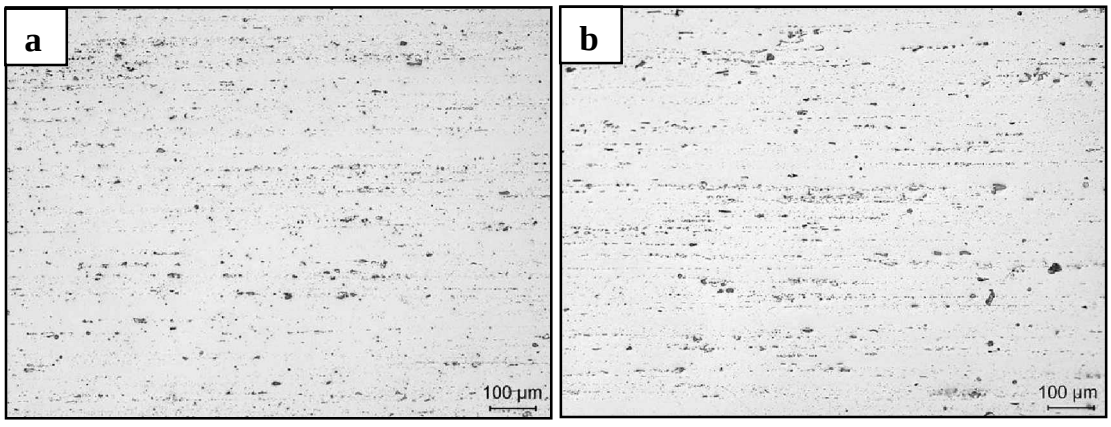

Figure 6.14. Microstructures after hot extrusion of 6082 alloy which was extruded from 100 mm to (a) 27 mm and (b) 44 mm

For determination of appropriate semi-solid temperature for AA6082 aluminum alloy, different specimens of 27 mm diameter were reheated to 630°C, 635°C, 640°C, and 645°C and hold for 5 minutes. The microstructures after reheating are shown in Figure 6.15. For the specimens of 630°C and 635°C, the lack of liquid phase is easily observed

from Figure 6.15. Moreover, grain boundaries are not clear for these two specimens at the end of 5 minutes holding time. It can be concluded that 630°C and 635°C are not enough for thixoforming. As the reheating temperature increases, the amount of liquid phase increases and grains become clearer as a result of penetration of liquid phase into grain boundaries. As one can see from Figure 6.15 (c) and (d), for 640°C and for especially 645°C liquid phase decorates grain boundaries.

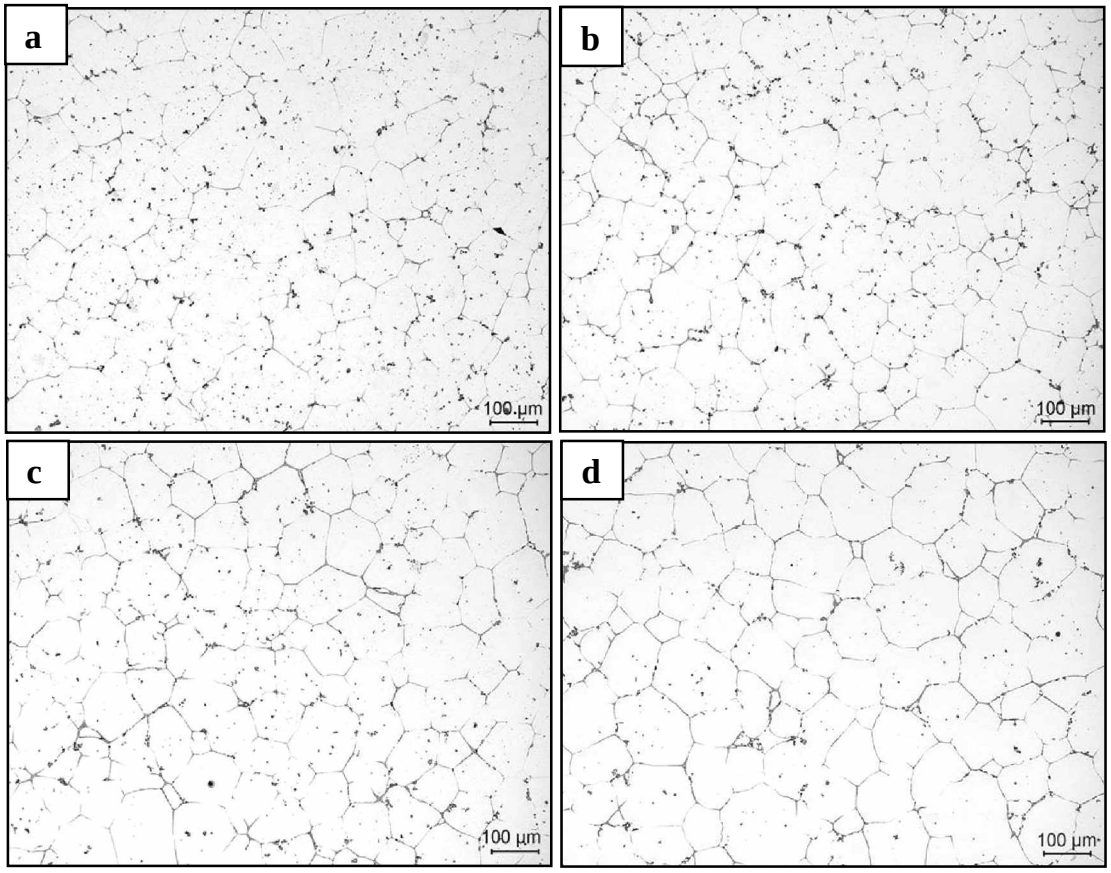

Figure 6.15. Microstructures of the samples of 27 mm diameter after reheating to (a) 630°C, (b) 635°C, (c) 640°C and (d) 645°C then holding for 5 minutes

In addition to above experiments where holding time is fixed and reheating temperature changes, some trials were also made by keeping reheating temperature fixed and varying holding time. By increasing the holding time, microstructural variations at low semi-solid temperatures were observed. In Figure 6.16, the microstructures of the specimens (27 mm diameter) which were heated to 630 °C and hold at that temperature for several holding times up to 30 minutes are seen. It can be seen that even for longer holding

times at 630 °C, grain boundaries are not clear and appropriate thixotropic structure does not form. Thus, it can be said that the amount of liquid phase is insufficient for 630 °C. As a result of above experiments, it can be easily concluded that reheating temperature is a more effective parameter compared to the holding time for thixotropic formation. Because, structural evolution seems to be very clear when heating temperature is increased while keeping holding time fixed (Figure 6.15). However for lower heating temperatures, increasing holding time has not much effect on thixotropic formation as shown in Figure 6.16.

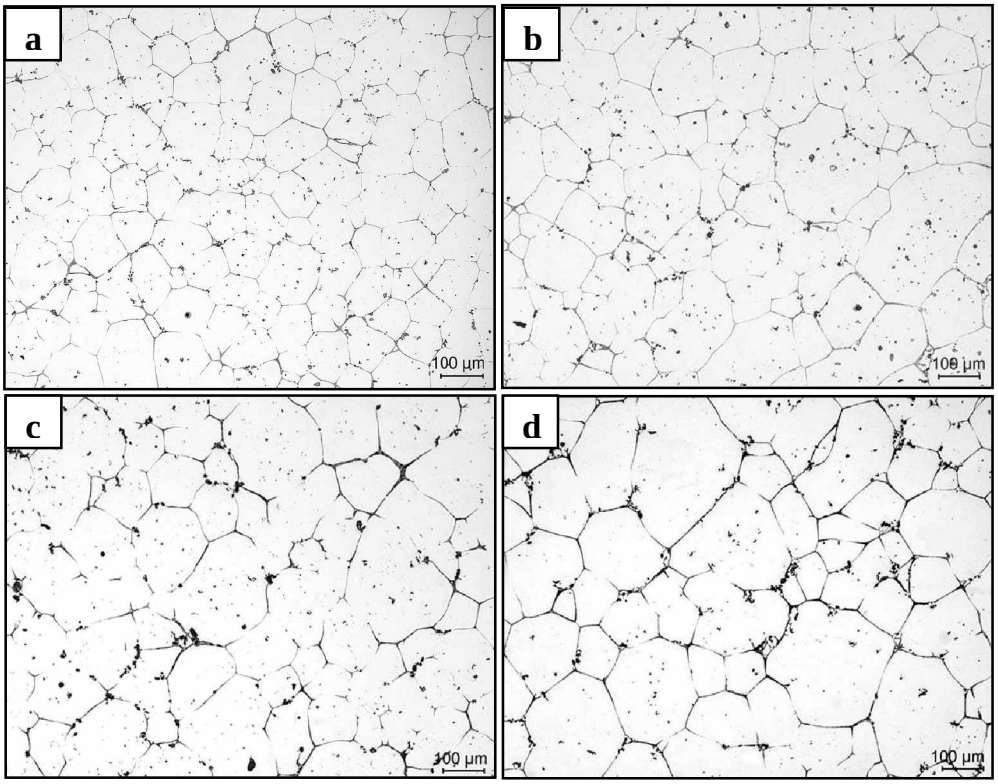

Figure 6.16. The microstructures of the specimens (27 mm diameter) which were hold at 630 °C for (a) 10, (b) 15, (c) 20 and (d) 30 minutes

From above experiments, it was concluded that 640 °C and 645 °C are appropriate temperatures for thixoforming. Macro appearance of reheated billets is particularly important in thixoforming. The billets must retain their shape after reheating phase. External appearance of several billets that were heated to 640 °C and 645 °C is shown in Figure 6.17. Deformation of the billet which was heated to 640 °C is small, whereas the

billet of 645 °C deforms to elephant foot shape by its own weight.

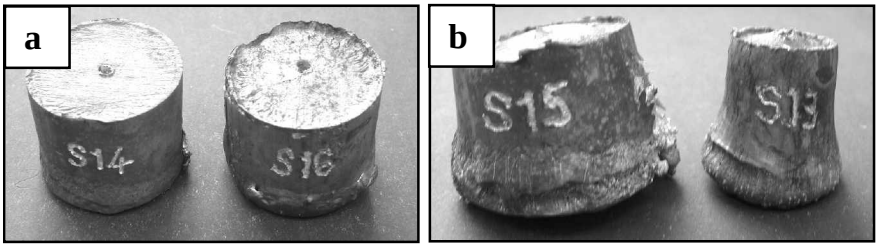

Figure 6.17. External appearance of the billets heated to 640 °C (a) and 645 °C (b)

In Figure 6.18 microstructures of specimens (27 mm diameter) subjected to several holding times at 640 °C are shown. After 20 minutes holding time, transformation into proper semi-solid slurry is completed and further holding leads to undesirable grain growth as shown in Figure 6.18 (d).

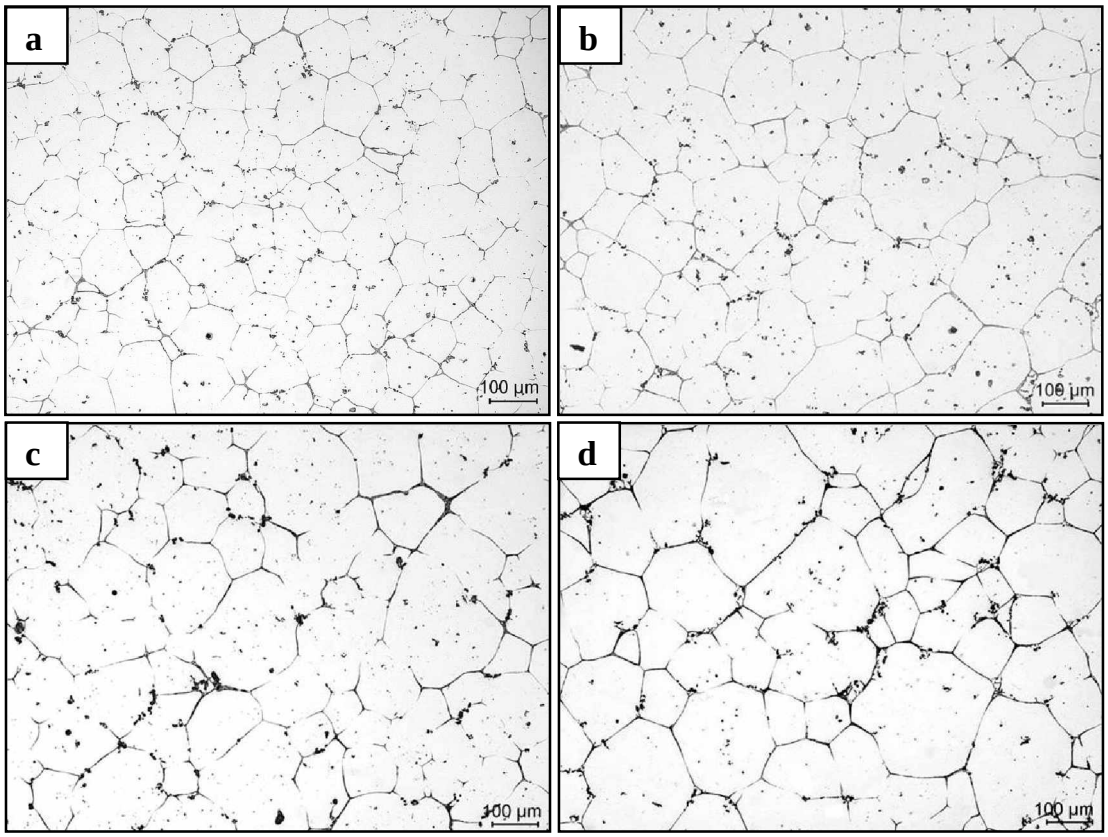

Figure 6.18. The microstructures of the specimens (27 mm diameter) which were hold at 640 °C for (a) 10, (b) 15, (c) 20 and (d) 30 minutes

Figure 6.19 represents the microstructures of specimens (27 mm diameter) which are subjected to several holding times at 645 °C. As shown in Figure 6.19 (c), after 15 minutes holding time appropriate thixotropic structure is obtained. Grains take hexagonal shape with increasing holding time because hexagon is thermodynamically more steady structure. As holding time increases, liquid occurs in form of fine crystals and α grain sizes gradually grow larger along with more spherical shape. At 645 °C, grains begin to take spherical shape after 15 minutes holding time for specimens with 27 mm diameter as shown in Figure 6.19 (c).

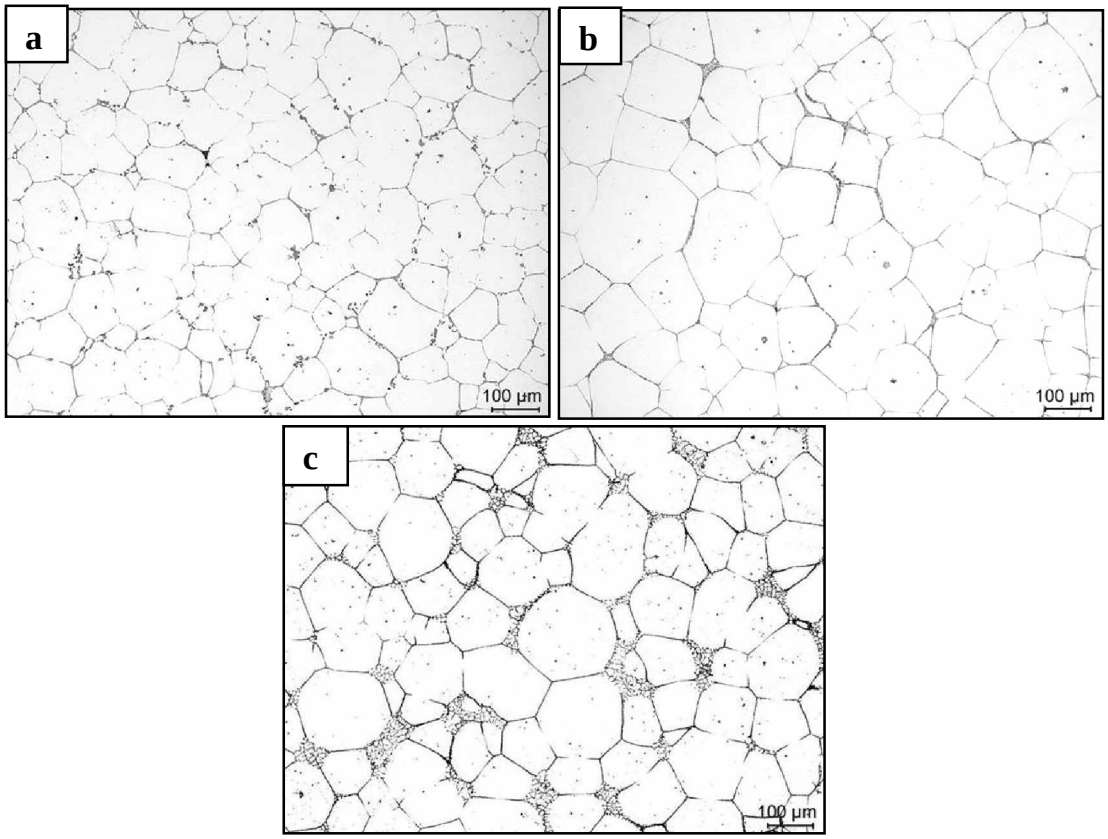

Figure 6.19. The microstructures of the specimens (27 mm diameter) which were hold at 645 °C for (a) 5, (b) 10, and (c) 15 minutes

Figure 6.20 and Figure 6.21 shows the microstructures of the 44 mm diameter specimens subjected to several holding times at 640 °C and 645 °C. Evolution of grain structure is clearer at 645 °C compared to 640 °C. As the holding time increased, the grains became more spheroidal in appearance and the liquid film became thicker.

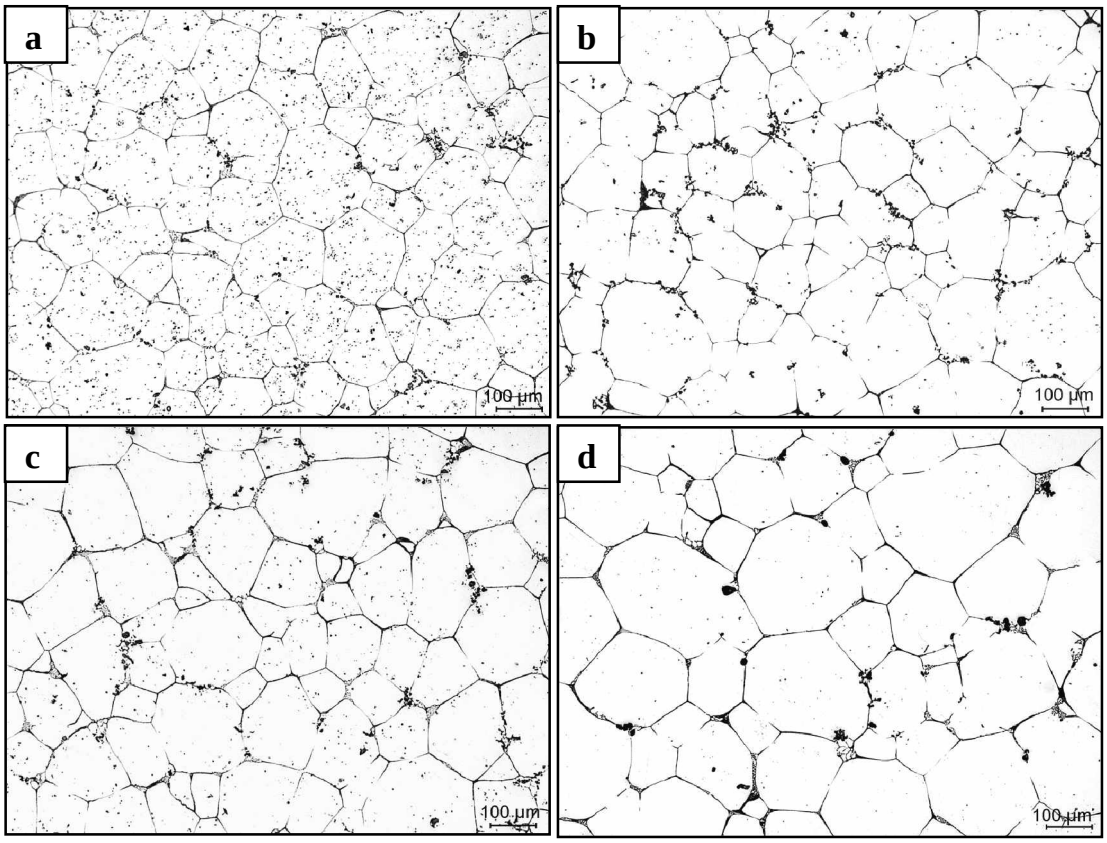

Figure 6.20. The microstructures of the specimens (44 mm diameter) which were hold at 640 °C for (a) 10, (b) 15, (c) 20 and (d) 30 minutes

It was observed that the degree of deformation during extrusion process influences the formation of thixotropic structure readily. It has a serious effect on grain size and morphology. For comparison, two kinds of specimen groups having different extrusion ratios were subjected to the same experimental conditions. As an example, the microstructures of the specimens of both 27 mm and 44 mm diameter subjected to 5 minutes holding time at 645 °C are shown in Figure 6.22. It can be seen from Figure 6.22 that as extrusion ratios increases grains disperse more homogeneously and grain size decreases. However; with increasing holding time, the effect of extrusion ratio on grain size is smaller. Specimens having 27 mm diameter have more homogeneity and smaller grain size than specimens having 44 mm diameter. Moreover, in accordance with Figure 6.19 and Figure 6.21 it can be said that liquid emerges earlier in the specimen with greater deformation ratio.

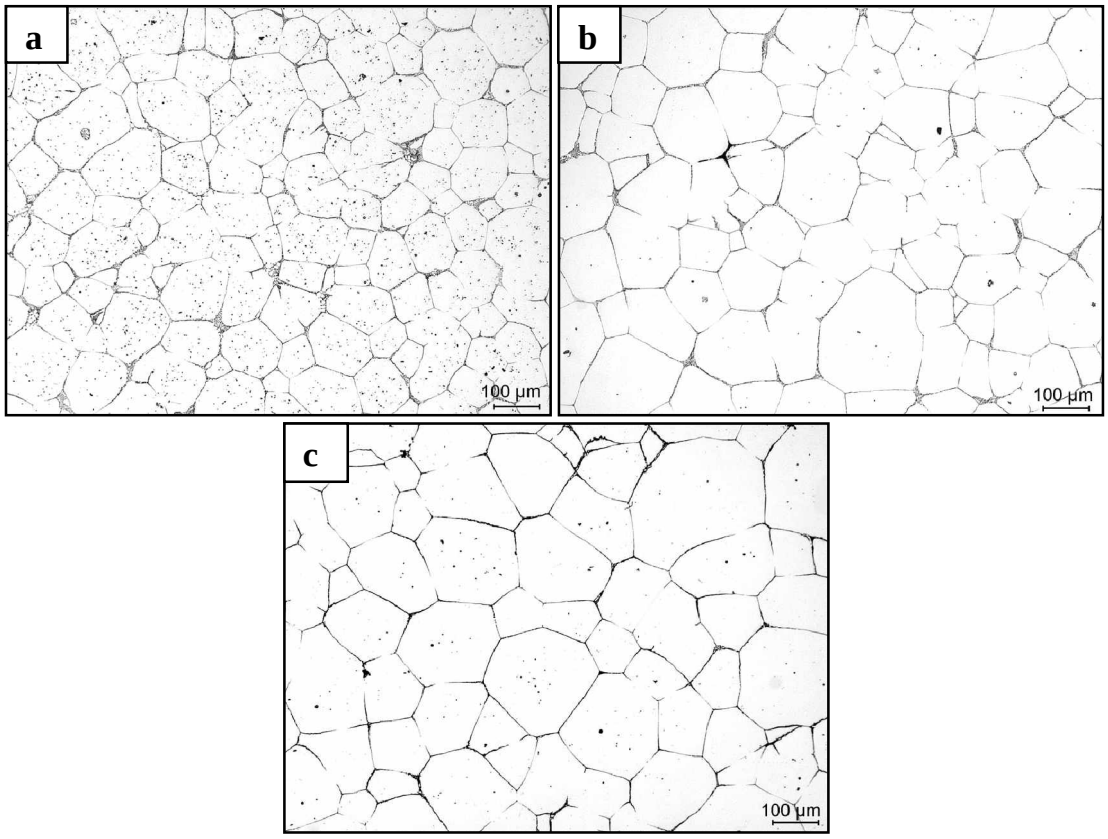

Figure 6.21. The microstructures of the specimens (44 mm diameter) which were hold at 645 °C for (a) 5, (b) 10, and (c) 15 minutes

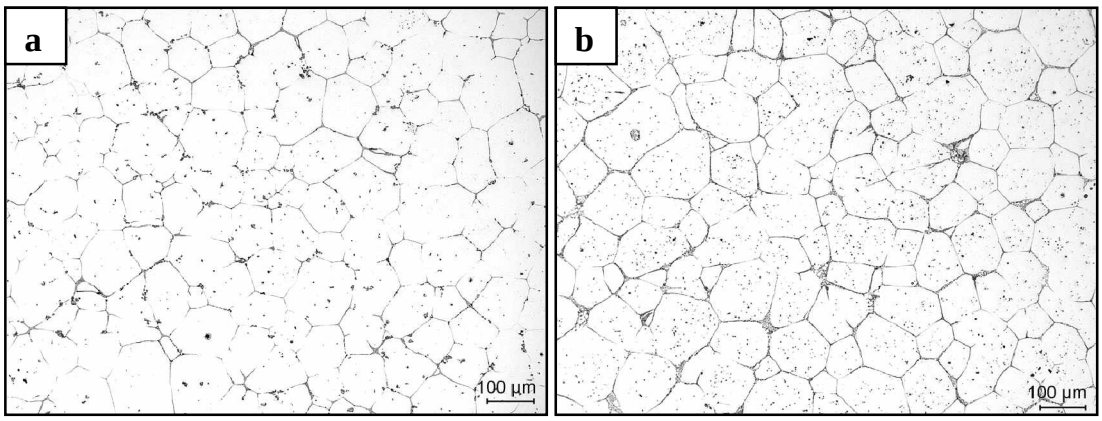

Figure 6.22. Microstructures of the specimens of (a) 27 mm and (b) 44 mm subjected to 5 minutes holding time at 645 °C

As shown in Figure 6.23, uncrystallized large grains are retained over all surface layers of which thickness approximately measured 3-4 mm. It is believed that lack of deformation on surface regions due to friction between die surface and extruded materials may become one reason for abnormal microstructures of surface layer. Due to the lack of deformation, recrystallization does not occur in these regions thus grains remain large in size.

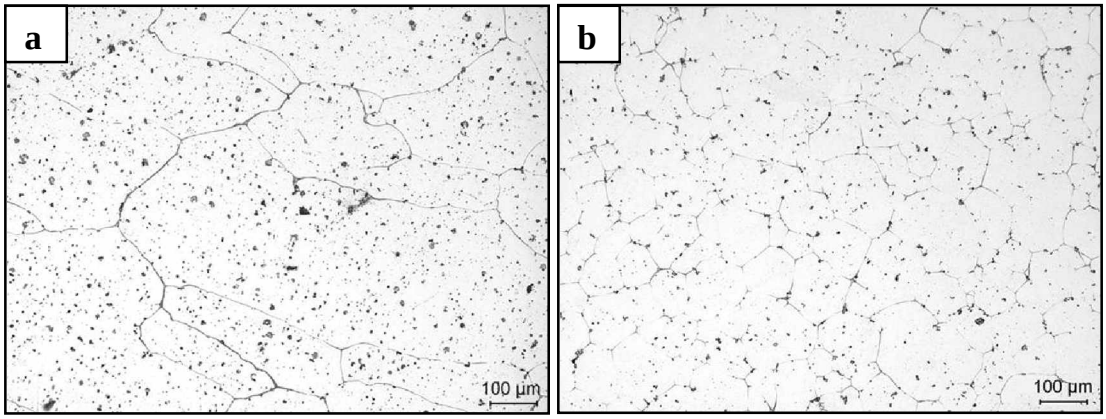

Figure 6.23. Microstructures of (a) surface region and (b) center of reheated samples

6.3 Thixoforming of A356 and AA6082 Aluminum Alloys

6.3.1. External Appearance of Thixoformed Parts

External view of thixoformed parts is shown in Figure 6.24 and Figure 6.25. Samples shown in Figure 6.24 were prepared for microstructural evaluation and hardness tests whereas samples shown in Figure 6.25 were prepared for tensile tests. Thixoforming trials were executed considering most successful heating conditions according to microstructural images found in Section 6.1 and Section 6.2. In this respect, four different heating conditions were applied for A356 and two different heating conditions for AA6082. Applied experimental conditions are as shown in Table 5.7.

Through the application of proposed press technology, several parts were produced. From Figure 6.24 and Figure 6.25, it is clear that complete die filled shape could be obtained. Although significant material flow (i.e. large deformation) occurred during

thixoforming, the material filled the cavity of die easily under experimental conditions. Surface of these parts also shows good condition. It is noteworthy that sticking tendency of a part toward die surface is higher for the parts formed using AA6082 than the parts formed using A356 because of higher working temperature of AA6082.

Figure 6.24. External appearance of thixoformed parts for microstructural evaluation and hardness tests

Figure 6.25. External appearance of thixoformed parts for tensile tests

6.3.2. Microstructural Investigation

Through microstructural examination of thixoformed parts, fine globular microstructures, which are characteristic microstructures of thixoformed parts, were observed in most of the cross-sectional area of a part.

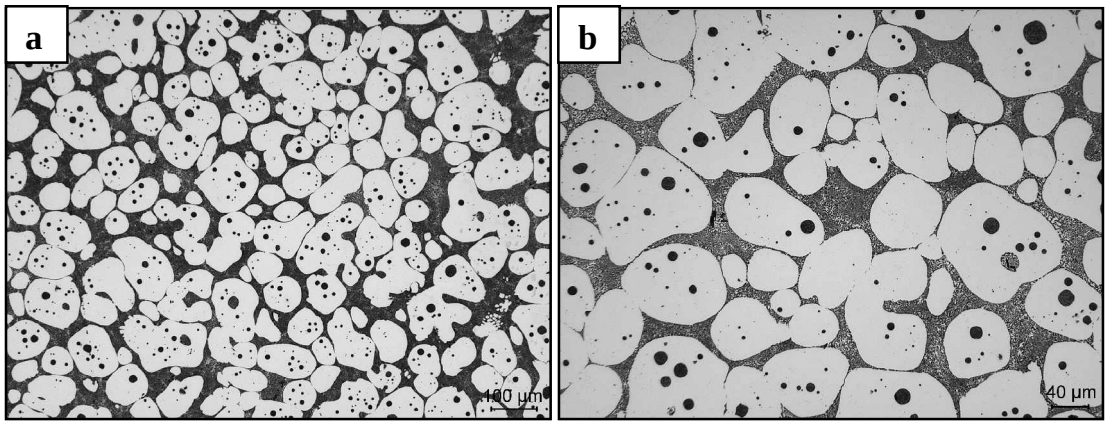

Figure 6.26. Microstructure of thixoformed A356 alloy in one step heating process, which were hold at 584 °C for 5 minutes

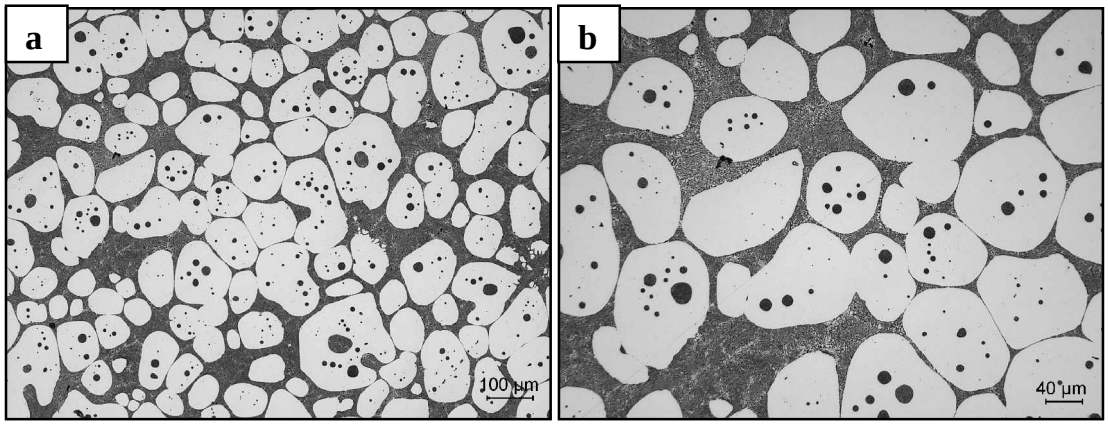

Figure 6.27. Microstructure of thixoformed A356 alloy in one step heating process, which were hold at 584 °C for 15 minutes

Figure 6.26 to Figure 6.29 shows typical microstructures of A356 alloy thixoformed under different heating conditions. In this alloy, the solid particles are surrounded by the liquid phase and the deformation is achieved mainly by liquid flow. The white areas in the micrograph correspond to the solid phase in the semi-solid state while the darker regions

consist of very fine eutectic. Grains are almost equiaxed, uniformly distributed in the liquid phase. Microstructures of thixoformed components are very similar to microstructures of reheated and quenched billets of Section 6.1. This is due to the laminar flow conditions maintained during die fill and the rheological behaviour of semi-solid metal slurries. The unique feature of the thixoforming process is retention of the feedstock microstructure in the formed part. From Figure 6.26 to Figure 6.29, the coalesced silica crystals were not observed because eutectic was completely melted during reheating.

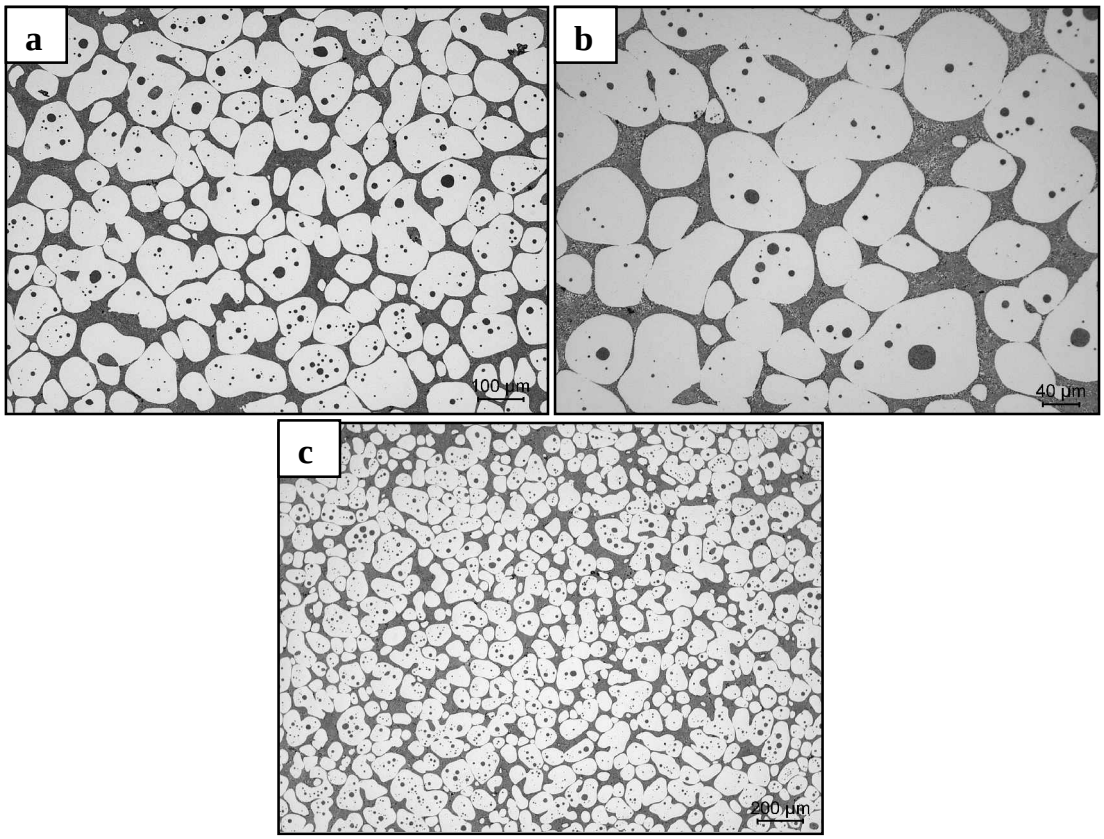

Figure 6.28. Microstructure of thixoformed A356 alloy in three- step heating process with T_{h1} =350 °C, t_{h1} =1 min, T_{h2} =575 °C, t_{h2} =1 min, T_{h3} =584 °C, t_{h3} =5 min

Figure 6.26 and Figure 6.27 corresponds to one-step heating with different holding times at 584 °C. As holding time increases, grain growth occurs. Grain globularization is completed after 5 minutes holding time and further holding leads to the coarsening of α-Al grains. Undesirable grain growth can decrease the mechanical properties. Both microstructures are successful; however, 5 minutes holding time is better in the point of

view of thixoformability.

Figure 6.28 and Figure 6.29 corresponds to three-step heating process. In both conditions, the distribution of grains is uniform throughout the specimen. In three-step heating, there is no much difference in grain sizes from one grain to another. The product with heating conditions T_{h1} =350 °C, t_{h1} =1 min, T_{h2} =575 °C, t_{h2} =1 min, T_{h3} =584 °C, t_{h3} =5 min (Figure 6.28) is the most successful one with respect to microstructures.

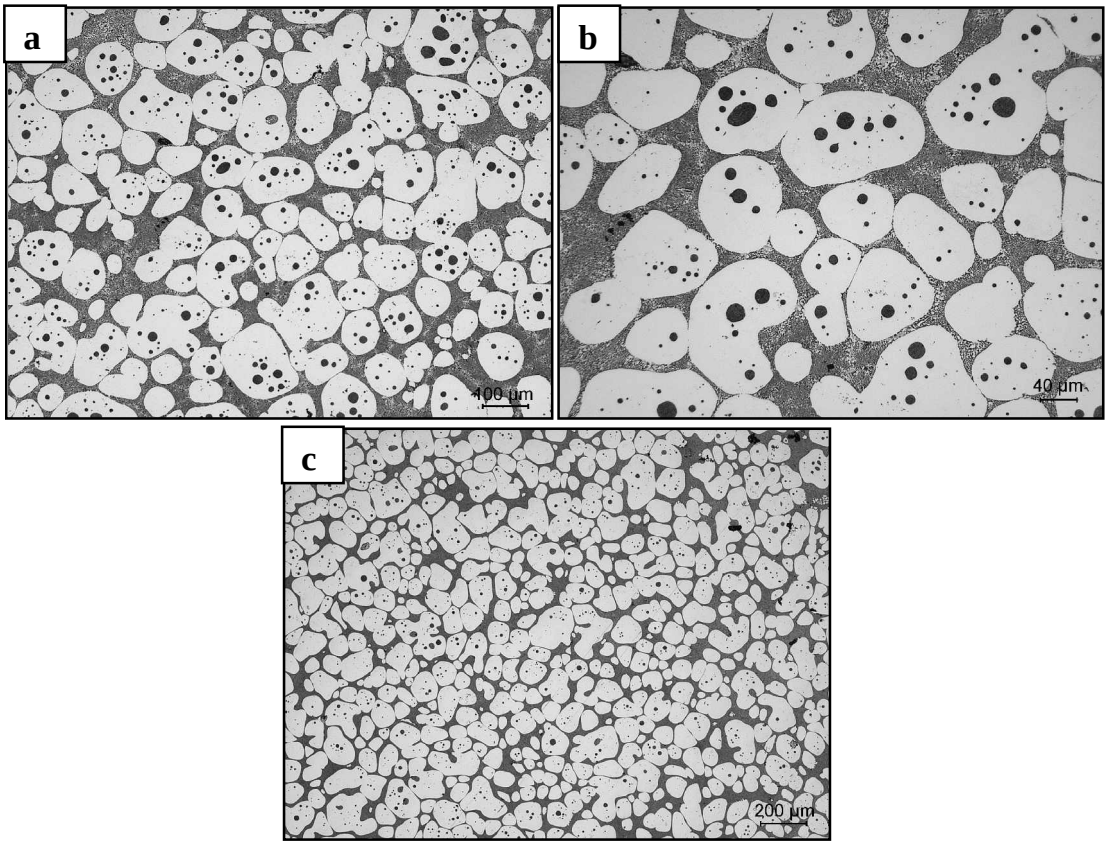

Figure 6.29. Microstructure of thixoformed A356 alloy in three- step heating process with T_{h1} =350 °C, t_{h1} =1 min, T_{h2} =575 °C, t_{h2} =3 min, T_{h3} =584 °C, t_{h3} =10 min

Figure 6.30 shows microstructure of thixoformed AA6082 alloy which was hold at 645 °C for 5 minutes. Total amount of liquid phase is quite insufficient in AA6082 alloy and solid particles contact each other. For this reason, the deformation in the semi-solid state originates mainly from the deformation of solid particles instead of movement of liquid phase. The result is segregation of solid and liquid phases. Figure 6.30 represents three different regions from this sample. It claims that the microstructure is very

heterogeneous. Liquid phase segregation was discovered in this sample, especially in second region (Figure 6.30 (b)). Grains have been elongated along the flow direction after thixoforming. This is due to the plastic deformation of solid grains. In third region of this part (Figure 6.30 (c)), primary grains remain largely unchanged.

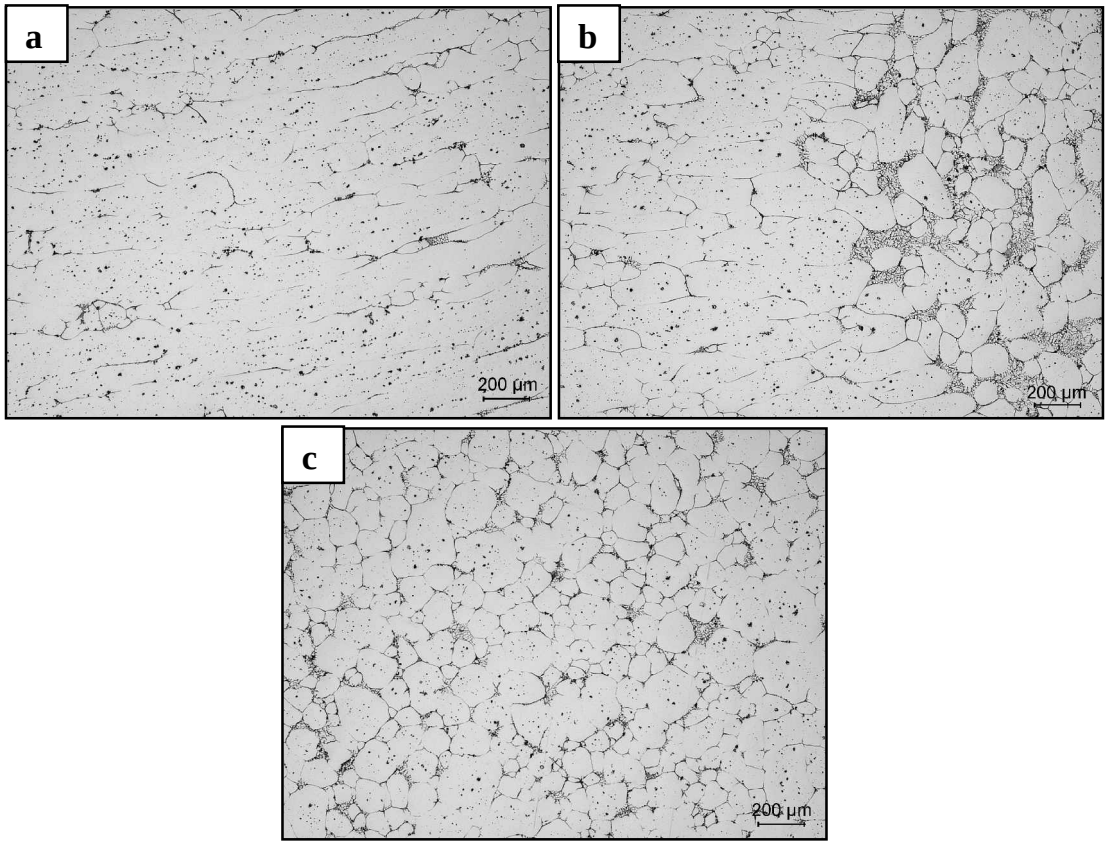

Figure 6.30. Microstructure of thixoformed AA6082 alloy under 5 minutes holding time at 645 °C

Figure 6.31 shows microstructure of thixoformed AA6082 alloy which was hold at 645 °C for 15 minutes. The clear difference of liquid phase fraction among three different regions can be confirmed from this figure. In Figure 6.31, liquid fraction is more intense in third region (Figure 6.31 (c)). Large elongated grains were also discovered in this sample, this is mainly because of deformation of solid grains during forming. The inhomogeneity of the microstructure may impair mechanical properties.

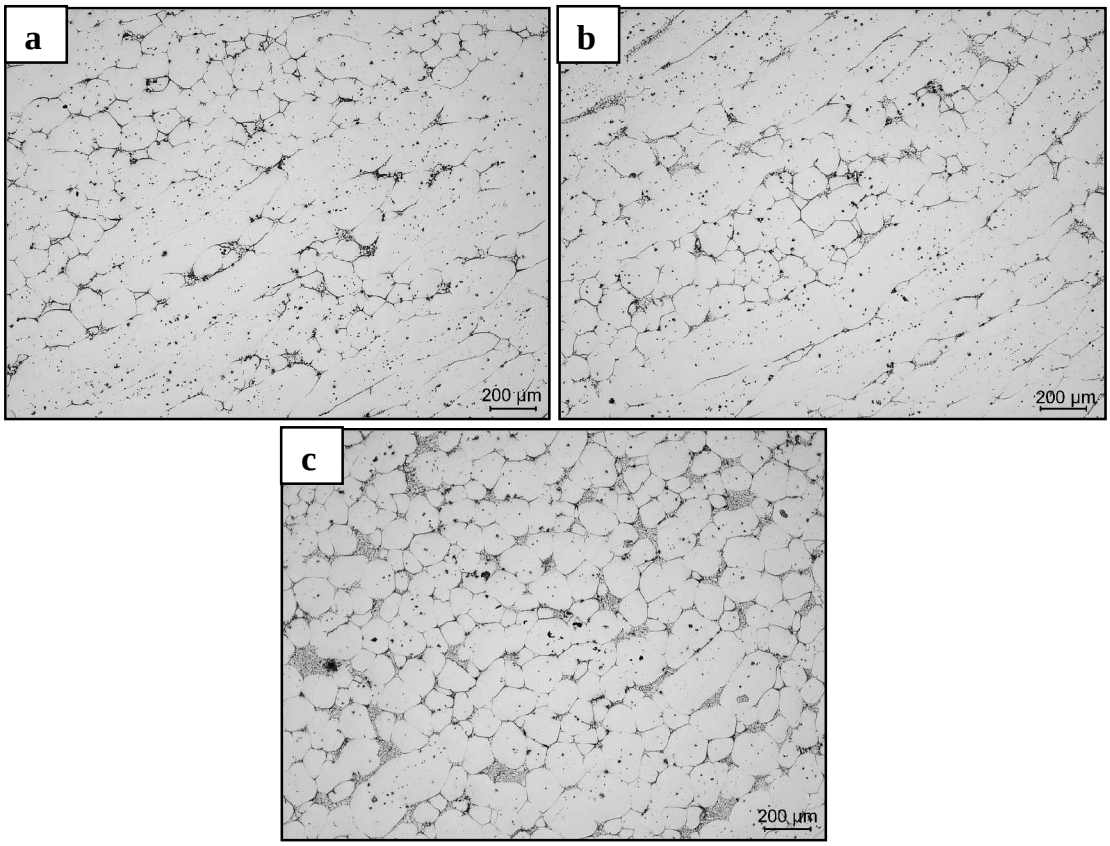

Figure 6.31. Microstructure of thixoformed AA6082 alloy with 15 minutes holding time at 645 °C

6.3.3. Mechanical Properties

Prior to forming, grains have to be as spherical as possible, in order to increase the fluidity of the semi-solid slurry. In addition, grain growth has to be minimal so that the final product has a small grain size exhibiting acceptable mechanical properties [19].

Figure 6.32 shows the hardness values before T6 heat treatment measured at each position in Figure 5.9. Experimental conditions corresponding to each product number is as shown in Table 5.7. For A356 alloy, the hardness values alter between 61-79 HV. For 6082 alloy, the hardness values alter between 45-56 HV. There is no general increasing or decreasing tendency of hardness values neither in longitudinal nor in transversal sections for any product.

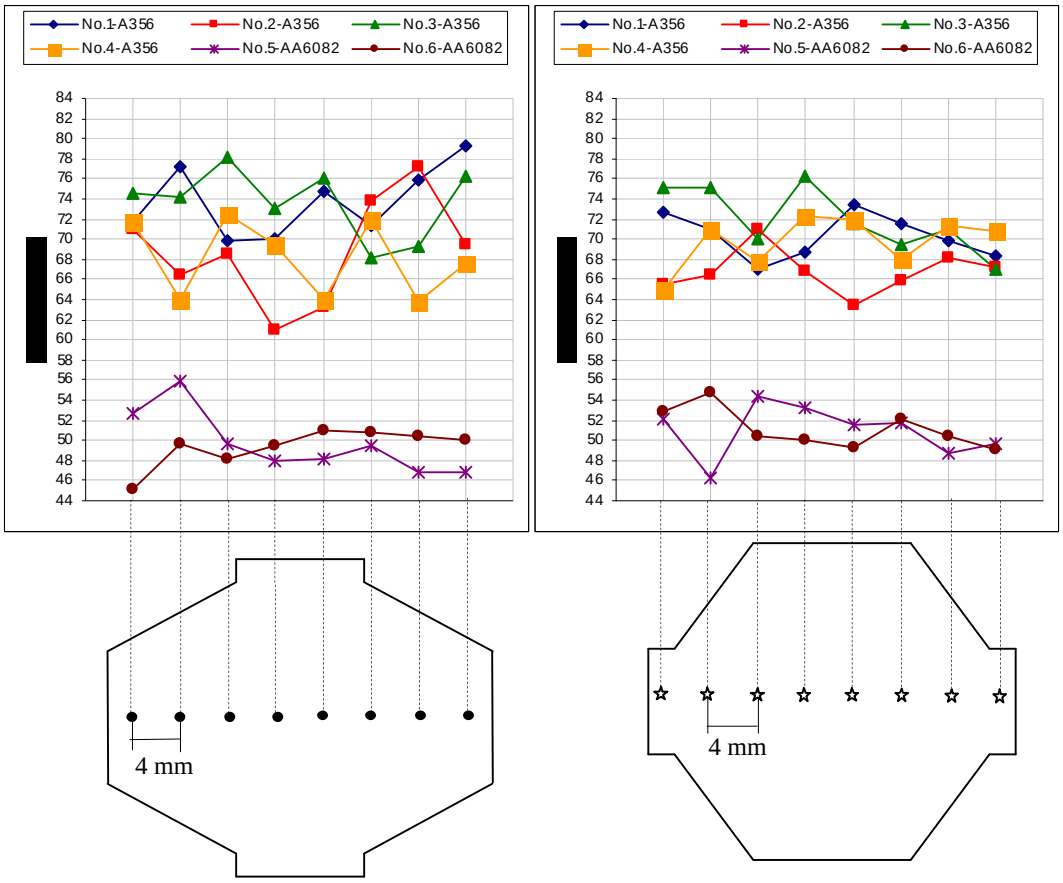

Figure 6.32. Hardness values of thixoformed samples on longitudinal (left) and transversal (right) sections before T6 heat treatment

Figure 6.33 shows average Vickers hardness values of samples before T6 heat treatment. When product number 1 and 2 or 3 and 4 are compared, it can be concluded that hardness values decrease with increasing holding time after 5 minutes for A356 alloy. Moreover; considering 5 minutes final holding time, three-step heating gives higher hardness value (product number 1 and 3). Product number 3 gives the highest hardness level before T6 heat treatment.

Figure 6.34 shows the hardness values after T6 heat treatment measured at each position in Figure 5.9. Experimental conditions corresponding to each product number is as shown in Table 5.7. For A356 alloy, the hardness values alter between 96-139 HV. For 6082 alloy, the hardness values alter between 95-132 HV. There is no general increasing or decreasing tendency of hardness values neither in longitudinal nor in transversal sections

for any product.

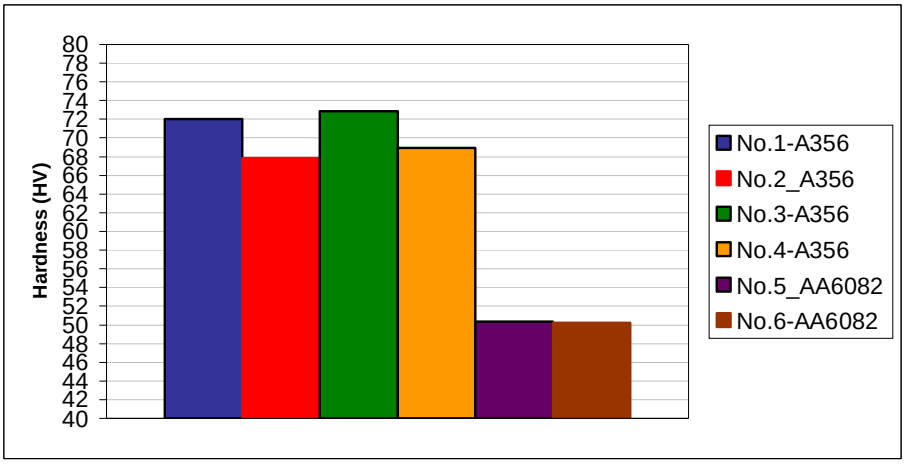

Figure 6.33. Average Vickers hardness values of thixoformed samples before T6 heat treatment

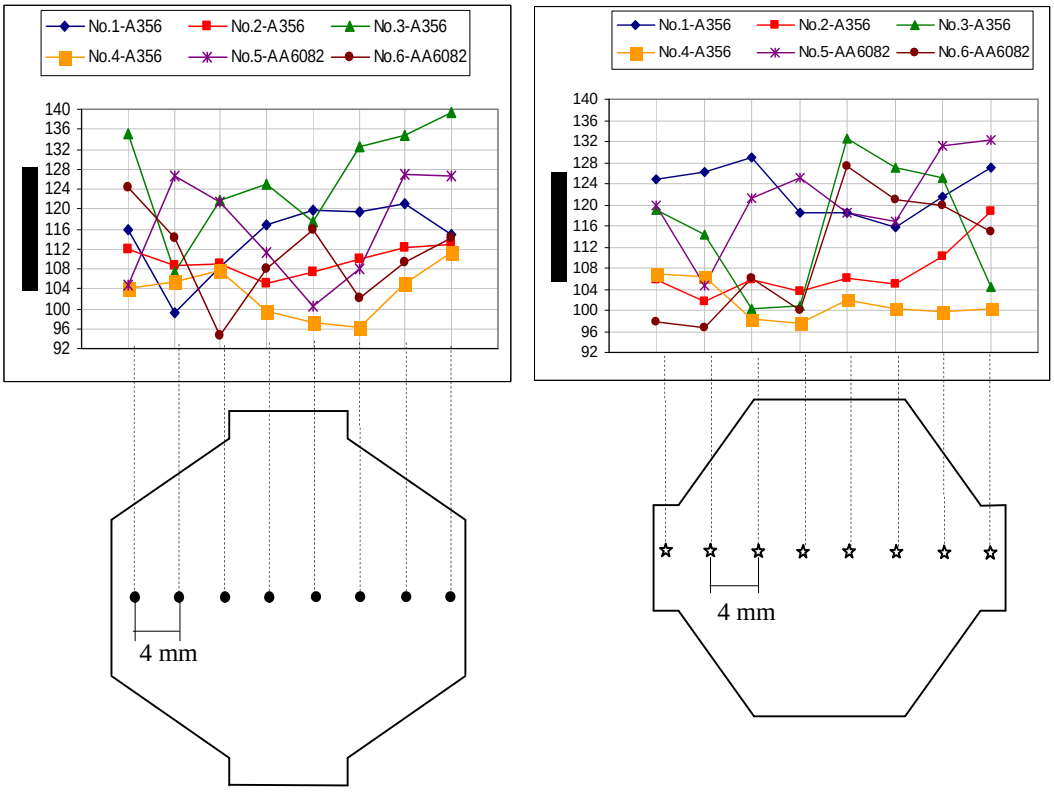

Figure 6.34. Hardness values of thixoformed samples on longitudinal (left) and transversal (right) sections after T6 heat treatment

Figure 6.35 shows average Vickers hardness values of samples after T6 heat treatment. It is clear that the response of AA6082 alloy to T6 heat treatment is very strong. The hardness values increased by more than 100% after T6 heat treatment. When product number 1 and 2 or 3 and 4 are compared, it can be concluded that hardness values decrease with increasing holding time after 5 minutes for A356 alloy. Moreover; considering 5 minutes final holding time, three-step heating gives higher hardness value (product number 1 and 3). Product number 3 gives the highest hardness level after T6 heat treatment.

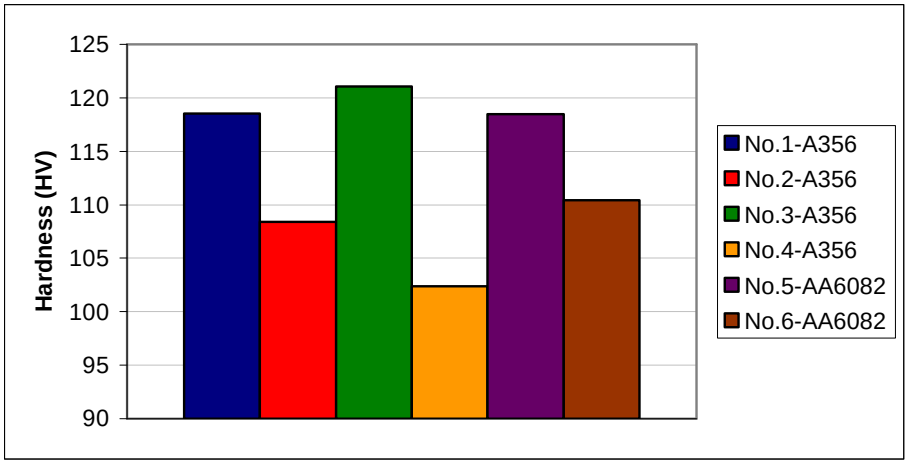

Figure 6.35. Vickers hardness values of thixoformed samples after T6 heat treatment

Tensile tests were performed to determine yield strength, tensile strength and elongation of thixoformed specimens. All tensile specimens were subjected to T6 heat treatment.

Table 6.1 represents tensile test results of all products after T6 heat treatment together with values found in literature as a whole. According to this table, mechanical properties of A356 alloy are in agreement with literature, even better. However, tensile properties of AA6082 alloy are lower than literature. This is possibly due to the heterogeneous microstructure and large elongated grains found in thixoformed AA6082 specimens.

Table 6.1. Tensile properties of A356 and AA6082 aluminum alloys after T6 heat treatment

Product no.	Material	Ultimate Tensile Strength (MPa)	Yield Strength (MPa)	Elongation (%)
1	A356	262.7	229.4	10.25
2	A356	254.6	206.4	11.1
3	A356	284	249.9	10.3
4	A356	258.6	210.1	11.2
5	AA6082	184.3	161.3	11.2
6	AA6082	189.3	174.9	10.8
Literature [32, 62]	A356	220-295	180-235	3-9
Literature [1, 15, 63, 64]	AA6082	310-370	260-330	3-8

Figure 6.36 shows average tensile properties of the examined specimens of A356 alloy. Experimental conditions corresponding to each product number is as shown in Table 5.7. Product number 1 and 2 corresponds to 5 minutes and 15 minutes holding time at 584 °C. A strong grain growth occurs after 5 minutes holding time for MHD A356 alloy. Undesirable grain coarsening causes the mechanical properties to decrease as shown in Figure 6.40 (Product number 2). As a result, it is important to prevent the coarsening of Si primary crystals for thixoforming to achieve a high level of strength values. Product number 3 corresponds to three-step heating with final holding time of 5 minutes. Three-heating gives rise to tensile properties with respect to one-step heating (comparison of product number 1 and 3).

Figure 6.37 shows average tensile test results for AA6082 alloy. Experimental conditions corresponding to each product number is as shown in Table 5.7. Results show that heating conditions have not much effect on tensile properties of SIMA 6082 alloy. For 15 minutes holding time at 645 °C, strength values are a little bit higher. The reason is that grain globularization is not completed after 5 minutes holding time for AA6082 alloy. Holding for 15 minutes instead of 5 minutes does not lead undesirable grain growth for AA6082 alloy, it is necessary to complete grain globularization. In this respect, holding more than 15 minutes may decrease strength values by causing undesirable grain growth.

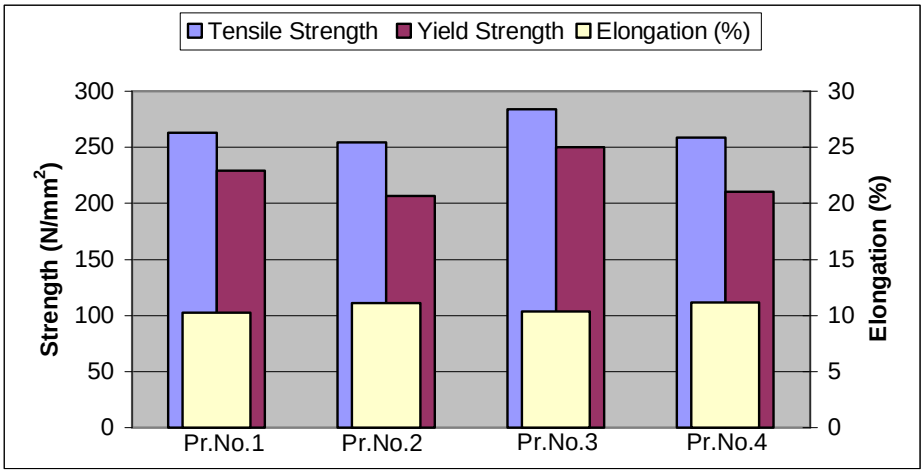

Figure 6.36. Tensile test results for thixoformed A356 alloys after T6 heat treatment

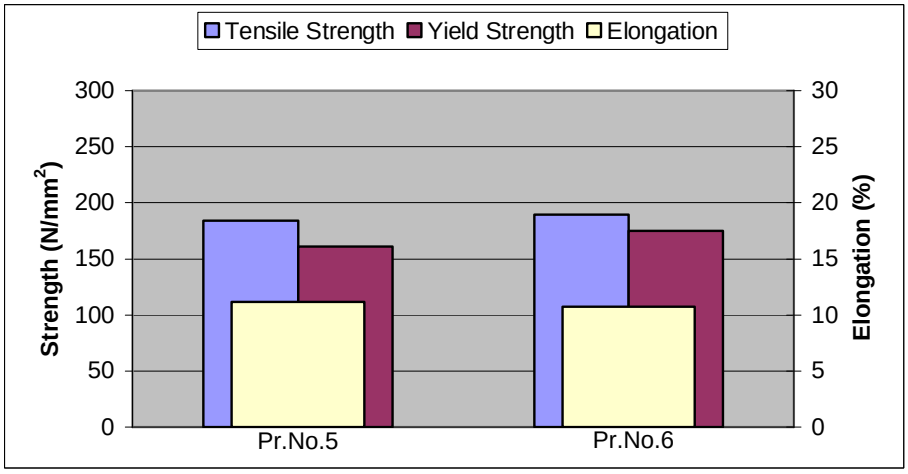

Figure 6.37. Tensile test results for thixoformed AA6082 alloys after T6 heat treatment

The mechanical properties of the manufactured components are in part satisfactory and indicate the great potential of thixoforming technology.

7. CONCLUSIONS

Thixoforming is a relatively new and promising technology that offers the possibility of forming complex aluminum parts with an exceptional quality and a reduction of processing steps. The production of a fine, equiaxed, globular microstructure is a must for the success of the thixoforming process. The present study showed that thixotropic structure can be successfully obtained using MHD casting route for A356 alloy and SIMA route for AA6082 aluminum alloy. In this study, the effect of heating conditions on thixoforming of A356 and AA6082 aluminum alloys was investigated.

Holding temperature, holding time and the number of reheating steps were considered as parameters in reheating experiments of MHD cast A356 alloy. Reheating practices revealed that three-step heating produces finer and more globular microstructure than one-step heating. Three-step heating is also useful to homogenously control the temperature distribution of semi-solid material. It was found that the holding time of the final step greatly affects the resulting microstructure. If the holding time of final step was short, globular microstructure was not obtained. On the other hand, too long holding time led to undesirable grain growth. Finest and most globular microstructure was obtained under the condition: 1 minute holding at 350 °C, 1 minute holding at 575 °C and 5 minute holding at 584 °C.

SIMA process was employed for thixotropic feedstock production of AA6082 alloy. The impact of the extent of deformation and reheating treatment parameters on the globularization of the grains in the 6082 alloy was investigated in this part of the study. It was concluded that reheating temperature is a more effective parameter compared to the holding time for thixotropic formation. Structural evolution seemed to be very clear when heating temperature was increased from 630 °C to 645 °C. At 645 °C, grains began to take spherical shape after 15 minutes holding time. Moreover, specimens of greater deformation degree showed more homogeneity and smaller grain size.

Finally, A356 and AA6082 aluminum alloys were thixoformed considering most successful heating conditions. Both alloys filled the die cavity easily under experimental conditions, also surface of the produced parts showed good condition. The microstructures and mechanical properties of the produced parts were investigated to get information about the obtained quality of the parts. The unique feature of the thixoforming process is retention of the feedstock microstructure in the formed part. Microstructures of thixoformed components were very similar to microstructures of reheated and quenched billets for A356 alloy. However, microstructures of thixoformed AA6082 alloys were very heterogeneous and included large elongated grains. The thixoformed specimens were given T6 heat treatment before mechanical testing. After T6 heat treatment, hardness measurements gave satisfactory results for both alloys. Tensile properties of A356 alloy were are in agreement with literature, even better. However, tensile test results of AA6082 alloy were found to be lower than literature values. This is possibly due to the liquid segregation and inhomogeneous microstructure found in AA6082 alloy.

REFERENCES

1. Giordano, P. and G. Chiarmetta, "New Rheocasting: A Valid Alternative to the Traditional Technologies for The Production of Automotive Suspension Parts", *Proceedings of the 8th International Conference on the Processing of Semi-solid Alloys and Composites*, 2004.

2. Fan, Z., "Semi-solid Metal Processing", *International Materials Reviews*, Vol. 47, No. 2, pp. 49-85, 2002.

3. Behrens, B., B. Haller, D. Fischer and R. Schober, "Investigations on Steel Grades and Tool Materials for Thixoforging", *Proceedings of the 8th International Conference on the Processing of Semi-solid Alloys and Composites*, 2004.

4. Henghua, Z., S. Guangjie, X. Luoping, X. Lin and T. Xuan, "Simulation and Optimization of Induction Heating Process of A356 Aluminum Alloy to Semi-solid State", *Proceedings of the 8th International Conference on the Processing of Semi-solid Alloys and Composites*, 2004.

5. Kopp, R., G. Winning and T. Möller, "Thixoforging of Aluminium Alloys", *Proceedings of International Conference on New Developments in Metallurgical Process Technology*, 1999, http://www.rwthaachen.de/sfb289/Wv/pdf/pub_ibf_ near netshape 97.pdf.

6. Ono Y., C. Zheng, F. G. Hamel, R. Charron and C. A. Loong, "Experimental Investigations on Monitoring and Control of Induction Heating Process for Semi-solid Alloys Using the Heating Coil as Sensor", *Measurement Science and Technology*, Vol. 13, pp. 1359-1365, 2002, http://www.iop.org/EJ/article/0957-0233/13/8/326/e20826.pdf.

7. Flemings, M. C., "Semi-solid Forming: The Process and the Path Forward", *Metallurgical Science and Technology*, Vol. 18, No. 2, pp.3-4, 2000.

8. Modigell, M. and J. Koke, "Time-dependent Rheological Properties of Semi-solid Metal Alloys", *Mechanics of Time-Dependent Materials*, Vol.3, pp. 15-30, 1999.

9. Dasgupta R., "Industrial Applications – The Present Status and Challenges We Face", *Proceedings of the 8th International Conference on the Processing of Semi-solid Alloys and Composites*, 2004.

10. Atkinson, H. V., "Modeling the Semisolid Processing of Metallic Alloys", *Progress in Materials Science*, Vol. 59, pp. 341-412, 2005.

11. Flemings, M. C., "Behavior of Metal Alloys in the Semi-solid State", *Metallurgical Transactions A*, Vol. 22A, pp. 957-980, 1991.

12. Kim, N. S. and C. G. Kang, "An Investigation of Flow Characteristics Considering the Effect of Viscosity Variation in the Thixoforming Process", *Journal of Materials Processing Technology*, Vol.103, pp. 237-246, 2000.

13. Tzimas, E. and A. Zavaliangos, "Material Selection for Semisolid Processing", *Materials and Manufacturing Processes*, Vol. 14, 1999, http://www.materials.drexel.edu/faculty/antonios/publications/papers_pdfs/MaterManuf.pdf.

14. Huang W., T. Li, X. Lin and L. Wang, "Formation of Semisolid Globular Structures under Shearing", *Proceedings of the 8th International Conference on the Processing of Semi-solid Alloys and Composites*, 2004.

15. Liu, D., H. V. Atkinson, P. Kapranos, W. Jirattiticharoean, and H. Jones, "Microstructural Evolution and Tensile Mechanical Properties of Thixoformed High Performance Aluminium Alloys", *Materials Science and Engineering*, Vol.A361, pp. 213-224, 2003.

16. Lee, S. Y. and S. Oh, “Thixoforming Characteristics of Thermo-mechanically Treated AA 6061 Alloy for Suspension Parts of Electric Vehicles”, *Journal of Materials Processing Technology,* Vol.130–131, pp. 587–593, 2002.

17. Winterbottom W. L., “Semi-solid Forming Applications: High Volume Automotive Products”, *Metallurgical Science and Technology*, Vol. 18, No. 2, pp. 5-10, 2000.

18. Liu, D., H. V. Atkinson and H. Jones, “Mtdata Thermodynamic Prediction of Suitability of Alloys for Thixoforming”, *Proceedings of the 8th International Conference on the Processing of Semi-solid Alloys and Composites*, 2004.

19. Tzimas, E. and A. Zavaliangos, “Evolution of Near-equiaxed Microstructure in the Semisolid State”, *Materials Science and Engineering,* Vol. A289, pp. 228-240, 2000.

20. Vieira, E. A., A. M. Kliauga, M. Ferrante, “Microstructural Evolution and Rheological Behaviour of Aluminum Alloys A356, and A356 + 0.5% Sn Designed for Thixocasting”, *Journal of Materials Processing Technology,* Vol. 155, pp. 1629-1633, 2004.

21. Roplekar, J. K. and J. A. Dantzig, "A Study of Solidification with a Rotating Magnetic Field" *International Journal of Cast Metals Research,* Vol. 14, pp. 79-95 2001.

22. Kirkwood, D. H., “Semi-solid Metal Processing”, *International Materials Reviews*, Vol.39, No. 5, pp. 173-189, 1994.

23. Dantzig, J. A., J. Winter and D. E. Tyler, “Process and Apparatus for Making Thixotropic Metal Slurries”, U.S. Patent 4,434,837, 1984.

24. Brabazon, D., D. J. Browne and A .J. Carr, “Mechanical Stir Casting of Aluminium Alloys form the Mushy State: Process, Microstructure and Mechanical Properties”, *Materials Science and Engineering*, Vol. A326, pp. 370-381, 2002.

25. Tzimas, E. and A. Zavaliangos, “A Comparative Characterization of Near-equiaxed Microstructures as Produced by Spray Casting, Magnetohydrodynamic Casting and the Stress Induced, Melt Activated Process”, *Materials Science and Engineering*, Vol. A289, pp. 217-227, 2000.

26. Buynacek, C. J. and W. L. Winterbottom, “High Volume Semi-solid Forming of Aluminum Master Cylinders”, *SAE 2000 World Congress*, 2000.

27. Kliauga, A. M. and M. Ferrante, “Comparison of Flow Behaviour and Microstructure and Texture Development of Aluminium Alloy A356 in Semisolid State Submitted to Two Different Thermomechanical Treatments”, *Materials Science and Technology*, Vol. 18, pp. 820-826, 2002.

28. Changming, L. and Z. Maohua, “Effects of Compressing and Remelting in SIMA Processing on Semi-solid Structure Evolution of an Al-Zn Wrought Alloy”, *Rare Metals*, Vol. 22, No. 3, pp. 185-191, 2003.

29. Wang, J. G., P. Lu, H. Y. Wang and Q. C. Jiang, “Effect of Predeformation on the Semisolid Microstructure of Mg-9Al-0.6Zn Alloy”, *Materials Letters*, Vol. 58, pp. 3852-3856, 2004.

30. Kirkwood, D. H., C. M. Sellars and L. G. E. Boyed, “Thixotropic Materials”, U.S. Patent 5,133,811, 1992.

31. Margarido, M. and M. H. Robert, “Influence of Thermomechanical Treatments on the Production of Rheocast Slurries by Partial Melting”, *Journal of Materials Processing Technology*, Vol. 133, pp. 149-157, 2003.

32. Haga, T. and P. Kapranos, “Billetless Simple Thixoforming Process”, *Journal of Materials Processing Technology*, Vol.130–131, pp. 581–586, 2002.

33. Salarfar, S., Akhlaghi F. and M. Nili-Ahmadabadi, "Influence of Pouring Conditions in the Inclined Plate Process and Reheating on the Microstructure of the Semi-solid A356 Aluminum Alloy", *Proceedings of the 8th International Conference on the Processing of Semi-solid Alloys and Composites*, 2004.

34. Grimmig, T., J. Aguilar, M. Fehlbier and A. Bührig-Polaczek, "Optimization of the Rheocasting Process under Consideration of the Main Influence Parameters on the Microstructure", *Proceedings of the 8th International Conference on the Processing of Semi-solid Alloys and Composites*, 2004.

35. Jirattiticharoean, W., H. Jones, H. V. Atkinson, I. Todd and P. Kapranos, "Thixoforming of Aluminum 7xxx Alloys Produced Using a Cooling Slope", *Proceedings of the 8th International Conference on the Processing of Semi-solid Alloys and Composites*, 2004.

36. Pan, Q. Y., M. Findon and D. Apelian, "The Continuous Rheoconversion Process (CRP): A Novel SSM Approach", *Proceedings of the 8th International Conference on the Processing of Semi-solid Alloys and Composites*, 2004.

37. Siegert, K. and S. Huber, "Forming of Spray Formed Copper Alloys with Injected Carbon", *Materials Science and Engineering,* Vol. A326, pp. 63-72, 2002.

38. Pan, Q. Y., D. Apelian and M. M. Makhlouf, "AlB_2 Grain Refined Al-Si Alloys: Rheocasting/Thixocasting Applications", *Proceedings of the 8th International Conference on the Processing of Semi-solid Alloys and Composites*, 2004.

39. Jung, H. K. and C. G. Kang, "Induction Heating Process of an Al-Si Aluminium Alloy for Semi-solid Die Casting and Its Resulting Microstructure", *Journal of Materials Processing Technology*, Vol. 120, pp. 355-364, 2002.

40. Jung, H. K., "The Induction Heating Process of Semi-solid Aluminium Alloys for Thixoforming and Their Microstructure Evaluation", *Journal of Materials Processing Technology*, Vol. 105, pp. 176-190, 2000.

41. Kapranos, P., R. C. Gibson, D. H. Kirkwood and C. M. Sellars, "Induction Heating and Partial Melting of High Melting Point Thixoformable Alloys", *Proceedings of the 4th International Conference on Semi-solid Processing Alloys and Composites*, 1996.

42. Fairchild Semiconductor 2002, "Induction Heating System Topology Review", http://www.fairchildsemi.com/an/AN/AN-9012.pdf.

43. Burnett R., "RF Induction Heating", http://www.richieburnett.co.uk/indheat.html.

44. Herring, D. H., "Induction Heating for the Rest of Us", *Industrial Heating*, Vol. 71, Iss. 5, pp. 12-13, 2004.

45. Ameritherm Inc., "About Induction Heating", http://ameritherm.com/aboutinduction.html.

46. Midson, S., V. Rudnev and R. Gallik, "Semi-solid Processing of Aluminum Alloys", *Industrial Heating*, Vol. 66, Iss. 1, 1999.

47. Zinn, S. and S. L. Semiatin, "Coil Design and Fabrication: Basic Design and Modifications", *Heat Treating*, pp. 32-36, June 1988.

48. Kopp, R., D. Neudenberger and G. Winning, "Different Concepts of Thixoforging and Experiments for Rheological Data", *Journal of Materials Processing Technology*, Vol. 111, pp. 48-52, 2001.

49. Wolf, A., J. Baur and G. C. Gullo, "Thixoforging", *Proceedings of the International Conference on New Developments in Forging Technology*, 2001.

50. Kang, C. G. and P. K. Seo, "The Effect of Gate Shape on the Filling Limitation in the Semi-solid Forging Process and the Mechanical Properties of the Products", *Journal of Materials Processing Technology*, Vol. 135, pp. 144-157, 2003.

51. McLelland, A. R. A., N. G. Henderson, H. V. Atkinson and D. H. Kirkwood, "Anomalous Rheological Behaviour of Semi-solid Alloy Slurries at Low Shear Rates", *Materials Science and Engineering*, Vol. A232, pp. 110-118, 1997.

52. Lapkowski, W., "Some Studies Regarding Thixoforming of Metal Alloys", *Journal of Materials Processing Technology*, Vol. 80-81, pp. 463-468, 1998.

53. Chen, C. P. and C. Y. A. Tsao, "Semi-solid Deformation of Non-dendritic Structures-Part I: Phenomenological Behaviour", *Acta Materialia*, Vol. 45, No. 5, pp. 1955-1968, 1997.

54. Yurko, J. A., R. A. Martinez and M. C. Flemings, "SSR^{TM}: The Spheroidal Growth Route to Semi-solid Forming", *Proceedings of the 8th International Conference on the Processing of Semi-solid Alloys and Composites*, 2004.

55. Xu, J., Z. Tian and L. Shi, "Study on New Al-Mg-Si Alloys for Semi-solid Processing", *Proceedings of the 8th International Conference on the Processing of Semi-solid Alloys and Composites*, 2004.

56. Hirt, G., R. Cremer, T. Witulski and H. C. Tinius, "Lightweight Near Net Shape Components Produced by Thixoforming", *Materials & Design*, Vol. 18, pp. 315-321, 1997.

57. Dong, J., J.Z. Cui, Q.C. Le and G.M. Lu, "Liquidus Semi-continuous Casting, Reheating and Thixoforming of a Wrought Aluminum Alloy 7075", *Materials Science and Engineering*, Vol.A345, pp. 234-242, 2003.

58. Altınel S. A., "Semi-solid Forming of Al-5083 and A356 Aluminum Alloys", M.S. Thesis, Boğaziçi University, 2003.

59. Zoqui, E. J., M. T. Sheata, M. Paes, V. Kao and E. Es-Sadiqi, "Morphological Evolution of SSM A356 During Partial Remelting", *Materials Science and Engineering*, Vol. A325, pp. 38-53, 2002.

60. ASTM B-917M-01 Standard, “Standard Practice for Heat Treatment of Aluminum Alloy Castings from All Processes”, 2001.

61. ASTM E-8M-04 Standard, “Standard Test Methods for Tension Testing of Metallic Materials”, 2004.

62. Cho, W.G. and C.G. Kang, “Mechanical Properties and Their Microstructure Evaluation in the Thixoforming Process of Semi-solid Aluminum Alloys”, *Journal of Materials Processing Technology,* Vol.105, pp. 269-277, 2000.

63. Hirt, G., R. Cremer, A. Winkelmann, T. Witulski and M. Zillgen, “Semi Solid Forming of Aluminium Alloys by Direct Forging and Lateral Extrusion”, *Journal of Materials Processing Technology,* Vol.45, pp. 359-364, 1994.

64. Wabusseg, H., G. Gullo, P. J. Uggowitzer, K. Steinhoff and H. Kaufmann, “Structure and Properties of AlMgSi1 Alloy Tailored for Semi-solid Forming”, *Journal of Materials Science,* Vol. 37, pp. 1173-1178, 2002.